CONTEMPORARY METHODOLOGICAL APPROACHES IN SCIENCE AND MATHEMATICS

EDITOR
PROF. HÜSNİYE SAĞLIKER, PH.D.

DOI: 10.5281/zenodo.19191850

Contemporary Methodological Approaches in Science and Mathematics

Edıtor

Prof. Hüsniye Sağlıker, Ph.D.

Publisher
Platanus Publishing®

Editor in Chief
Prof. Hüsniye Sağlıker, Ph.D.

Cover & Interior Design
Platanus Publishing®

The First Edition
March, 2026

ISBN
978-625-8513-85-7

Platanus Publishing®
Address: Natoyolu Cad. Fahri Korutürk Mah. 157/B, 06480, Mamak, Ankara, Turkey.

Phone: +90 312 390 1 118
web: www.platanuspublishing.com
e-mail: platanuskitap@gmail.com

Platanus Publishing®

İÇİNDEKİLER

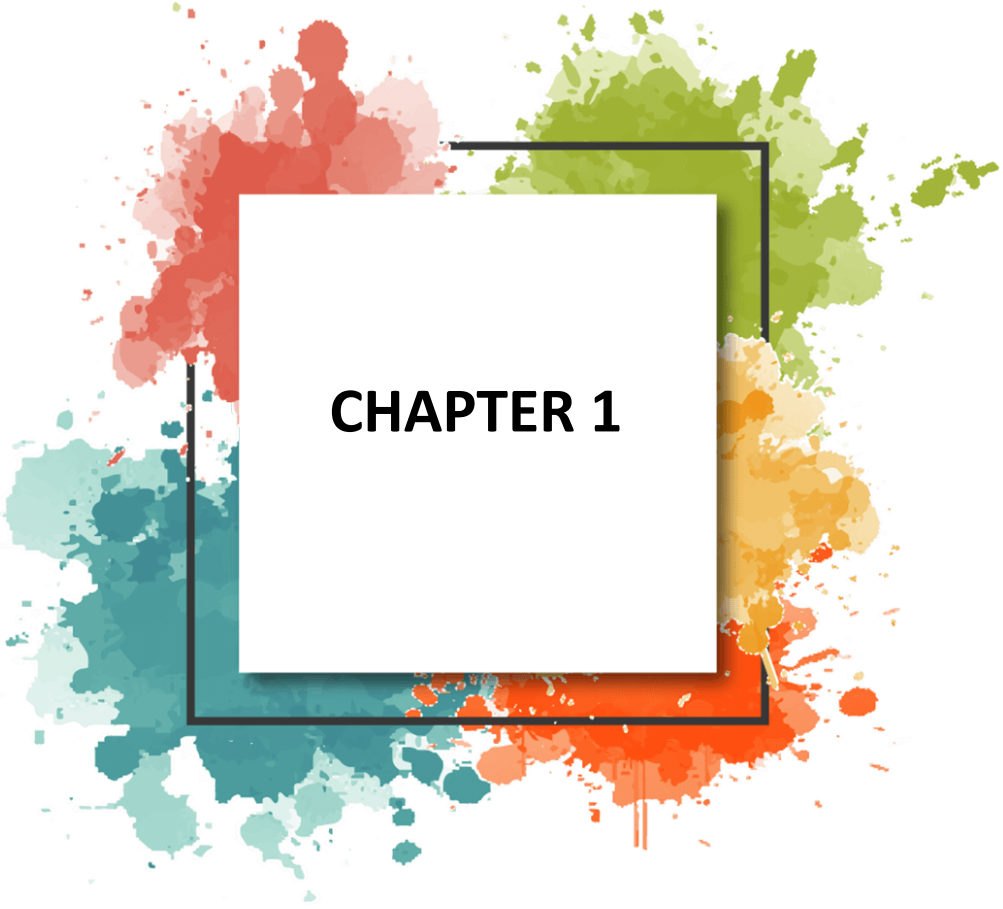
CHAPTER 1

A Generator-Based Methodological Framework for Earthquake Magnitude Modeling: The Gumbel–Weibull Distribution and a Turkey Application

Selen Çakmakyapan[1]

1. Introduction

Earthquake magnitude is one of the most fundamental variables in probabilistic seismic hazard and risk analysis, as it directly reflects the amount of released seismic energy and governs the potential impact of seismic events. Reliable statistical modeling of earthquake magnitudes is therefore essential for understanding seismic risk, estimating return periods, and supporting risk-informed decision-making. However, empirical earthquake catalogs often exhibit pronounced asymmetry, heavy-tailed behavior, and heterogeneous distributional structures that challenge the adequacy of classical probability models.

A broad range of probability distributions has been employed in the literature to model earthquake magnitudes, including exponential, log-normal, Weibull, gamma, Cauchy, logistic, and Gumbel distributions. Among these, Gumbel- and Weibull-based models have received particular attention due to their connection with extreme value theory and their suitability for modeling maximum earthquake magnitudes. Extreme value theory suggests that block maxima of earthquake magnitudes may follow Type I (Gumbel) or Type III (reflected Weibull) distributions. Despite their widespread use, empirical evidence indicates that these classical models often struggle to simultaneously capture central clustering and tail behavior, especially in regions characterized by complex tectonic settings. In particular, Gumbel models have been reported to overestimate extreme magnitudes, while Weibull-based models may underestimate large events.

A comprehensive summary of probability distributions that have been employed in previous studies for modeling earthquake magnitudes across different regions and magnitude ranges is presented in Table 1.

[1] Assist, Prof., Department of Statistics, Istanbul Medeniyet University, 34700, Istanbul, Turkey, ORCID: 0000-0002-1878-2181

Table 1. Probability distributions used for modeling earthquake magnitudes in previous studies

Distribution	Reference(s)	Earthquake Magnitude (Mw)	Region
Normal	Rahman and Hossain (2019)	$3.5 \leq Mw \leq 5.0$	Bangladesh
Log-normal	Patel et al. (1976); Rahman and Hossain (2019); Pasari (2019)	$5.0 \leq Mw \leq 7.0$	India, Bangladesh
Weibull	Makjanic (1972); Yegulalp and Kuo (1974); Patel et al. (1976); Ferraes (2003); Yakovlev et al. (2006); Roy (2014); Rahman et al. (2018); Rahman and Hossain (2019); Selçuk and Yücemen (2000)	$5.5 \leq Mw \leq 7.5$	Global, Bangladesh, Turkey
Gamma	Rahman and Hossain (2019)	$4.0 \leq Mw \leq 6.0$	Bangladesh
Cauchy	Rahman and Hossain (2019)	$3.0 \leq Mw \leq 5.5$	Bangladesh
Logistic	Rahman and Hossain (2019)	$3.0 \leq Mw \leq 5.5$	Bangladesh
Gumbel	Nordquist (1945); Burton (1979); Kijko (1984); Al-Abbasi and Fahmi (1985, 1991); Ameer et al. (2004); Kijko (2002); Rahman and Hossain (2019); Kestel and Yücemen (2000)	$6.0 \leq Mw \leq 8.0$	Global, Turkey
Birnbaum–Saunders	Lillo et al. (2018)	$6.5 \leq Mw \leq 8.0$	Italy, Mediterranean region
Extreme Birnbaum–Saunders	Lillo et al. (2018)	$6.5 \leq Mw \leq 8.0$	Italy, Mediterranean region
Exponential	Ferraes (2003)	$3.5 \leq Mw \leq 5.5$	Argentina
Rayleigh	Ferraes (2003)	$3.5 \leq Mw \leq 5.5$	Argentina
Inverse Gaussian	Matthews et al. (2002); Pasari (2019)	$6.0 \leq Mw \leq 8.0$	Global, India
Wald	Pasari (2019)	$6.0 \leq Mw \leq 8.0$	India

Distribution	Reference(s)	Earthquake Magnitude (Mw)	Region
Truncated Exponential	Dhanya (2019); Raschke (2014)	$5.5 \leq Mw \leq 7.5$	India, Germany
Generalized Pareto	Dhanya (2019)	$5.5 \leq Mw \leq 7.5$	India, Germany
Gumbel III	Mohammadi et al. (2016)	$6.0 \leq Mw \leq 7.8$	Iran
Bounded Exponential	Raschke (2014)	$5.5 \leq Mw \leq 7.5$	Germany
Pareto	Charpentier and Durand (2015)	$6.0 \leq Mw \leq 8.0$	France, Global

Motivated by these limitations, recent statistical research has increasingly focused on the development of flexible distributional frameworks through generator-based construction mechanisms. Such approaches allow the generation of new distribution families by embedding a baseline distribution within a suitable generator, thereby enhancing flexibility without resorting to mixture models or overly complex parameterizations. Within this context, the present study introduces a new family of continuous probability distributions, referred to as the Gumbel–G family, constructed by employing the Gumbel distribution as a generator within the T–X framework.

The proposed Gumbel–G family provides a unified and extensible structure for generating flexible distributions capable of accommodating skewness, tail heaviness, and diverse hazard rate shapes. As a specific and practically relevant member of this family, we focus on the Gumbel–Weibull (GW) distribution, which is obtained by selecting the Weibull distribution as the baseline model. The GW distribution inherits the interpretability of the Weibull distribution while benefiting from the additional flexibility introduced by the Gumbel-based generator mechanism.

To demonstrate the usefulness of the proposed framework, the statistical properties of the GW distribution are derived in detail, including its probability density function, cumulative distribution function, hazard function, quantile function, and moments. Parameter estimation is carried out using the maximum likelihood method, and the performance of the GW distribution is evaluated through comprehensive comparisons with several classical distributions commonly used in earthquake magnitude modeling.

The empirical application focuses on earthquake magnitude data from Turkey, a tectonically complex region located along the Alpine–Himalayan seismic belt and characterized by frequent moderate earthquakes and rare but highly destructive large events. This setting provides a challenging and realistic testbed for assessing the adequacy of flexible probabilistic models. Through model fitting, information-criterion-based comparisons, hazard analysis, and return period estimation, the study demonstrates that the GW distribution offers improved performance and interpretable risk measures compared to traditional models.

The main contributions of this study can be summarized as follows:

(i) a new continuous probability distribution derived from the Weibull distribution using a Gumbel-based generator approach is introduced, and its fundamental statistical properties are examined in detail;

(ii) the parameters of the proposed GW distribution are estimated using the maximum likelihood method, and the model's flexibility is assessed through its hazard function and tail behavior;

(iii) the performance of the proposed model is evaluated using an earthquake catalog comprising events that occurred in Turkey between 1999 and 2023 above a specified magnitude threshold, and is compared with several classical distributions commonly employed in the literature.

Overall, this work contributes to the literature by proposing a new Gumbel-based distribution family and by illustrating the practical advantages of one of its key members, the Gumbel–Weibull distribution, for earthquake magnitude modeling and seismic risk assessment.

The remainder of this paper is organized as follows: Section 2 presents the proposed Gumbel–G family and the Gumbel–Weibull (GW) distribution, Section 3 describes the estimation procedure, Section 4 reports the empirical results and model comparisons, Section 5 discusses the findings, Section 6 concludes the paper, and Section 7 provides the references.

2. Methodological Background and Motivation

Extreme value theory (EVT) provides a well-established probabilistic framework for modeling rare and extreme events and has long been employed in seismology to characterize earthquake magnitudes. Classical EVT-based models, such as the Gumbel, Weibull, and generalized extreme value (GEV) distributions, have been widely used to represent maximum or large earthquake magnitudes (Gumbel, 1958; Lomnitz, 1966; Kijko, 1984). Despite their theoretical appeal, these models often impose restrictive assumptions on tail behavior and hazard

rate structure, which may limit their ability to adequately represent the complex statistical characteristics observed in real earthquake catalogs.

Earthquake magnitude data frequently exhibit different statistical behaviors across magnitude ranges. While low- and moderate-magnitude earthquakes tend to occur more frequently and display relatively regular patterns, large and destructive earthquakes are rare and are typically associated with extreme-value behavior. This heterogeneity suggests that modeling a wide range of earthquake magnitudes using a single distributional structure may not yield uniform performance across all magnitude regimes. Indeed, several studies indicate that considering earthquake magnitudes under different magnitude ranges or threshold-based frameworks may support the notion that the statistical properties of large and rare earthquakes can be more reliably characterized when magnitude-dependent behaviors are taken into account (Lomnitz, 1966; Kijko, 2002; Pisarenko and Sornette, 2004; Pisarenko et al., 2010).

To address these challenges, recent research has increasingly focused on more flexible modeling strategies. Generalized distributions, generator-based distribution families, and mixture models have been proposed to better accommodate the complex structure of earthquake magnitude data (Zografos and Balakrishnan, 2009; Alzaatreh et al., 2013; Bourguignon et al., 2014). However, mixture models often introduce difficulties related to parameter identifiability, interpretability, and numerical stability, while some generalized models may exhibit excessive or insufficient tail behavior over specific magnitude intervals. These issues complicate the reliable assessment of magnitude-dependent seismic risk (Kagan and Schoenberg, 2001; Lombardi and Marzocchi, 2019).

Motivated by these methodological considerations, the present study adopts a generator-based approach to extend the Weibull distribution using a Gumbel generator, resulting in a new continuous probability distribution referred to as the Gumbel–Weibull (GW) distribution. This construction aims to enhance the flexibility of the Weibull distribution in modeling earthquake magnitudes, particularly with respect to tail behavior and hazard rate curvature, while avoiding the structural and interpretational complexities typically associated with mixture models.

2.1. Statistical Framework of the Gumbel-G Distribution Family and the Gumbel–Weibull Distribution

In this study, a new family of continuous probability distributions is first introduced by employing a Gumbel-based generator mechanism. This family, referred to as the Gumbel-G distribution family, provides a general framework for extending baseline distributions through the incorporation of a Gumbel generator. The Gumbel-G family preserves the support structure of the baseline distribution while introducing additional parameters derived from the Gumbel distribution, allowing for enhanced control over tail behavior and the overall curvature of the distribution.

The primary motivation for the Gumbel-G distribution family arises from the limitations of classical distributions when modeling data characterized by heterogeneous statistical behavior, such as earthquake magnitudes. Earthquake magnitude data often exhibit varying frequency patterns, tail behaviors, and risk structures across different magnitude ranges. In such settings, fixed-structure distributions may fail to provide adequate flexibility. The Gumbel-G approach addresses this issue by integrating the extreme-value modeling capability of the Gumbel distribution with a wide class of baseline distributions, thereby enabling a more adaptable probabilistic representation.

Within this general framework, the present study focuses on a specific member of the Gumbel-G family, namely the Gumbel–Weibull (GW) distribution. The Weibull distribution is widely used in earthquake magnitude modeling due to its flexibility arising from scale and shape parameters. However, the classical Weibull distribution may exhibit limited adaptability in capturing the behavior of large and rare earthquakes, particularly in the upper tail of the distribution. By incorporating a Gumbel generator into the Weibull baseline, the proposed GW distribution aims to overcome these limitations.

One of the key statistical features of the Gumbel–Weibull distribution is the additional flexibility it provides in modeling tail behavior. Accurate probabilistic representation of large earthquakes is crucial for reliable seismic hazard and risk analyses. The GW distribution retains the fundamental scale structure of the Weibull distribution while allowing the upper tail to be more sensitively shaped through the Gumbel generator parameters. This feature enables a more consistent representation of the heterogeneous risk structure observed across different earthquake magnitude ranges.

In addition to tail flexibility, the GW distribution exhibits a highly adaptable hazard function structure. Depending on the parameter configuration, the hazard function can take increasing, decreasing, unimodal, or non-monotonic forms. Such versatility is particularly valuable in seismic applications, where magnitude-dependent risk does not necessarily follow a simple monotonic pattern. Compared to classical Weibull and Gumbel models, this constitutes a notable advantage.

From an analytical perspective, an important strength of the Gumbel-G family, and of the Gumbel–Weibull distribution in particular, is the availability of closed-form expressions for key statistical functions. The cumulative distribution function, probability density function, survival function, and quantile function can all be derived explicitly. This analytical tractability facilitates both theoretical investigation and practical implementation. Moreover, quantile-based measures of skewness and kurtosis can be naturally defined, providing robust and interpretable shape descriptors.

Based on the general framework outlined in this section, the next subsection presents the mathematical formulation of the Gumbel-G distribution family and

provides the explicit cumulative and density functions of its special member, the Gumbel–Weibull distribution.

2.1.1. Gumbel–Weibull Distribution as a Special Case of the Gumbel–G Family

Let $F(x)$ and $f(x)$ denote the cumulative distribution function (cdf) and probability density function (pdf) of the Gumbel distribution, respectively. These functions are given in Eqs. (1) and (2). The Gumbel distribution is widely used in extreme value modeling due to its ability to characterize rare and extreme events. In this formulation, $\alpha \in \mathbb{R}$ represents the location parameter and β>0 denotes the scale parameter.

$$F(x) = e^{-e^{-\left(\frac{x-\alpha}{\beta}\right)}}, \quad x \geq 0 \tag{1}$$

$$f(x) = \frac{1}{\beta} e^{-\left(\frac{x-\alpha}{\beta}\right)}, \quad x \geq 0 \tag{2}$$

Similarly, the cumulative distribution function and probability density function of the Weibull distribution are defined in Eqs. (3) and (4), respectively. Owing to its flexible scale and shape parameters, the Weibull distribution has been extensively applied in reliability analysis, engineering, and geophysical studies. Here, a>0 denotes the scale parameter, while b>0 is the shape parameter.

$$F(x) = 1 - e^{-\left(\frac{x}{b}\right)^{a}}, \quad x \geq 0 \tag{3}$$

$$f(x) = \frac{a}{b}\left(\frac{x}{b}\right)^{a-1}, \quad x \geq 0 \tag{4}$$

To enhance the adaptability of probability modeling, it is often necessary to consider more flexible distributional structures derived from classical baseline distributions. In this study, the Gumbel distribution is employed as a generator to construct a novel family of continuous distributions. When a distinct distribution

F is generated for each baseline distribution G, the Gumbel function acts as a generator within the framework proposed by Alzaatreh et al. through the T–X (transformer) mechanism. Under this framework, merging the Gumbel generating function with the cumulative distribution function of a baseline distribution leads to a broader class of continuous distributions, referred to as the Gumbel–G family. In particular, by adopting the Weibull distribution as the baseline distribution, a more flexible and powerful probability distribution, namely the Gumbel–Weibull (GW) distribution, is obtained.

Within the T–X generator framework, the baseline cumulative distribution function $G(x)$ is mapped onto the positive real line through the transformation $-\log\{1-G(x)\}$, which corresponds to a logarithmic transformation of the survival function of the baseline distribution. This transformation ensures that the generator operates on an appropriate domain while preserving the support of the baseline model. By applying the Gumbel generating function to the transformed baseline distribution, the resulting Gumbel–G distribution is obtained. The corresponding Gumbel–G transformation adopted in this study is therefore formally expressed in Eq. (5).

$$Gumbel - G(x) = \int_0^{-\log(1-G(x))} e^{-e^{-\left(\frac{t-\alpha}{\beta}\right)}} dt \tag{5}$$

For the Weibull baseline, the cumulative distribution function of the resulting Gumbel–Weibull distribution is given in Eq. (6). In this expression, $\alpha \in \mathbb{R}$ represents the location parameter, while a, b, and $\beta>0$ denote shape and the scale-related parameters of the distribution. The corresponding probability density function of the GW distribution is obtained by differentiating Eq. (6) with respect to x

$$G(x) = exp\left[-exp\left[\frac{\beta-\left(\frac{x}{b}\right)^a}{\alpha}\right]\right], \; x > 0 \tag{6}$$

$$g(x) = -\frac{a}{\alpha b}\left(\frac{x}{b}\right)^{a-1} exp\left[\frac{\beta-\left(\frac{x}{b}\right)^a}{\alpha} - exp\left[\frac{\beta-\left(\frac{x}{b}\right)^a}{\alpha}\right]\right], \; x > 0 \tag{7}$$

The proposed GW distribution retains the fundamental characteristics of the Weibull distribution while incorporating the extreme-value modeling capability of the Gumbel generator. This combination yields a distribution with enhanced flexibility, particularly in the upper tail, which is crucial for modeling rare and large-magnitude events. Consequently, the GW distribution serves as a suitable and effective special case within the broader Gumbel–G family for earthquake magnitude modeling.

The survival function, commonly denoted by $S(x)$, is a fundamental concept in survival and reliability analysis and represents the probability that a random variable exceeds a given threshold. For a non-negative random variable T, the survival function is defined as $S(x)=P(T>x)$. In the context of earthquake

magnitude modeling, the survival function provides a probabilistic description of the likelihood that an earthquake magnitude exceeds a specified level, which is particularly relevant for assessing the risk of large and extreme events. Based on the definition $S(x) = 1 - G(x)$, the survival function of the proposed Gumbel–Weibull (GW) distribution is obtained from Eq. (8) as

$$S(x) = 1 - G(x) = 1 - exp\left[-exp\left[\frac{\beta-\left(\frac{x}{b}\right)^{a}}{\alpha}\right]\right], \quad x > 0 \tag{8}$$

The hazard function characterizes the instantaneous risk associated with the occurrence of an event, conditional on the event not having occurred before a given magnitude level. In the present setting, the hazard function can be interpreted as a magnitude-dependent risk measure, describing the conditional likelihood of observing an earthquake with magnitude in the neighborhood of x, given that no larger magnitude has occurred.

The hazard function of the GW distribution is defined as the ratio of the probability density function to the survival function and is given in Eq. (9) by

$$h(x) = \frac{g(x)}{S(x)} = \frac{-\frac{a}{\alpha b}\left(\frac{x}{b}\right)^{a-1} exp\left[\frac{\beta-\left(\frac{x}{b}\right)^{a}}{\alpha} - exp\left[\frac{\beta-\left(\frac{x}{b}\right)^{a}}{\alpha}\right]\right]}{1-exp\left[-exp\left[\frac{\beta-\left(\frac{x}{b}\right)^{a}}{\alpha}\right]\right]}, \qquad x > 0 \tag{9}$$

where the explicit form of $g(x)$ and $S(x)$follows from Eqs. (6) and (8), respectively, and the parameters satisfy $\alpha, \beta, a, b > 0$.

An important feature of the proposed GW distribution is the flexibility of its hazard function. Depending on the parameter configuration, the hazard function can exhibit increasing, decreasing, unimodal, or non-monotonic shapes, including bathtub and inverted bathtub patterns. Such behavior is particularly desirable in earthquake magnitude modeling, where the risk associated with increasing magnitude does not necessarily follow a simple monotonic trend.

The density, survival, and hazard functions of the GW distribution are illustrated in Figures 1a–1c, respectively. Figure 1a demonstrates the flexibility of the proposed model in capturing different density shapes. The hazard function plots shown in Figure 1c further confirm this flexibility, displaying initially increasing patterns followed by monotonic decreases, as well as inverted bathtub and reversed J-shaped behaviors. These results indicate that the GW distribution

is capable of accommodating a wide range of statistical behaviors through appropriate parameter choices, making it a robust and adaptable model for earthquake magnitude data.

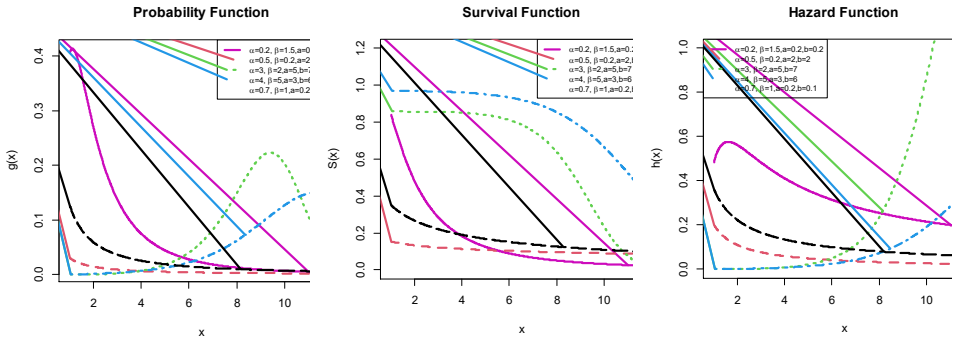

a. Plots for Density Function

b. Plots for Survival Function

Plots for Hazard Function

Figure 1. Probability density, survival, and hazard functions of the GW distribution for selected parameter values.

The quantile function plays an important role in the theoretical and practical analysis of probability distributions, as it provides an alternative and robust approach for characterizing distributional properties such as the median, mode, skewness, and kurtosis. Quantile-based measures are particularly advantageous in the presence of skewed or heavy-tailed data, where moment-based measures may be unstable or difficult to interpret. In seismological applications, quantiles are also of interest since they have been used to describe the relationship between earthquake magnitudes and geoelectric or geophysical indicators.

Using the cumulative distribution function of the Gumbel–Weibull (GW) distribution given in Eq. (6), the quantile function of the GW model is obtained by inversion and is expressed in Eq. (10) as

$$Q(u) = G^{-1}(u) = b[\beta - \alpha \ln(-lnu)]^{\frac{1}{a}}, \quad u \sim U(0,1). \tag{10}$$

The quantile function in Eq. (10) enables the direct computation of location and shape characteristics of the distribution. In particular, the median of a continuous probability distribution is defined as the point at which the cumulative

distribution function equals 0.5. By substituting u=0.5 into Eq. (10), the median of the proposed GW distribution is obtained as

$$Q(0.5) = b[\beta - \alpha \ln(-ln0.5)]^{\frac{1}{a}} \quad (11)$$

To further characterize the shape of the GW distribution, quantile-based measures of skewness and kurtosis are considered. These measures are less sensitive to extreme observations and provide robust descriptors of asymmetry and tail behavior. Bowley's skewness coefficient, based on quartiles, is defined in Eq. (12) as

$$Bowley - S = \frac{Q\left(\frac{3}{4}\right) - 2Q\left(\frac{1}{2}\right) + Q\left(\frac{1}{4}\right)}{Q\left(\frac{3}{4}\right) - Q\left(\frac{1}{4}\right)} \quad (12)$$

Similarly, Moors' kurtosis measure, which is based on octiles and captures tail thickness and peakedness, is given in Eq. (13) by

$$Moors - K = \frac{Q\left(\frac{7}{8}\right) - Q\left(\frac{5}{8}\right) + Q\left(\frac{3}{8}\right) - Q\left(\frac{1}{8}\right)}{Q\left(\frac{6}{8}\right) - Q\left(\frac{2}{8}\right)} \quad (13)$$

Here, $Q(\cdot)$denotes the quantile function defined in Eq. (10). The availability of explicit expressions for the quantile function and the associated shape measures further highlights the analytical tractability of the proposed GW distribution and facilitates its application in both theoretical studies and empirical earthquake magnitude modeling.

Table 2. Values of some moments measures for the GW distribution

a	b	α	β	Median	S	K
2	2	6	7	6,065996	-0,01045	1,298646
3	2	4	10	4,509911	0,028346	1,249883
4	3	2	9	5,298869	0,058889	1,246597
5	4	3	6	5,919786	-0,01311	1,260686
6	4	8	11	6,204824	-0,06996	1,318133
7	2	4	5	2,611173	-0,0913	1,351605
8	3	7	6	3,923882	-0,17232	1,681846
9	6	2	12	7,960153	0,064463	1,246244
10	6	5	8	7,540809	-0,06081	1,295029
1	5	3	6	5,975229	-0,03116	1,265216
12	8	2	4	9,106501	-0,03241	1,265593

Table 2 reports selected quantile-based summary measures of the Gumbel–Weibull (GW) distribution for different combinations of the model parameters. The variation in the median values across parameter settings highlights the flexibility of the GW distribution in capturing different central tendency levels. Moreover, the skewness (S) and kurtosis (K) measures exhibit noticeable changes depending on the parameter configuration, indicating that the distribution is capable of representing a wide range of asymmetry and tail behaviors.

In particular, both positive and negative skewness values are observed, suggesting that the GW distribution can accommodate left-skewed and right-skewed data structures. Similarly, the kurtosis values vary across parameter combinations, reflecting different degrees of tail heaviness and peakedness. These results illustrate that the shape of the GW distribution can be effectively controlled through its parameters, which is essential for modeling heterogeneous earthquake magnitude data characterized by varying tail behavior.

Overall, the numerical results presented in Table 2 provide further empirical support for the analytical flexibility of the proposed GW distribution and complement the theoretical properties discussed in the preceding sections.

The moments of a probability distribution play a crucial role in statistical analysis, as they provide essential information about the location, dispersion, and overall shape of the distribution. In the context of seismic risk analysis and the

identification of early warning signals for critical transitions, it has been recognized that certain statistical indicators, such as the expected value and variance, may exhibit anomalous behavior prior to catastrophic events. This phenomenon has been previously investigated using earthquake catalogs, as demonstrated by Scheffer et al. (2009).

Motivated by the integral representations and expansion techniques presented in Gradshteyn and Ryzhik (2007), the rth raw moment of the random variable Xassociated with the Gumbel–Weibull (GW) distribution can be derived from the probability density function given in Eq. (7). The rth raw moment is defined as

$$E(X^n) = \int_0^{\infty} x^n g(x) dx = \int_0^1 Q^n(u) du$$

where $Q(u)$denotes the quantile function of the GW distribution.

By substituting the explicit form of the quantile function and applying a binomial series expansion, the above expression can be rewritten as

$$\begin{aligned} E(X^n) &= b^n \beta^{\frac{n}{a}} \int_0^1 \left[1 - \frac{\alpha}{\beta} \ln(-lnu)\right]^{\frac{n}{a}} du \\ &= \sum_{k=0}^{\infty} \binom{\frac{n}{a}}{k} \left(-\frac{\alpha}{\beta}\right)^k k \int_0^1 \ln(-lnu)\, du \\ &= -\sum_{k=0}^{\infty} \binom{\frac{n}{a}}{k} \left(-\frac{\alpha}{\beta}\right)^k kC \end{aligned} \quad (14)$$

where C denotes the Euler constant, and the convergence condition $|-\alpha/\beta \ln(-lnu)| < 1$ must be satisfied.

The expression in Eq. (14) provides a general representation for the raw moments of the GW distribution and highlights its analytical tractability. Although closed-form expressions for higher-order moments may not always be available, the series representation enables numerical evaluation and facilitates the study of moment-based characteristics such as the mean and variance. This property further supports the applicability of the GW distribution in modeling complex and heterogeneous data structures, including earthquake magnitude data.

2.2. Estimation

In this section, parameter estimation for the Gumbel–Weibull (GW) distribution is carried out using the maximum likelihood estimation (MLE) method. Let $X_1, X_2, \ldots, X_n$ denote an observed random sample from the GW

distribution. Based on a complete sample, the log-likelihood function of the GW distribution, denoted by $\ln L$, is given by Eq. (12).

$$\ln L = nlna - nlnb + (a-1)\sum_{i=1}^{n}(lnx_i - lnb) - nln\alpha + \sum_{i=1}^{n}\frac{\beta-\left(\frac{x_i}{b}\right)^a}{\alpha} - \sum_{i=1}^{n} exp\left(\frac{\beta-\left(\frac{x_i}{b}\right)^a}{\alpha}\right) \quad (12)$$

The maximum likelihood estimators of the model parameters a, b, α, and β are obtained by differentiating the log-likelihood function with respect to each parameter. The corresponding score equations are derived by setting the partial derivatives of $\ln L$ equal to zero. The expressions for the partial derivatives with respect to a, b, α, and β are presented in Eq. (13).

$$\frac{\partial \ln L}{\partial a} = \frac{n}{a} + \sum_{i=1}^{n} ln\, x_i + nln\, b - \frac{1}{\alpha}\sum_{i=1}^{n}\left(\frac{x_i}{b}\right)^a ln\left(\frac{x_i}{b}\right),$$

$$\frac{\partial \ln L}{\partial b} = \frac{n-a+1}{b} + \frac{a\sum_{i=1}^{n}\left(\frac{x_i}{b}\right)^a\left(1-exp\left(\frac{\beta-\left(\frac{x_i}{b}\right)^a}{\alpha}\right)\right)}{\alpha b},$$

$$\frac{\partial \ln L}{\partial \alpha} = \frac{1}{\alpha} - \sum_{i=1}^{n}\frac{\beta-\left(\frac{x_i}{b}\right)^a}{\alpha^2}\left(1 + exp\left(\frac{\beta-\left(\frac{x_i}{b}\right)^a}{\alpha}\right)\right),$$

$$\frac{\partial \ln L}{\partial \beta} = \frac{n}{\alpha} - \frac{1}{\alpha}\sum_{i=1}^{n} exp\left(\frac{\beta-\left(\frac{x_i}{b}\right)^a}{\alpha}\right). \quad (13)$$

Due to the nonlinear structure of the resulting likelihood equations, closed-form solutions for the maximum likelihood estimators are not available. Consequently, the estimation problem is solved numerically using an iterative optimization procedure. In this study, the Nelder–Mead algorithm is employed to maximize the log-likelihood function, as it does not require gradient information and has been shown to perform reliably for complex likelihood surfaces.

The numerical optimization is implemented in the R programming environment using the AdequacyModel package. Initial parameter values are selected to ensure numerical stability and convergence of the algorithm. The

resulting estimates, denoted by $\hat{a}$, $\hat{b}$, $\hat{\alpha}$, and $\hat{\beta}$, correspond to the parameter values that maximize the log-likelihood function of the GW distribution.

The MLE framework adopted here provides a consistent and efficient approach for parameter estimation and forms the basis for subsequent inferential procedures and empirical applications of the proposed GW distribution.

3. Study Area

In this section, two comprehensive earthquake catalogs from Turkey are utilized to evaluate the performance of the proposed Gumbel–Weibull (GW) distribution in seismic risk analysis. Turkey represents a highly suitable study region due to its complex tectonic setting and frequent seismic activity, resulting from the interaction of the Anatolian, Eurasian, African, and Arabian plates.

Turkey is geographically located between latitudes 36°–42°N and longitudes 26°–45°E and is among the most seismically active countries in the Mediterranean–Alpine–Himalayan seismic belt. The country hosts several major active fault systems, including the North Anatolian Fault Zone, the East Anatolian Fault Zone, and the Aegean extensional fault system. The spatial distribution of active faults is illustrated in Figure 3, highlighting the structural complexity and seismic heterogeneity of the region.

The Catalog: To perform the seismic risk analysis, earthquake events with magnitude values $M \geq 4.5$ recorded between 17 August 1999 and 30 April 2023 are considered. The earthquake data are obtained from the catalog of the Boğaziçi University Kandilli Observatory which provides one of the most reliable and widely used seismic datasets for Turkey. The catalog is publicly accessible at http://www.koeri.boun.edu.tr/scripts/istot.asp.

The catalog was intentionally analyzed over a fixed observation window (17 August 1999–30 April 2023) to ensure a stable and consistently processed dataset for methodological model development and comparison. The objective of the study is not real-time forecasting, but rather the evaluation of a flexible probabilistic framework under a clearly defined empirical setting.

In this study, for each seismic event, the maximum reported magnitude value among different magnitude types (e.g., M_D: duration magnitude, M_L: local magnitude, M_W: moment magnitude, M_S: surface-wave magnitude, and M_B: body-wave magnitude) is used. This approach ensures consistency in representing the largest seismic impact associated with each earthquake event and reduces potential bias arising from magnitude-type discrepancies.

The spatial distribution of earthquake epicenters across Turkey for the selected dataset is presented in Figure 2 that uses a broader catalog for visualization. The map illustrates the widespread seismic activity across the

country, with dense clustering observed along major fault zones. This spatial heterogeneity further motivates the need for flexible probabilistic models capable of capturing diverse magnitude behaviors, particularly in regions characterized by varying tectonic regimes.

By combining a long-term and spatially extensive earthquake catalog with a flexible statistical modeling framework, the present study aims to provide a comprehensive assessment of the GW distribution's suitability for modeling earthquake magnitudes in Turkey.

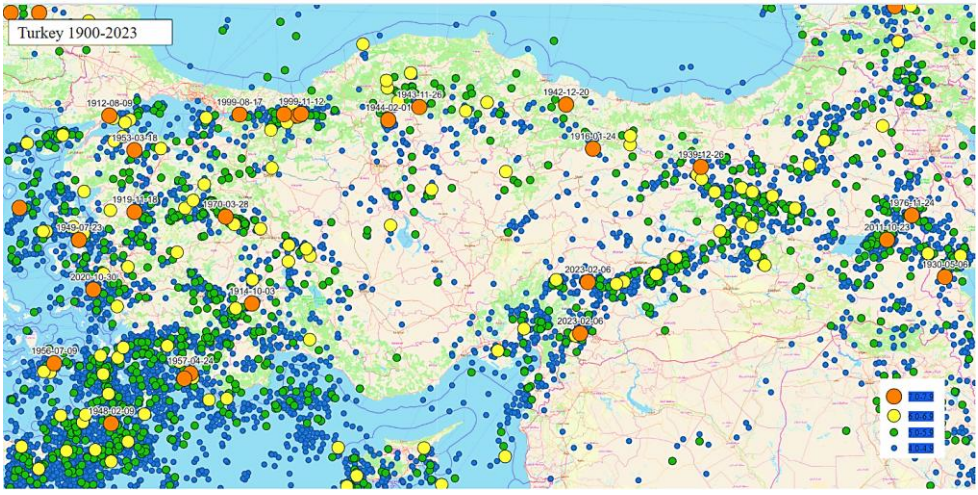

Figure 2. Epicenter map of earthquakes in Turkey between years 1900 and 2023.

The active fault map of Turkey is given in Figure 3. According to the active fault map of Turkey, the North Anatolian Fault (NAF) and East Anatolian Fault (EAF), as well as the Eastern Anatolia, Marmara and Aegean regions are the highest earthquake risk areas in Turkey.

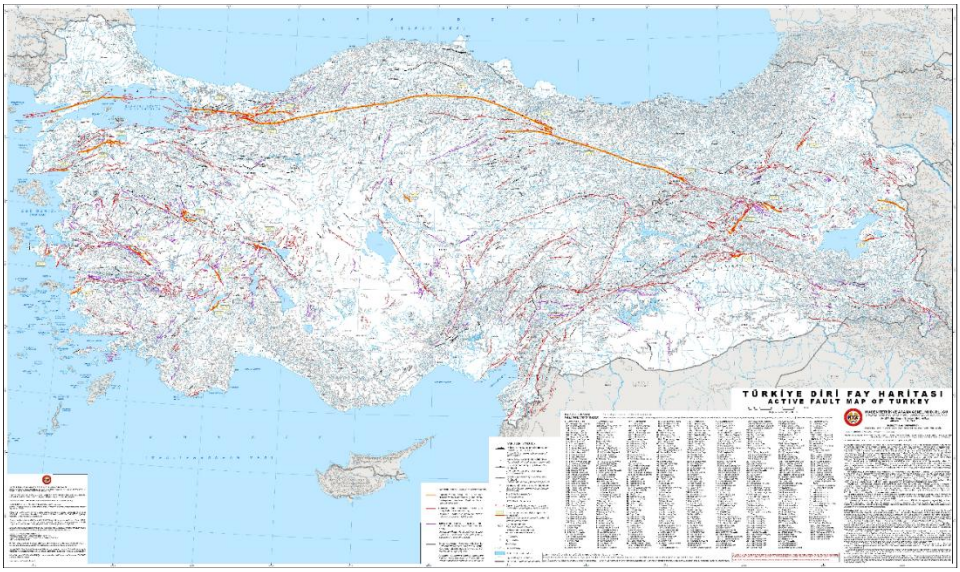

Figure 3. The active fault map of Turkey (Emre et al., 2013)

4. Results

In this section, a descriptive statistical analysis of earthquake magnitudes in Turkey is presented to provide an empirical overview of the data structure prior to model fitting. Understanding the basic distributional characteristics of the magnitude data is essential for motivating the use of flexible probabilistic models in seismic risk analysis. Summary statistics for earthquakes with magnitudes greater than 4.5 during the period from 17 August 1999 to 30 April 2023 are reported in Table 2.

As shown in Table 3, the dataset consists of 503 earthquake events, with magnitudes ranging from 4.5 to 7.7. The mean magnitude is 4.9, while the median is slightly lower at 4.8, indicating a concentration of events near the lower bound of the selected magnitude threshold. The mode equal to 4.5 further confirms that a substantial proportion of earthquakes occur at or just above the threshold magnitude.

The skewness value of 2.15051 indicates a pronounced right-skewed distribution, reflecting the presence of relatively few but significantly larger magnitude events. This asymmetry is further supported by the high kurtosis value of 6.3945, which suggests a heavy-tailed distribution with a higher probability of extreme values compared to a normal distribution. Such characteristics are commonly observed in earthquake magnitude data and pose challenges for classical symmetric or light-tailed models.

The standard deviation of 0.49531 reflects moderate dispersion around the central tendency; however, the combination of right skewness and high kurtosis highlights the heterogeneity of the magnitude distribution. These findings suggest that while most earthquake events cluster around moderate magnitudes, the tail behavior associated with larger earthquakes plays a critical role in the overall risk structure.

Overall, the descriptive results presented in Table 3 provide clear empirical evidence that earthquake magnitudes in Turkey exhibit asymmetry, heavy-tailed behavior, and concentration near lower magnitude levels. These features strongly motivate the use of flexible distributional models, such as the proposed Gumbel–Weibull distribution, that are capable of accommodating skewness and tail variability within a unified probabilistic framework. In the following section, the performance of the GW model is evaluated and compared with alternative distributions using goodness-of-fit criteria.

Table 3. Summary statistics of earthquakes greater than 4.5 magnitudes (Mw) in Turkey for the period of 17.08.1999 to 30.04.2023

N	503	**Variance**	0.24533
Min.	4.5	**St. Deviation**	0.49531
Max.	7.7	**Skewness**	2.15051
Mean	4.9	**Std. Error of Skewness**	0.109
Median	4.8	**Kurtosis**	6.3945
Mode	4.5	**Std. Error of Kurtosis**	0.217

The average earthquake magnitude in the dataset is 4.9, indicating that most events cluster around moderate magnitude levels. However, the skewness and kurtosis values reported in Table 3 clearly show that the magnitude distribution is neither symmetric nor light-tailed. The pronounced positive skewness reflects the presence of relatively few but substantially larger earthquakes, while the high kurtosis indicates a heavy-tailed distribution with an elevated probability of extreme values.

The histogram of earthquake magnitudes greater than 4.5, presented in Figure 4, provides a visual confirmation of these distributional characteristics. A strong concentration of events is observed near the lower bound of the magnitude threshold, particularly around magnitude 4.5, followed by a rapidly decreasing frequency as magnitude increases. At the same time, the presence of a long right tail extending toward higher magnitudes highlights the importance of accurately modeling extreme events.

The standard deviation reflects moderate dispersion around the central tendency; however, the combined evidence from skewness, kurtosis, and the histogram indicates substantial heterogeneity in the magnitude distribution. Such

features pose challenges for classical symmetric or light-tailed probability distributions and underscore the need for flexible models capable of capturing both central clustering and tail behavior.

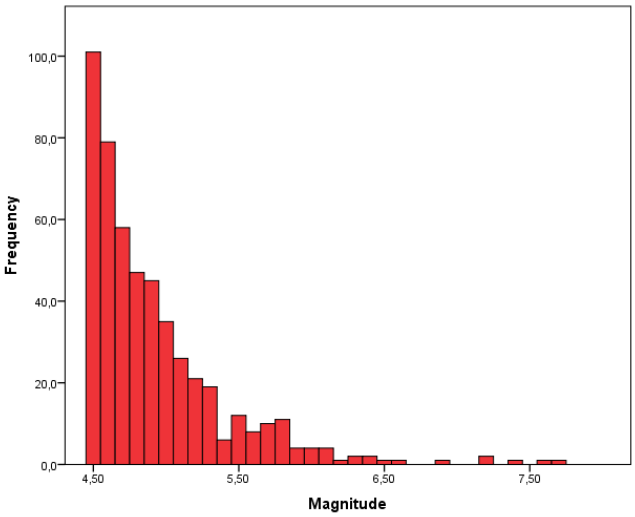

Figure 4. Histogram of earthquake data with magnitude greater than 4.5 in Turkey for the period of 17.08.1999 to 30.04.2023.

When modeling earthquake magnitude data, probability distributions are commonly employed to describe the underlying statistical structure. The suitability of a given distribution depends critically on its ability to accommodate skewness and heavy tails, as observed in the present dataset. These empirical characteristics motivate the use of advanced distributional models and fitting techniques to identify the best-performing distribution for earthquake magnitude modeling. In the following subsection, the proposed Gumbel–Weibull distribution is fitted to the data and its performance is systematically compared with alternative models using formal goodness-of-fit criteria.

To gauge the success of these models and facilitate an informed choice among competing distributions, we employed several statistical measures, namely the Akaike Information Criterion (AIC), Bayesian Information Criterion (BIC), Consistent Akaike Information Criterion (CAIC), and Hannan-Quinn Information Criterion (HQIC). These criteria serve as invaluable tools in model selection and comparison by balancing the goodness of fit against the complexity of the models. By considering these metrics collectively, we aimed to identify the most suitable probability distribution for characterizing the earthquake data. Our approach integrates both established models from the literature and a novel distribution, providing a comprehensive framework for evaluating and selecting

the most appropriate model for earthquake data analysis. This methodological synthesis, grounded in statistical rigor, enhances our understanding of the underlying distributional patterns and contributes to the broader field of seismic risk modeling.

Table 4. MLEs and the values of AIC, CAIC, BIC and HQIC statistics

Distribution	MLE	Errors	AIC	CAIC	BIC	HQIC
GW	0.0197 1.68541 0.21064 0.39479	0.0008 0.0530 0.0049 0.0382	3259.709	3259.718	3285.601	3268.804
Exp	4.45782	0.0411	58686.43	58686.43	58693.81	58688.91
Weibull	7.41667 4.68610	0.0422 0.0062	21048.47	21048.47	21063.22	21053.42
Log-normal (2p)	1.48951 0.09943	0.0009 0.0006	14115	14115	14129.75	14119.95
Rayleigh	3.17025	0.0146	42772.11	42772.11	42779.48	42774.59
Frechet	0.90585	0.0068	75232.89	75232.89	75240.26	75235.37
Gumbel	0.30714 4.26044	0.0023 0.0029	10879.6	10879.6	10894.35	10884.55

Table 4 presents the maximum likelihood estimates (MLEs) of the model parameters along with several widely used information criteria, namely the Akaike Information Criterion (AIC), Consistent Akaike Information Criterion (CAIC), Bayesian Information Criterion (BIC), and Hannan–Quinn Information Criterion (HQIC), for the proposed Gumbel–Weibull (GW) distribution and a set of competing classical models.

Among all considered distributions, the GW model yields the lowest values of AIC, CAIC, BIC, and HQIC, indicating a superior balance between goodness of fit and model complexity. This result suggests that the GW distribution provides the most adequate statistical representation of the earthquake magnitude data compared to the alternative models examined, including exponential, Weibull, log-normal, Rayleigh, Fréchet, and Gumbel distributions. The consistently smaller information criterion values obtained for the GW model demonstrate its ability to capture both the central clustering of moderate-magnitude earthquakes and the heavy-tailed behavior associated with larger events. In contrast, classical distributions either lack sufficient flexibility to model tail behavior or exhibit poorer overall fit when model complexity is taken into account.

Overall, the results summarized in Table 4 provide strong empirical evidence supporting the effectiveness of the proposed GW distribution for earthquake

magnitude modeling in Turkey. The systematic improvement observed across multiple information criteria underscores the robustness of the GW model and highlights its potential as a reliable alternative to conventional probability distributions in seismic risk analysis.

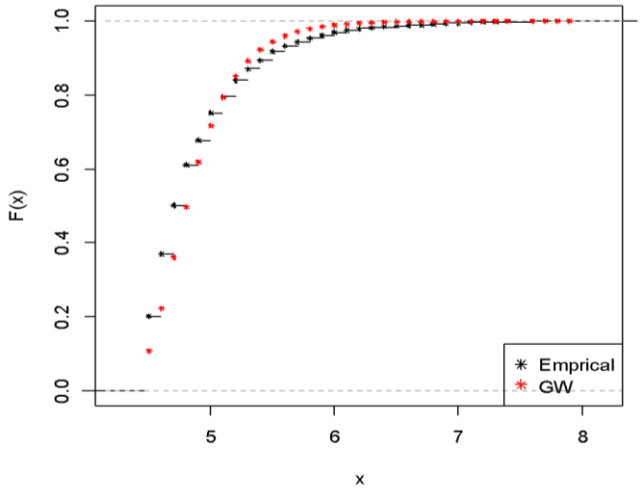

Figure 5. Empirical and theoretical CDF curves for the earthquake magnitude data and the fitted GW distribution.

Figure 5 compares the empirical cumulative distribution function (CDF) of earthquake magnitudes with the theoretical CDF obtained from the fitted Gumbel–Weibull (GW) distribution. The close agreement between the empirical points and the fitted GW curve indicates that the proposed model adequately captures the overall distributional structure of the data across the observed magnitude range. In particular, the alignment observed in the upper tail region suggests that the GW distribution is capable of representing the probabilistic behavior of larger and less frequent earthquakes.

Beyond goodness-of-fit considerations, the hazard function derived from the GW model provides additional insight into the magnitude-dependent dynamics of seismic risk. In this context, the hazard rate represents the instantaneous conditional likelihood of observing an earthquake of a given magnitude, assuming that no larger-magnitude event has occurred. This interpretation allows the assessment of how seismic risk evolves across different magnitude levels.

Table 5. Hazard rates for some magnitudes

Magnitude	4.5	5	5.5	6	6.5	7	7.5	8
Hazard Rate	1.0668	3.0750	3.2879	3.1419	2.9626	2.7968	2.6491	2.5197

Table 5 reports the estimated hazard rates for selected earthquake magnitudes. The results indicate that the hazard rate varies with magnitude, reflecting non-uniform risk dynamics across the magnitude spectrum. For example, the hazard rate increases from magnitude 4.5 to 5.5 and subsequently exhibits a gradual decrease for larger magnitudes. This non-monotonic pattern suggests that the risk associated with earthquake occurrence does not increase uniformly with magnitude but instead depends on the underlying distributional structure captured by the GW model.

Overall, the combined evidence from the empirical-theoretical CDF comparison in Figure 5 and the magnitude-specific hazard rates in Table 5demonstrates that the GW distribution not only provides a good statistical fit to the earthquake magnitude data but also yields interpretable hazard-based measures that are relevant for seismic risk assessment.

An important practical outcome of probabilistic earthquake magnitude modeling is the estimation of return periods, which quantify the expected time interval between earthquakes exceeding a given magnitude threshold. In this study, return periods are derived directly from the fitted **Gumbel–Weibull (GW)** distribution, which was identified as the best-performing model based on information criteria.

Let $F(m)$denote the cumulative distribution function of the GW distribution. The probability that an earthquake has a magnitude equal to or greater than a specified level $m$is given by the exceedance probability

$$P(M \geq m) = 1 - F(m).$$

Assuming that earthquake occurrences follow a stationary Poisson process, the return period $T(m)$associated with magnitude $m$or greater can be expressed as

$$T(m) = \frac{1}{\lambda\, P(M \geq m)},$$

where λrepresents the mean annual rate of earthquake occurrences above the minimum magnitude threshold.

In the present study, a total of 503 earthquakes with magnitudes $M \geq 4.5$were recorded between 17 August 1999 and 30 April 2023, corresponding to an observation period of approximately 23.70 years. Accordingly, the annual occurrence rate is estimated as

$$\lambda = \frac{503}{23.70} \approx 21.22 \text{ events per year.}$$

Table 6. Exceedance probabilities and return periods for selected earthquake magnitudes based on the GW distribution

Magnitude (m)	**Exceedance Probability P(M ≥ m)**	**Return Period T(m) (years)**
5.0	0.283204	0.166
5.5	0.055824	0.844
6.0	0.011132	4.233
6.5	0.002419	19.483
7.0	0.000573	82.217

Using the GW distribution with parameters estimated via maximum likelihood, exceedance probabilities and corresponding return periods were computed for selected magnitude levels. The results indicate a rapid increase in return periods with increasing magnitude. For example, earthquakes with magnitude $m = 5.0$are associated with relatively short return periods, while the expected waiting time increases substantially for larger magnitudes. In particular, the return period is estimated to be less than one year for magnitudes around 5.5, increases to several years for magnitudes near 6.0, and exceeds several decades for magnitudes greater than 6.5. For very large magnitudes, such as $m \geq 7.5$, the estimated return periods extend to several years.

These findings demonstrate that the GW-based framework provides not only an improved statistical fit to earthquake magnitude data but also yields interpretable and practically relevant risk measures. Compared to classical frequency–magnitude approaches based on the Gutenberg–Richter relationship, the proposed distribution-based method explicitly accounts for skewness and tail behavior in the data, offering a flexible and data-driven alternative for return period estimation in seismic risk analysis.

5. Discussion

This study introduced a flexible probabilistic framework for modeling earthquake magnitudes based on the Gumbel–Weibull (GW) distribution, constructed as a special member of the broader Gumbel–G family. The motivation for this approach arises from the well-documented limitations of classical magnitude distributions in capturing the asymmetric and heavy-tailed structure of earthquake data, particularly in tectonically complex regions such as Turkey. Rather than aiming to predict earthquake occurrence in a temporal or deterministic sense, the proposed framework focuses on improving the statistical representation of earthquake magnitude distributions and associated risk measures.

Empirical analyses conducted using Turkish earthquake data from 1999 to 2023 revealed pronounced right skewness, high kurtosis, and strong tail behavior, indicating substantial departures from symmetry and light-tailed assumptions. These characteristics were consistently reflected in descriptive statistics, graphical diagnostics, and hazard-based measures. Such features pose significant challenges for traditional distributions, including exponential, Gumbel, and Weibull models, which often lack sufficient flexibility to simultaneously capture central clustering and extreme events.

Model fitting and comparative analyses based on multiple information criteria (AIC, CAIC, BIC, and HQIC) demonstrated that the GW distribution consistently outperformed competing models considered in this study. This superiority highlights the ability of the Gumbel-based generator mechanism to enhance tail modeling while maintaining analytical tractability and interpretability. The results suggest that embedding classical distributions within a generator-based framework can substantially improve goodness of fit without resorting to overly complex or opaque model structures.

Beyond overall fit, hazard and return period analyses provided additional insight into magnitude-dependent seismic risk. The estimated hazard functions exhibited non-monotonic behavior, indicating that the likelihood structure of earthquake magnitudes cannot be adequately described by simple monotonic assumptions. Furthermore, return period estimates derived from the GW distribution suggest that moderate-magnitude earthquakes (approximately 5.0–5.5) occur relatively frequently, whereas larger events (magnitude ≥ 6.5) are associated with substantially longer waiting times. These findings underscore the importance of explicitly modeling tail behavior when assessing seismic risk and interpreting the potential impact of rare but highly destructive earthquakes.

From a broader perspective, the proposed framework should be viewed as a complementary statistical approach rather than a replacement for physics-based

seismic models. Although the GW distribution does not explicitly incorporate fault mechanics or rupture processes, it provides a statistically coherent tool for evaluating the probability structure of large earthquakes. In contrast to physically based models—which may be complex, computationally demanding, and difficult to calibrate at large scales—the proposed statistical framework is particularly well suited for analyzing extensive earthquake catalogs and identifying general distributional patterns.

Several limitations should also be acknowledged. The analysis assumes time-independent earthquake magnitudes, consistent with standard probabilistic seismic hazard analysis practices, but does not account for temporal dependence or clustering effects. Moreover, potential inconsistencies across earthquake catalogs may influence parameter estimation, highlighting the importance of cross-validation and sensitivity analyses. Finally, while maximum likelihood estimation performed well in this study, alternative estimation or optimization methods may be explored in future work to address potential numerical challenges.

In addition, the empirical application is based on a fixed; therefore, the reported parameter estimates and return-period values should be interpreted as estimates conditional on the analyzed observation window. Updating the catalog with newly recorded events may refine the estimates, and this constitutes a natural direction for future validation.

6. Conclusion

In this study, a new probabilistic modeling framework based on the Gumbel–Weibull distribution was proposed and applied to earthquake magnitude data from Turkey. By introducing the Gumbel–G family and focusing on the Gumbel–Weibull distribution as one of its key members, the study provided a systematic and extensible approach for enhancing classical magnitude models.

Comprehensive empirical results demonstrated that earthquake magnitudes in Turkey exhibit strong asymmetry, heavy-tailed behavior, and concentration near lower magnitude thresholds. The proposed GW model successfully captured these characteristics and consistently outperformed several widely used distributions according to multiple information-based criteria. The availability of closed-form expressions for key distributional functions further supports the analytical convenience and practical applicability of the model.

The hazard and return period analyses illustrated the potential of the proposed framework to generate interpretable and decision-relevant risk measures. By providing improved estimates of exceedance probabilities and return periods, the GW distribution may contribute to probabilistic seismic hazard analysis, seismic risk mapping, and engineering-oriented risk assessments. In this sense, the

proposed model offers a flexible statistical tool that can complement existing methodologies used by earthquake engineers and risk analysts.

Future research may extend this framework in several directions. Other members of the Gumbel–G family may be explored to assess their suitability for different seismic settings or magnitude ranges. Incorporating spatial or temporal dependence structures, such as fault-based classification or time-dependent seismicity models, may further enhance the realism of the approach. Additionally, hybrid frameworks that combine the statistical flexibility of generator-based distributions with physically motivated constraints represent a promising avenue for future investigation.

Beyond its seismological application, the proposed Gumbel–G framework offers a general methodological contribution to distributional modeling in science and mathematics. In particular, its generator-based construction may be adapted to other domains characterized by skewness, tail heterogeneity, and non-standard hazard structures, such as reliability, environmental extremes, and risk analysis. The proposed framework is readily updateable and can be re-estimated as new earthquake records become available, enabling periodic reassessment of magnitude distributions and risk measures.

7. References

Afet ve Acil Durum Yönetimi Başkanlığı (AFAD). (2023). 06 Şubat 2023 Kahramanmaraş (Pazarcık ve Elbistan) depremleri arazi çalışmaları ön değerlendirme raporu (Sürüm 1, revize). Ankara, Türkiye: Author.

Al-Abbasi, J. N., & Fahmi, K. J. (1985). Estimating maximum magnitude earthquakes in Iraq using extreme value statistics. Geophysical Journal International, 82(3), 535–548.

Al-Abbasi, J. N., & Fahmi, K. J. (1991). GEMPAK: A FORTRAN-77 program for calculating Gumbel's first, third, and mixture upper earthquake magnitude distributions employing maximum likelihood estimation. Computers & Geosciences, 17(2), 271–290.

Alzaatreh, A., Lee, C., & Famoye, F. (2013). A new method for generating families of continuous distributions. Metron, 71(1), 63–79.

Bhattacharya, P., & Bhattacharjee, R. (2009). A study on Weibull distribution for estimating the parameters. Wind Engineering, 33(5), 469–476.

Burton, P. W. (1979). Seismic risk in southern Europe through to India examined using Gumbel's third distribution of extreme values. Geophysical Journal of the Royal Astronomical Society, 59(2), 249–280.

Emre, Ö., Duman, T. Y., Özalp, S., Elmacı, H., Olgun, Ş., & Şaroğlu, F. (2013). Active fault map of Turkey with explanatory text (Special Publication Series No. 30, 1:1,250,000 scale). Ankara, Turkey: General Directorate of Mineral Research and Exploration (MTA).

Firuzan, E. (2008). Statistical earthquake frequency analysis for Western Anatolia. Turkish Journal of Earth Sciences, 17(4), 741–762.

Gradshteyn, I. S., & Ryzhik, I. M. (2007). Table of integrals, series, and products (7th ed.). Amsterdam, Netherlands: Academic Press.

Gumbel, E. J. (1958). Statistics of extremes. New York, NY: Columbia University Press.

Hagiwara, Y. (1974). Probability of earthquake occurrence as obtained from a Weibull distribution analysis of crustal strain. Tectonophysics, 23(3), 313–318.

Kagan, Y. Y. (2010). Statistical distributions of earthquake numbers: Consequence of branching process. Geophysical Journal International, 180(3), 1313–1328.

Kartal, R. F., Kadirioğlu, F. T., & Zünbül, S. (2015, October). Kinematics of the North Anatolian Fault Zone [Conference presentation]. 19th Active Tectonics Research Group Conference.

Kijko, A. (1984). Is it necessary to construct empirical distributions of maximum earthquake magnitudes? Bulletin of the Seismological Society of America, 74(1), 339–347.

Kijko, A. (2002, September 9–13). Statistical estimation of maximum regional earthquake magnitude mmax (Paper Ref. FW: 022). In Proceedings of the 12th European Conference on Earthquake Engineering. London, England: Elsevier Science Ltd.

Lomnitz, C. (1966). Statistical prediction of earthquakes. Reviews of Geophysics, 4(3), 377–393.

Makjanić, B. (1972). A contribution to the statistical analysis of Zagreb earthquakes in the period 1869–1968. Pure and Applied Geophysics, 95, 80–88.

Yegulalp, T. M., & Kuo, J. T. (1974). Statistical prediction of the occurrence of maximum magnitude earthquakes. Bulletin of the Seismological Society of America, 64(2), 393–414.

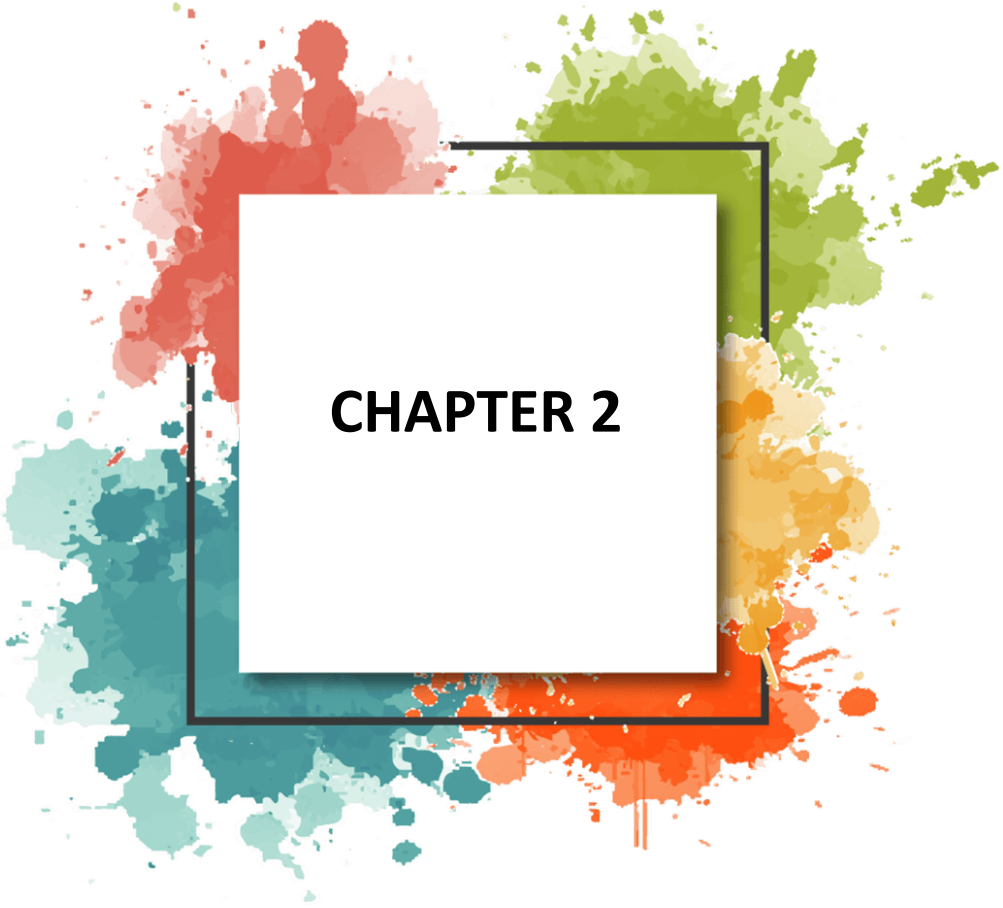
CHAPTER 2

Mammal Fauna of Edirne Province

Beytullah Özkan[1] & Serbülent Paksuz[2]

1. INTRODUCTION

Approximately 6,500 mammal species live in the world. There are 26-29 orders of mammals in the world. Of these, 10 orders are extinct, and 16 orders are alive today. Currently, 25% of mammals are under various threats such as environmental and human impact. In Turkey, only placental mammals live.

Located in the Palearctic zoogeographic region, Turkey, due to its geographical location, shows a much richer variety of mammal species compared to European countries. Turkey also includes the distribution areas of mammals of European, Asian, and African origin (Walker et al., 1975; Corbet, 1978; Wilson and Reeder, 1993; Yiğit et al., Mitchell-Jones et al. 1999; 2006; https://www.tramem.org/memeliler, 2026; https://www.tramem.org/memeliler, 2026).

Approximately 171 mammal species belonging to 7 orders (1- Eulipothyla (Insectivora) (3 families, 22 species), 2- Chiroptera (6 families, 43 species), 3- Lagomorpha (1 family, 2 species), 4- Rodentia (9 families, 69 species), 5- Carnivora (7 families, 20 species), 6- Artiodactyla (3 families, 9 species), 7- Cetacea (5 families, 12 species) live in Turkey (Sözen and Çolak, 2025) (Table 1).

Approximately 73% of the species that make up the mammal fauna of Turkey are small mammals (Eulipothyla, Chiroptera, Rodentia and Lagomorpha), and approximately 27% are large mammals (Carnivora, Artiodactyla and Cetacea) (Kumerloeve, 1975; Corbet, 1978; Kurtonur et al., 1996; Mitchell-Jones et al. 1999; Yiğit et al., 2006; Sözen and Çolak, 2025; https://www.tramem.org/memeliler, 2026), (Table 1)

[1] Assoc. Prof., Trakya University, Faculty of Science, Department of Biology, Balkan Campus 22030 Edirne, ORCID: 0000-0003-0050-7031

[2] Assist. Prof., Trakya University, Faculty of Education, Department of Primary Education, İsmail Hakkı Tonguç Campus 22030 Edirne, ORCID: 0000-0002-2645-9843

Table 1. Mammals living in Turkey (order, family and species).

Order	Family	Species
1 - EULIPOTYPHLA (Insectivores)	3	22
2 - CHIROPTERA (Bats)	6	43
3 - LAGOMORPHA (Hares)	1	2
4 - RODENTIA (Rodents)	9	69
5 - CARNIVORA (Carnivores)	7	20
6 - ARTIODACYLA (Even-Toaed Ungulates)	3	9
7 – CETACEA (Whales and Dolphins)	5	12
Total 7	29	177

There are 13 species endemic to Turkey, and 12 species are regionally endemic or have a very large distribution in Turkey. *Oryctolagus cuniculus*, *Rattus rattus, R. norvegicus*, and *Myocastor coypus* are four species that were introduced to Turkey later (Mursaloğlu, 1973; Lowe et al., 2000; Kryštufek and Vohralík, 2001). The European squirrel (*Sciurus vulgaris*) populations in Eastern Anatolia are also human-induced (Mursaloğlu, 1973). Additionally, there are 10 domesticated mammal species in Turkey (Corbet, 1978; Sözen and Çolak, 2025).

The mammals in Turkey are native species. They do not undergo seasonal migration. Of the mammal species in Turkey, 28 are endangered, 8 are endemic, 1 is an invasive species introduced by humans (e.g., *Myocastor coypus*), 5 are harmful, and 3 are extinct (Lowe et al., 2000; Sözen and Çolak, 2025).

Some mammal species living in Turkey are threatened on a global or regional scale. Due to factors such as habitat degradation, rapid population growth, pollution, and hunting, some mammal species have reached the point of extinction. Some of the important threatened mammals in Turkey include the Anatolian leopard (*Panthera pardus tulliana*), striped hyena (*Hyaena hyaena*), Anatolian wild sheep (*Ovis orientalis*), red deer (*Cervus elaphus*), fallow deer (*Dama dama*), roe deer (Capreolus capreolus), Hatay mountain gazelle (*Gazella gazella*), hooked-horned mountain goat (Rupicapra rupicabra), wolf (*Canis lupus*), brown bear (*Ursus arctos*), otter (*Lutra lutra*), wild cat (Felis silvestris), lynx (Lynx lynx), caracal (*Lynx caracal*), swamp cat (*Felis chaus*), Mediterranean monk seal (*Monachus monachus*), Anatolian ground squirrel (*Spermophilus xanthophrymnus*), and Euphrates hares (*Allactaga euphratica*) (Can, 2004; Corbet, 1978; 2004; Sözen and Çolak, 2025) are included.

Equus onager, Elephas maximus, and *Bos primigenius* were found in Turkey before the modern period but later became extinct (Kumerloeve, 1975). Castor fiber, Acinonyx jubatus, Panthera leo, and Dama mesopotamica became extinct in Turkey in the 19th century; *Panthera tigris* became extinct in the 1980s (Corbet, 1978; Can, 2004; Sözen and Çolak, 2025).

The Turkish Thrace region, located in the European part of Turkey, covers an area of 23,500 km². It is surrounded by the sea on three sides (Aegean, Marmara, and Black Seas) and bordered by Bulgaria and Greece on the land. Thrace, a relatively low-lying region, has its highest point at Mahya Mountain (1,035 m). The average altitude of the Thrace region is around 180 m. The highlands of Thrace are formed by the Yıldız Mountains (Istranca) in the north, the Ganos and Koru Mountains in the south, and the hills around the Saros Bay. The Ergene and lower Meriç basins are located in the middle of these areas, and these areas have an anthropogenic steppe character (Dönmez, 1968).

With a surface area of 6,276 km2 and an elevation of 41 m above sea level, Edirne province is located in the west of the Thracian Peninsula in the Marmara Region. It is surrounded by Kırklareli and Tekirdağ provinces to the east, Greece to the west, Bulgaria to the north, and Çanakkale province to the south. The Istranca Mountains in the north, the anthropogenic steppe-character Ergene Basin in the central part, and the mountains and plateaus and the Meriç Delta in the south constitute the surface features of the province. Its highest point is Yerlisu Hill (726 meters). 61% of Edirne province consists of agricultural land, 18% of forest, 9% of meadows and pastures, and 12% of non-agricultural land. Certain sections of the Meriç, Tunca, Arda, and Ergene Rivers are within the province's borders. The Meriç River forms a natural border with Greece (Dönmez, 1968) (Figure 1).

Figure 1. Map of Turkish Thrace and Edirne province.

Edirne and its surroundings have a continental climate. Summers are hot and dry, and winters are very cold and harsh. Located in the Marmara and Meriç Basins, Edirne Province falls into the semi-humid climate type according to general humidity indices. In the south of the province, in the Enez district and along the coastline in the Saroz Bay of the Aegean Sea, a Mediterranean climate prevails, with hot and dry summers and mild and rainy winters. The Northern Lalapaşa Forests and Koru Mountains, which have the healthiest oak forests within Edirne province, provide habitat, feeding, and breeding grounds for vertebrate and invertebrate animals. Edirne province also has scattered groves, maquis, heathlands, and pine plantations. Due to deforestation (anthropogenic), agricultural areas and pastures have developed in the open spaces. The following trees are found in the forests: hairy oak (*Quercus cerris*), gall oak (*Q. infectoria*), Hungarian oak (*Q. frainetto*), Istranca oak (*Q. hartwissiana*), sessile oak (*Q. petraea*), hornbeam (*Carpinus betulus*), maple (*Acer campestre*), hazelnut (*Coryllus avellana*), dogwood (*Cornus mas*), plum (Prunus sp.), wild pear (*Pyrus elaeagrifolia*), rosehip (Rosa canina), peony (*Paeonia tenuifolia*), and mullein (*Clematis integrifolia*) (Anonymous, 2015a).

2. METHOD

In the identification of mammals in Edirne province, information obtained from various studies, sources, and interviews with local people was combined and used. Live traps were used to capture small mammals, and camera traps were used for medium and large mammals. For flying mammals, bats, an ultrasonic bioacoustic recorder (Widlife Song Meter SM4BAT FS Bioaccustics Recorder) and a bat hand detector (Magenda Bat5) were used at night. If there were caves near each study area, the caves were visited, and perching bats were observed without disturbing them, and species identifications were made. In the field studies, mammal specimens caught with live traps were identified, their characteristics were recorded, GPS records were taken, photographs were taken along with their habitats, and the examined specimens were released back into the area where they were caught. In addition, videos and photographs of mammals were taken with a camera during the field studies, and the study area was photographed. Medium and large mammals were searched for in these areas using binoculars. All types of traces in the study areas (feces, hair, dead animals, skin and bone remains, pellets, footprints, gnawed plants and seeds, nests, etc.) were investigated, and the information obtained was evaluated taking into account the biotope characteristics of the region. In addition, surveys were conducted with the local people, and the accuracy of the information obtained was investigated and evaluated in the study (Figure 2).

Figure 2. Devices and equipment used during fieldwork.

Fieldwork was conducted in the relevant localities using appropriate research methods for each mammal group without harming any living organisms. As a result of all these studies, the mammal species identified from each locality/research area are listed and presented in a table. The Turkish and Latin names of the listed mammal species are written in the table, and their international (IUCN, BERN, CITES) and national conservation status (OSB, MAKK) is indicated. In addition, whether the species are endemic, the number of individuals, density, reproduction, and monitoring indicators were also evaluated (Table 3).

3. RESULTS

According to various scientific studies conducted to date, approximately 171 mammal species live in Turkey. 70 (41%) live in Thrace, and 62 (36%) live within the borders of Edirne province (Tables 1, 2, 3).

As a result of various studies conducted in and around Edirne province to date, the mammals currently living within the borders of Edirne province have been identified and their distributions have been examined. As a result of these studies, a total of 62 mammal species were identified within the borders of Edirne province, including 61 terrestrial and 1 marine species (dolphin – Turciops truncatus), belonging to 7 orders, 19 families and 39 genera. Among the mammals, bats (Chiroptera) are found with 24 species (24%) (38.7%), rodents (Rodentia) with 18 species (17.8%), carnivores (Carnivora) with 11 species (17.8%), insectivores (Eulipotyphla) with 4 species (6.5%), even-toed ungulates (Artiodactyla) with 3 species (4.8%), rabbits (Lagomorpha) with 1 species each

(1.6%), and whales and dolphins (Cetacea) with 1.6% each (Çağlar, 1965; Spitzenberger, 1968; Kurtonur, 1972). 1975, 1982, 1992; Mursaloğlu, 1973; Doğramacı, 1974; Corbet, 1978; Kıvanç, 1988; Albayrak, 1988, 1999; Kurtonur and Özkan, 1990, 1991, 1992; Doğramacı and Tez, 1991; Gosling and Baker, 1991; Kurtonur et al., 1994; Özkan and Kurtonur, 1994; Özkan, 1987, 1995, 1999a, 1999b, 2006a, 2006b; 2018, 2019a, 2019b, 2024, 2026; Simson et al., 1995; Civitelli et al., 1995; Filippucci et al., 1995; Krystufek et al., 1997; Öztürk, 1998; Benda and Horacek, 1998; Özkan, and Kurtonur, 1994; Çolak et al., 2000; Niermann et al., 2001; Kryštufek and Vohralik, 2001; Yiğit et al., 2003; Özkan et al., 2003; Krystufek et al., 2004; Krystufek and Vohralik, 2005; Çolak, Çolak and Yiğit, 2005; Kryštufek and Vohralik, 2009; Krystufek et al., 2009a; Krystufek et al., 2009b; Doğan, 2010; Paksuz and Özkan, 2011; Gruychev, 2012, 2017; Milchev and Gorgiev, 2012; Özkan and Paksuz, 2015; Anonymous, 2015a; Anonymous, 2015b; Anonymous, 2016; Chloë and Legakis, 2016; Nedyakov et al., 2018; Anonymous, 2023; Sözen and Çolak, 2025), (Tables 1, 2, 3). The orders, families, genera, and species of mammals currently living in Edirne province are shown in Tables 1, 2, and 3, along with their international and national criteria in Table 3, and the species distribution of the orders is shown in Figure 3.

Table 2. Mammals of Edirne province and their orders, families, genus, species and percentages.

MAMMALIA				
Order	Family	Genus	Species	%
1 - EULIPOTYPHLA (Insectivores)	3	3	4	6,5
2 - CHIROPTERA (Bats)	3	9	24	38,7
3 - LAGOMORPHA (Hares)	1	1	1	1,6
4 - RODENTIA (Rodents)	6	14	18	29
5 - CARNIVORA (Carnivores)	3	8	11	17,8
6 - ARTIODACYLA (Even-Toaed Ungulates)	2	3	3	4,8
7 – CETACEA (Whales and Dolphins)	1	1	1	1,6
Total 7	19	39	62	

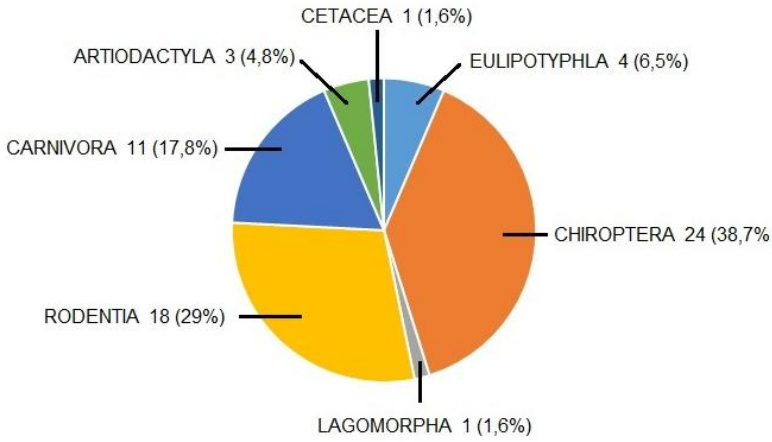

Figure 3. Order-level distribution of mammal species in Edirne province.

Table 3. Mammals of Edirne province, their international convention and national convention legislation status.

ORDER/Family/*Scientific name*	**Cammon Name**	**Turkish Name**	**Abundance**	**International Convention Status of Species**				**National Convention Status of Species**		**Detection Methods**
				ENDEMIC	**IUCN**	**CITES**	**BERN**	**MAF**	**CHCD**	
EULIPOTYPHLA (Insectivores)										
Erinaceidae (Hedgehogs)										
1. *Erinaceus roumanicus* Barret-Hamilton, 1900	Northern White-breast Hedgehog	Kirpi	Moderate	-	LC	-	-	Protected	-	1, 2, 3
Talpidae (Moles)										
2. *Talpa europaea* Linnaeus, 1758	European Mole	Köstebek	Moderate	-	LC	-	-	Protected	-	1, 2, 3, 5
Soricidae (Shrews)										
3. *Crocidura suaveolens* (Pallas, 1811)	Lesser White-toothed Shrew	Küçük Sivriburunlu Bahçefaresi	Unknown	-	LC	-	EK II	Protected	-	1, 3, 4
4. *Crocidura leucodon* (Hermann, 1780)	Becolored Shrew	Sivriburunlu Bahçefaresi	Unknown	-	LC	-	EK III	Protected	-	1, 3, 4
CHIROPTERA (Bats)										
Rhinolophidae (Horseshoes Bats)										
5. *Rhinolophus ferrumequinum* (Schreber, 1774)	Greater Horseshoe Bat	Nalburunlu Büyükarasa	Unknown	-	LC	-	EK III	Protected	-	1, 3, 6, 7, 8

6. *Rhinolophus mehelyi* Matschie, 1901	Mehely's Horseshoe Bat	Mehely Yarasası	Unknown	-	VU	-	EK II	Protected	-	1, 3, 6, 7
7. *Rhinolophus hipposideros* (Bechstein, 1800)	Lesser Horseshoe Bat	Nalburunlu Küçüky arasa	Unknown	-	LC	-	EK II	Protected	-	3, 6
Vespertilionidae (Vesper Bats)										
8. *Myotis bechsteinii* (Kuhl, 1818)	Bechstein's Bat	Büyükkulaklı Yarasa	Unknown	-	NT	-	EK II	Protected	-	1, 3, 6, 7, 8
9. *Myotis blythii* (Tomes, 1857)	Lesser Mouse-eared Myotis	Farekulaklı Küçük Yarasa	Unknown	-	LC		EK II	Protected	-	3, 6, 7
10. *Myotis capaccinii* (Bonaparte, 1837)	Long-fingered Bat	Uzunayaklı Yarasa	Unknown	-	VU	-	EK II	Protected	-	1, 3, 6, 7
11. *Myotis daubentonii* (Kuhl,1819)	Daubenton's Bat	Su Yarasası	Unknown	-	LC	-	EK II	Protected	-	1, 3, 6, 7, 8
12. *Myotis emerginatus* (E. Geoffory, 1806)	Geoffroy's Ba	Kirpikli Yarasa	Unknown	-	VU	-	EK II	Protected	-	3, 6, 8
13. *Myotis myotis* (Borkhausen, 1797)	Greater Mouse-eared Bat	Farekulaklı Büyük Yarasa	Unknown	-	LC	-	EK II	Protected	-	3, 6, 8
14. *Myotis mystacinus* (Kuhl, 1819)	Whiskered Bat	Bıyıklı Yarasa	Unknown	-	LC	-	EK II	Protected	-	3, 6, 8,
15. *Myotis nattereri* (Kuhl, 1818)	Natterer's Bat	Saçaklı Yarasa	Unknown	-	LC	-	EK II	-	-	3, 6, 7
16. *Pipistrellus kuhlii* (Kuhl, 1819)	Kuhl's Pipistrelle	Beyazyakalı Yarasa	Unknown	-	LC	-	EK II	Protected	-	3, 6, 7
17. *Pipistrellus nathusii* (Kayserling & Blasius, 1839)	Nathusius' Pipistrelle	Pürtüklü Yarasa	Common	-	LC	-	EK II	Protected	-	1, 3, 6, 8
19. *Pipistrellus pipistrellus* (Scheber, 1774)	Common Pipistrelle	Cüce Yarasa	Common	-	LC	-	EK II	Protected	-	1, 3, 6, 8
19. *Pipistrellus pygmaeus* (Leach, 1825)	Soprano Pipistrelle	Cüce Yarasa	Common	-	LC	-	EK II	Protected	-	1, 3, 6, 8
20. *Nyctalus lasiopterus* Shreber, (1780)	Greater Noctule	Büyük Akşamcı Yarasa	Rare	-	NT	-	EK II	Protected	-	1, 6, 7, 8
21. *Nyctalus leisleri* (Kuhl, 1818)	Leisler's Bat	Küçük Akşamcı Yarasa	Unknown	-	LC	-	EK II	Protected	-	1, 6, 7, 8
22. *Nyctalus noctula* (Schreber, 1774)	Common Noctule	Akşamcı Yarasa	Unknown	-	LC	-	EK II	Protected	-	1, 3, 6, 7, 8
23. *Vespertilio murinus* Linnaeus, 1758	Parti-coloured Bat	Çift Renkli Yarasa	Unknown	-	LC	-	EK II	Protected	-	1, 3, 6, 7, 8
24. *Plecotus austriacus* (Linnaeus, 1758)	Grey Long-eared Bat	Gri Uzunkulaklı Yarasa	Unknown	-	LC	-	EK II	Protected	-	3, 6, 7, 8
25. *Plecotus auritus* (Linnaeus, 1758)	Brown Long-eared Bat	Kahverengi Uzunkulaklı Yarasa	Unknown	-	LC	-	EK II	Protected	-	3, 6, 7, 8
26. *Eptesicus serotinus (*Schereber, 1774)	Serotine Bat	Genişkanatlı Yarasa	Unknown	-	LC	-	EK II	Protected	-	3, 6, 7, 8

27. *Barbastella barbastellus* (Schereber, 1774)	Barbastelle	Basıkburunlu Yarasa	Unknown	-	NT	-	EK II	Protected	-	3, 6, 7, 8
Molossidae (Free-tailed Bats)										
28. *Tadarida teniotus* (Rafinesque, 1814)	European Free-tailed Bat	Serbest kuyruklu Yarasa	Unknown	-	LC	-	EK II	Protected	-	3, 6, 7, 8
LAGOMORPHA (Hares)										
Leporidae (Rabbits and Hares)										
29. *Lepus europaeus* (Pallas, 1778)	Europaean Hare	Kır Tavşanı, Yabani Tavşan	Moderate	-	LC	-	EK III	-	Hunting Animal	1, 2, 3, 4, 5
RODENTIA (Rodents)										
Sciuridae (Ssquirrels)										
30. *Sciurus vulgaris* Linnaeus, 1758	Eurasian Red Squirrel	Avrupa Sincabı	Rare	-	LC	-	EK III	Protected		1, 2, 3, 4, 5
31. *Spermophilus citellus* (Linnaeus, 1766)	Europaean Ground Squirrel	Gelengi, Yer Sincabı, Kazık sıçanı	Moderate	-	VU	-	EK III	Protected	-	1, 2, 3, 4, 5
Cricetidae (Cricetids)										
32. *Nothocricetulus migratorius* (*Cricetulus migratorius*) (Pallas, 1773)	Grey Dwarf Hamster	Avurtlak	Unknown	-	LC	-	-	-	-	1, 3
33. *Arvicola amphibius* (Linnaeus, 1758)	Eurasian Water Vole	Su Sıçanı	Unknown	-	LC	-	-	Protected	-	1, 3, 5
34. *Microtus mystacinus* (deFilippi, 1865)	Caspian Drey Vole	Uzun kuyruklu çayır faresi	Moderate	-	LC	-	-	-	-	1, 3
35. *Microtus arvalis* (Pallas, 1778)		Tarla faresi	Unknown	-	LC	-	-	-	-	3
Spalacidae (Blind Mole Rats)										
36. *Nannospalax leucodon* (Nordmann, 1840)	Lesser Blind Mole Rat	Körfare	Common	-	DD	-	-	-	-	1, 2, 3, 4, 5
Muridae (Mouses and Rats)										
37. *Micromys minutus* (Pallas, 1771)	Eurasian Harvest Mouse	Hasat Faresi	Rare	-	NT	-	-	Protected	-	1, 3, 5
38. *Apodemus flavicollis* (Melchior, 1834)	Yellow-necked Fiel Mouse	Orman Faresi	Common	-	LC	-	-	-	-	1, 3
39. *Apodemus sylvaticus* (Linnaeus, 1758)	Long-tailed Field Mouse	Tarla faresi	Common	-	LC	-	-	-	-	1, 3
40. *Rattus rattus* (Linnaeus, 1758)	House Rat	Ev Sıçanı	Moderate	-	LC	-	-	-	-	1, 2, 3
41. *Rattus norvegicus* (Berkenhout, 1769)	Brown Rat	Göçmen Sıçan	Common	-	LC		-	-	-	1, 2, 3

42. *Mus macedonicus* Petrov & Ruzic, 1983)	Macedonian Mouse	Makedonya Ev Faresi	Moderate	-	LC	-	-	-	-	1, 2, 3
43. *Mus domesticus* Rutty, 1772	House Mouse	Ev faresi	Common	-	LC	-	-	-	-	1, 2, 3
Gliridae (Dormouses)										
44. *Glis glis* (Linnaeus, 1766)	Edible Dormouse	Yediuyur, Kataliks	Moderate	-	LC	-	EK III	Protected	-	1, 3, 4
45. *Dryomys nitedula* (Pallas, 1779)	Forest Dormouse	Ağaç Faresi, Cevizkıran	Moderate	-	LC	-	EK III	Protected	-	1, 2, 3, 4, 5
46. *Myomimus roachi* (Bate, 1937)	Roach' Mouse-tailed Dormouse (Ground Dormouse)	Yer Yediuyuru	Rare	-	VU	-	EK II	Protected	-	1, 2, 3, 4, 5
Myocastoridae (Nutrias)										
47. *Myocastor coypus* (Molina, 1758)	Coypu	Su Maymunu	Common	-	LC	-	-		-	1, 2, 3, 4, 5
CARNIVORA (Carnivores)										
Canidae (Dogs)										
48. *Canis lupus* Linnaeus, 1758	Grey Wolf	Kurt	Moderate	-	LC	EK 2	EK II	Protected	--	1, 2, 3, 4, 5
49. *Canis aureus* Linnaeus, 1758	Golden Jackal	Çakal	Moderate	-	LC	-	-	-	Hunting Animal	1, 2, 3, 4, 5
50. *Vulpes vulpes* (Linnaeus, 1758)	Red Fox	Tilki	Common	-	LC	-	-	-	Hunting Animal	1, 2, 3, 4, 5
Mustelidae (Weasels)										
51. *Martes foina* (Erxleben, 1777)	Beech Marten	Kaya Sansarı	Rare	-	LC	-	EK III	-	Hunting Animal	1, 2, 3, 5
52. *Martes martes* (Linnaeus, 1758)	Pine Marten	Ağaç sansarı	Unknown	-	LC	-	EK III	Protected	Hunting Animal	2, 3
53. *Meles meles* (Linnaeus, 1758)	Eurasian Badger	Porsuk	Rare	-	LC	-	EK III	-	Hunting Animal	1, 2, 3
54. *Lutra lutra* (Linnaeus, 1758)	Eurasian Otter	Su Samuru	Rare	-	NT	EK 1	EK II	Protected	-	1, 2, 3, 4, 5
55. *Mustela nivalis* Linnaeus, 1766	Least Weasel	Gelincik	Rare	-	LC	-	EK III	-	Hunting Animal	1, 2, 3, 5
56. *Mustela putorius* Linnaeus, 1758	Western Polecat	Kokarca	Rare	-	LC	-	EK III	-	Hunting Animal	1, 2, 3
57. *Vormela peregusna* (Guldenstaedt, 1770)	Marbled Polecat	Alaca Kokarca	Unknown	-	VU	-	EK II	Protected	-	1, 2, 3
Felidae (Cats)										
58. *Felis silvestris* Schreber, 1777	Europaean Wildcat	Yaban Kedisi	Rare	-	LC	EK 2	EK II	Protected	-	1, 2, 3, 4
ARTIODACTYLA (Even-Toaed Ungulates)										
Suidae (Pigs)										
59. *Sus scrofa* Linnaeus, 1758	Wild Boar	Yaban Domuzu	Common	-	LC	-	-	-	Hunting Animal	1, 2, 3, 4, 5

Cervidae (Deer)											
60. *Cervus elaphus* Linnaeus, 1758	Red Deer	Ulu Geyik, Kızıl Geyik	Unknown	-	LC	EK 1	EK III	-	-	2, 3, 5
61. *Capreolus capreolus* (Linnaeus, 1758)	European Roe Deer	Karaca	Unknown	-	LC	-	EK III	Protected	-	1, 2, 3, 4, 5
CETACEA (Whales and Dolphins)										
Delphinidae (Dolphins)										
62. *Tursiops truncatus* Montagu, 1821	Common Bottlenose Dolphin	Yunus, Afalina	Unknown	-	LC	EK 2	EK II	-	-	1, 2, 5

Detection methots: 1- observation , 2- questionary, 3- literature, 4- camera trap, 5- sign, 6- bioacoustic record, 7- bat sond detector, 8- bat mist net

Table 4. Mammals of Edirne province, Their oder, families, genus, species and international convention and national convention status.

Order	n	nus	ɛci	International Convention Status of Species				National Convention Status of Species	
				DEMIC	IUCN	CITES	BERN	MAF	CHCD
7	19	39	62	-	LC=50 NT=5 VU=6 DD=1	Appendix 1=2 Appendix 2=3 Unlisted=95	Appendix II =30 Appendix III=13 Unlisted= 19	Protection=40 Unlisted=22	Hunting Animals=9 Unlisted=91

2.1. Evaluation of Mammals According to International and National Criteria.

2.1.1. Evaluation of Mammals According to International Criteria.

There are no endemic (END = Species unique to the region) mammal species in Edirne province (Tables 3, 4).

When the mammals in Edirne province are evaluated according to IUCN (International Union for Conservation of Nature and Natural Resources);

50 species (1- *Erinaceus roumanicus*, 2- *Talpa europaea*, 3- *Crocidura suaveolens*, 4- *Crocidura leucodon*, 5- *Rhinolophus ferrumequinum*, 6- *Rhinolophus hipposideros*, 7- *Myotis blythi,* 8- *Myotis daubentonii*, 9- *Myotis myotis,* 10- *Myotis mystacinus*, 11- *Myotis nattereri,* 12- *Pipistrellus kuhlii,* 13- *Pipistrellus nathusii*, 14- *Pipistrellus pipistrellus*, 15- *Pipistrellus pygmaeus*, 16- *Nyctalus leisleri*, 17- *Nyctalus noctula*, 18- *Vespertilio murinus,* 19- *Plecotus austriacus*, 20- *Plecotus auritus,* 21- *Eptesicus serotinus*, 22- *Tadarida teniotus,* 23- *Lepus europaeus*, 24- *Sciurus vulgaris*, 25- *Cricetulus migratorius,* 26- *Arvicola amphibius,* 27- *Microtus mystacinus*, 28- *Microtus arvalis*, 29-

Apodemus flavicollis, 30- *Apodemus sylvaticus*, 31- *Rattus rattus,* 32- *Rattus norvegicus*, 33- *Mus macedonicus,* 34- *Mus domesticus*, 35- *Glis glis*, 36- *Dryomys nitedula,* 37- *Myocastor coypus,* 38- *Canis lupus*, 39- *Canis aureus,* 40- *Vulpes vulpes*, 41- *Martes foina,* 42- *Martes martes,* 43- *Meles meles*, 44- *Mustela nivalis,* 45- *Mustela putorius,* 46- *Felis silvestris*, 47- *Sus scrofa,* 48- *Cervus elaphus*, 49- *Capreolus capreolus*, 50- *Tursiops truncatus*) LC (common species category) kategorisindedir (Şekil 5), (Tablo 3, 4).

5 species are in the NT category (1- Myotis bechsteinii, 2- Nyctalus lasiopterus, 3- Barbastella barbastellus, 4- Micromys minutus, 5- Lutra lutra NT (Species that are not currently endangered but are candidates for inclusion in the VU, EN or CR category in the near future) (Figure 4), (Tables 3, 4).

6 species (1- *Rhinolophus mehelyi*, 2- *Myotis capaccinii*, 3- Myotis emerginatus, 4- *Spermophilus citellus*, 5- *Myomimus roachi* and 5- *Vormela peregusna*) are classified as VUL (vulnerable, sensitive, critically endangered in the wild) (Figure 4 and Tables 3, 4).

1 species (1- *Nannospalax leucodon*) is classified as DD (Species for which insufficient information is available) (Figure 4), (Tables 3, 4).

When the mammals in Edirne province are evaluated according to CITES (Convention on International Trade in Endangered Species of Wild Animals and Plants);

2 species (1- *Lutra lutra*, 2- *Cervus elaphus*) are in Annex 1 (Includes species whose species are threatened with extinction and whose trade is therefore subject to strict regulations and permitted only in exceptional circumstances); 3 species (1- *Canis lupus* and 2- *Felis silvestris* and 3- *Tursiops truncatus*) are in Annex 2 (Includes species whose trade is subject to certain principles in order to prevent uses incompatible with their survival, although they are not absolutely threatened with extinction) (Figure 4 and Tables 3, 4).

When the mammals in the region are assessed according to the BERN CONVENTION (European Convention on the Conservation of Wild Life and Habitats);

30 species (1- *Crocidura suaveolens*, 2- *Rhinolophus ferrumequinum*, 3- *Rhinolophus mehelyi*, 4- Rhinolophus hipposideros, 5- *Myotis bechsteinii*, 6- *Myotis blythi*, 7- *Myotis capaccinii,* 8- *Myotis daubentonii*, 9- *Myotis emerginatus*, 10- *Myotis myotis*, 11- *Myotis mystacinus*, 12- *Myotis nattereri*, 13- *Pipistrellus kuhlii*, 14- *Pipistrellus nathusii*, 15- *Pipistrellus pipistrellus*, 16- *Pipistrellus pygmaeus*, 17- *Nyctalus lasiopterus*, 18- *Nyctalus leisleri*, 19- *Nyctalus noctula*, 20- Bicolored Bat - 21- *Plecotus austriacus*, 22- *Plecotus auritus*, 23- *Eptesicus serotinus*, 24- *Barbastella barbastellus*, 25- *Tadarida*

teniotus, 26- *Myomimus roachi*, 27- *Canis lupus,* 28- *Lutra lutra*, 29-*Vormela peregusna*, 30- *Tursiops truncatus* are in the Annex II (Strictly Protected Species) category: (Tables 3, 4).

13 species (1- *Crocidura leucodon*, 2- *Rhinolophus ferrumequinum*, 3- *Lepus europaeus*, 4- *Sciurus vulgaris*, 5- *Spermophilus citellus*, 6- *Glis glis*, 7- *Dryomys nitedula*, 8- *Martes* foina, 9- *Martes martes*, 10- *Meles meles*, 11- *Mustela putorius,* 12- *Cervus elaphus*, 13- *Capreolus capreolus* are in the ANNEX III (Animal Species in Requirement of Protection) category (Table 3, 4).

2.1.2. Evaluation of Mammals According to National Criteria.

According to AFA (Ministry of Agriculture and Forestry), 40 mammal species (1- *Erinaceus roumanicus*, 2- *Talpa europaea*, 3- *Crocidura suaveolens*, 4- *Crocidura leucodon*, 5- *Rhinolophus ferrumequinum*, 6- *Rhinolophus mehelyi*, 7- *Rhinolophus hipposideros,* 8- *Myotis bechsteinii*, 9- *Myotis blythi*, 10- *Myotis capaccinii*, 11- *Myotis daubentonii*, 12- *Myotis emerginatus*, 13- *Myotis myotis*, 14- *Myotis mystacinus*, 15- *Pipistrellus kuhlii*, 16- *Pipistrellus nathusii*, 17- *Pipistrellus pipistrellus*, 18- *Pipistrellus pygmaeus*, 19- *Nyctalus lasiopterus*, 20- *Nyctalus leisleri*, 21- *Nyctalus noctula*, 22- *Vespertilio murinus*, 23- *Plecotus austriacus,* 24- *Plecotus auritus*, 25- *Eptesicus serotinus*, 27- *Barbastella barbastellus*, 26- Tadarida teniotus, 27- *Sciurus vulgaris*, 28- *Spermophilus citellus*, 29- *Arvicola amphibius*, 30- *Micromys minutus*, 31- *Glis glis*, 32- *Dryomys nitedula*, 33- *Myomimus roachi*, 34- *Canis lupus*, 35- *Martes foina*, 36- *Martes martes*, 37- *Lutra lutra*, 38- *Vormela peregusna*, 39- *Felis silvestris,* 40- *Capreolus capreolus* are in Annex III (protecred) category. Other species are not listed (Figure 5 and Tables 3, 4).

9 mammal species (1- *Lepus europaeus*, 2- *Canis aureus*, 3- *Vulpes vulpes*, 4- *Martes foina*, 5- *Martes martes*, 6- *Meles meles,* 7- *Mustela nivalis*, 8- *Mustela putorius*, 9- *Sus scrofa*) are in the Annex III (protected) category. Other species are not listed (Figure 5 and Tables 3, 4).

According to the CHCD (Central Hunting Commission Decision), 9 mammal species (1- *Lepus europaeus*, 2- *Canis aureus*, 3- *Vulpes vulpes*, 4- *Martes foina*, 5- *Martes martes*, 6- *Meles meles*, 7- *Mustela nivalis*, 8- *Mustela putorius*, 9- *Sus scrofa*) are in the Annex II (game) category. Other species are not listed (Figure 5), (Tables 3, 4).

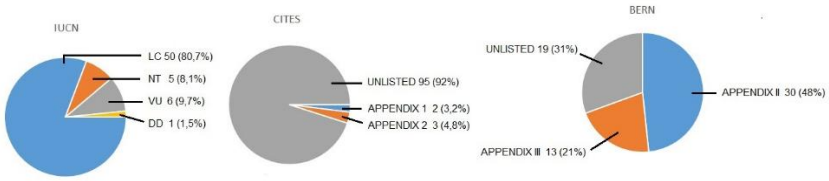

Figure 4. Evaluation of mammal species in Edirne province according to international criteria (IUCN, BERN, CITES).

Figure 5. Evaluation of mammal species in Edirne province according to national criteria (MAF, CHCD).

3. DISCUSSION AND CONCLUSION

The first systematic studies on mammals in Thrace were initiated by Çağlar (1965), Mursaloğlu (1973), Kurtonur (1972, 1975, 1982, 1991, 1992), Kurtonur and Özkan (1994, 1999a, 1999b, 2006a, 2006b), Kıvanç (1988), Albayrak (1998, 1991) and Doğramacı (1974, 1991), and new mammal species were identified for Turkish Thrace and Edirne province, and new distribution areas of mammals were determined. Later, Özkan (1987, 1995) conducted studies on mammal species in Edirne as his postgraduate thesis. Kurtonur and Özkan served as Turkey coordinators in the international project "Atlas of European Mammals" and updated the mammal species of Turkish Thrace (Mitchell-Jones et al. 1999). Subsequently, various studies on mammals conducted by domestic and international scientists in different directions have determined the current mammals of Edirne province. It has been observed that aquatic mammals such as otters and coypus avoid the polluted Ergene River.

3.1. Order Eulipotyphla (Insectivores)

A total of 4 species belonging to 3 families of the order Eulipotyphla (Insectivores) have been identified. *Erinaceus roumanicus* (northern white-breast hedgehog) and *Talpa europaea* (European mole) and their nests have been observed in all types of habitats within the borders of Edirne province. Other

shrew species (*Crocidura suaveolens* (Lesser White-toothed Shrew) and *Crocidura leucodon* (Becolored Shrew) have been captured alive by traps, particularly in forests, groves, and rocky scrub areas (Spitzenberger, 1968; Kumerloeve, 1975; Krystufek and Vohralik, 2001; Krystufek et al., 2009a; Anonymous, 2015a; Anonymous, 2015b; Anonymous, 2016 https://www.tramem.org/memeliler, 2026) (Tables 2, 3).

Figurel 6. A) *Erinaceus roumanicus* (Northern White-breast Hedgehog) and B) *Talpa europaea* (European mole)

3.2. Order Chiroptera (Bats)

A total of 24 bat species belonging to 3 families and 9 genera have been identified within the order Chiroptera. New studies and research have increased the number of bat species from 14 to 24. It is the mammal group with the most species in Edirne province (Tables 2, 3). While there are approximately 54 caves in Kırklareli province, the number of caves has decreased within the borders of Edirne province due to the impact of stone quarries. Specimens, particularly of horseshoe bats, have been found in the unregistered Manastır Cave in Enez, while other bat species have been identified in abandoned houses, forests, and wetlands in residential areas. Bats use tree hollows, ruins, and rock crevices for wintering or migrate to other regions. In 2009, 1 bat (*Myotis capaccinii* (Long-fingered Bat) was identified in a cave near the village of Koyunbaba in Kırklareli, 400 km to the west, in Greece (Paksuz, 2009). Geographically, Edirne province contains habitats rich in flat areas and wetlands. The wetlands formed by the confluence of the Meriç, Tunca, and Arda rivers in the city center of Edirne, as well as the rice fields along the entire Meriç River and the wetlands of Gala Gölü National Park in the south, are among the most important feeding, sheltering, and breeding grounds for bats. *Myotis bechsteinii*, *Myotis mystacinus, Nyctalus lasiopterus*, *Plecotus auritus*, *Eptesicus serotinus*, *Barbastella barbastellus* and *Tadarida teniotus* are among the bat species recently recorded in Edirne province. The most common bats are mostly species belonging to the genus *Pipistrellus*, which are found especially in populated areas (Çağlar, 1965; Kumerloeve, 1975; Kumerloeve, 1975; Altringham, 1996; Kurtonur et al., 1996; Benda and Horacek, 1998; Anonymous, 2015a; Anonymous, 2016; https://www.tramem.org/memeliler, 2026), (Figure 6 and Tables 2, 3).

Figure 7. Nadir orman yarasalarından Myotis bechsteinii (Bechstein's bat).

Figure 8. *Nyctalus lasiopterus* (Greater Noctule) recorded in Turkey.

3.3. Order Lagomorpha (Rabbits and Hares)

One species of rabbit belonging to one family and one genus within the order Hare has been identified. The European Hare (Lepus europaeus), a game animal, has been found to inhabit woodlands, groves, shrublands, pastures, and agricultural areas. Due to its status as a game animal and environmental pressures, its population is not experiencing rapid growth (Kumerloeve, 1975; Kurtonur et

al., 1996; Mitchell-Jones et al., 1999; Kryštufek and Vohralik, 2001; Anonymous, 2015a; Anonymous, 2016; https://www.tramem.org/memeliler, 2026) (Figure 9).

Figure 9. *Lepus europaeus* (Europaean hare) (A. Çıtak)

3.4. Order Rodentia (Rodents)

Eighteen rodent species belonging to 6 families and 14 genera of the order Rodentidae have been identified. They generally include small mammals. In Edirne province, it is the second most abundant mammal group. It includes species adapted to all kinds of habitats. *Sciurus vulgaris*, distributed in Thrace, Turkey, is sparsely distributed in forests, groves, gardens, and urban forests. *Spermophilus* citellus is distributed in anthropogenic steppe areas, pastures, agricultural areas, and the southern coastal region. Population presence changes over the years. Population density is considerably higher in the area at the entrance of Gala Gölü National Park compared to other areas (Özkan, 1987; Anonim, 2015a). *Arvicola amphibius* has only one old record, from Sazlıdere stream west of Edirne city. *Nannospalax leucodon* maintains a stable population in pastures and open areas. *Micromys minutus* is a rare species and has been recorded in rice fields (Özkan et al., 2003). *Rattus norvegicus*, which flees to settlements due to Meriç River floods, causes significant agricultural damage due to its excessive population density (Doğramacı, 1974; Özkan, 1987; Anonim, 2015a) (Figures 10, 11, 12, 13, 14).

Figure 10. *Sciurus vulgaris* (Eurasian red squirrel).

Figure 11. *Spermophilus citellus* (Europaean Ground Squirrel).

Figure 12. *Nannospalax leucodon* (Lesser blind mole rat).

Figure 13. A) *Apodemus flavicollis* (Yellow-necked fiel mouse) and B) *Dryomys nitedula* (Forest dormouse).

Figure 14. *Micromys minutus* (Harvest mouse)

Figure 15. *Myomimus roachi* (Roach' Mouse-tailed dormouse / ground dormouse).

Figure 16. *Glis glis* (Edible dormouse).

The tree dormouse *Glis glis* is a new record from the northern Lalapaşa forests within Edirne province. *Dryomys nitedula* is found in moderate density in all wooded areas, forests, groves, and orchards (Kurtonur, 1972; Mursaloğlu, 1973; Kurtonur, 1975; Kurtonur and Özkan, 1990; Doğramacı and Tez, 1991; Kurtonur, 1992). The rare and endangered Roach' mouse-tailed dormouse/ground dormouse *Myomimus roachi* is found especially in orchards with old fruit trees such as walnut, mulberry, and plum, in willow trees along stream banks, and in groves with old oak trees. It is a mammal included in the "Species Conservation Action Plan" for Edirne province (Özkan and Paksuz, 2015). Records are known from 11 localities within the Edirne province. Furthermore, the world's first specimen of a ground dormouse from which a chromosome (2n=44) was

extracted is from Turkish Thrace (Civitelli et al., 1995). Its population is endangered due to habitat changes and human impact. A quarry near Lalapaşa-Vaysal village is located 300 meters from the ground dormouse's habitat. The cutting down of old, hollow walnut and mulberry trees that provide nesting and shelter for the ground dormouse in this habitat threatens the future of this species. A sand quarry located near İpsala-Sarpdere village in the south of the province also endangers the habitat of this species. The access roads of the newly constructed "18 March 1915 Bridge" across the Dardanelles Strait have caused significant damage to the *Myomimus roachi* habitat in Gallipoli (Özkan, 1987; Kurtonur and Özkan, 1991; Mitchell-Jones et al. 1999; Anonim, 2015a; Özkan, 2019a) (Figures 13, 15, 16).

Myocastor coypus – coypu, native to South America, was brought to Europe in the early 1900s for fur production and is known to have arrived in the Meriç and Tunca rivers via Bulgaria after the 1980s. The first scientific record in Turkish Thrace was given by Özkan (Özkan and Kurtonur, 1994; Özkan, 1999a). After the 1990s, it spread south via the Meriç River and is now distributed in the Meriç basin and the wetlands of Gala Gölü National Park in the Enez-İpsala districts. It is currently distributed across more than half of Turkish Thrace (Gosling and Baker, 1991; Kurtonur et al., 1994; Kumerloeve, 1975; Lowe et al., 2000; Özkan, 2018; Özkan, 2019b; Anonymous, 2022; Anonymous, 2023; Özkan, 2026) (Figure 17).

Figure 17. An invasive species *Myocastor coypus*–coypu and Gala Lake National Park.

3. 5. Order Carnivora (Carnivorous)

Eleven carnivore species belonging to 3 families and 8 genera of the order Carnivora have been identified. They are medium-sized mammals. They are the mammal group most frequently involved in road accidents at night. While *Canis lupus* was once found throughout the province when forests were more abundant and human influence was less, today it is represented in small populations in the Lalapaşa forests in the north and the Koru and Hisarlı mountains and the forests between them in the south. The game animals *Canis aureus* and *Vulpes vulpes* are found in moderate numbers in all habitats of the province. Lutra lutra, an aquatic mammal species, is found, albeit rarely, in all wetlands such as rivers, streams, lakes, and ponds. Local people mention that it moves from one wetland

to another in search of food. While it was once hunted for its fur, it is now protected. *Vormela peregusna* is one of the rarest carnivore groups. It is known from the Hisarlı Mountain and the vicinity of Sazlıdere village near Edirne. *Felis silvestris* is seen, albeit rarely, in all habitats of the province. It is a victim of road accidents, especially at night during breeding season. Other carnivorous species are sparsely distributed (Kumerloeve, 1975; Kurtonur et al., 1994; Kurtonur et al., 1996; Krystufek et al., 1997; Mitchell-Jones et al. 1999; Çolak et al., 2000; Yiğit et al., 2006; Özkan, 2006b; Anonymous, 2015a; Özkan, 2019b) (Figures 1F8, 19, 20).

Figure 18. A) *Canis lupus* (Grey wolf) and B) *Canis aureus* (Golden jackal).

Figure 19. A) *Vulpes vulpes* (Red fox) and B) *Lutra lutra* (*Eurasian otter*).

Figure 20. A) *Meles meles* (Eurasian badger) and B) *Felis silvestris* (Europaean wildcat).

3.6. Order Artiodactyla (Even-Toated Ungulates)

Three species belonging to 2 families and 3 genera within the order Artiodactyla (even-toed ungulates) have been identified. The game animal, *Sus scrofa*, is found throughout the province. Its habitats include forests, groves, meadows, pastures, and agricultural areas. *Cervus elaphus* is currently only found sporadically in the Lalapaşa forests and Koru Mountains. Due to recent human pressure, hunting, and habitat degradation, its presence throughout the province is inevitable. *Capreolus capreolus* is also seen, albeit in small numbers, in suitable habitats throughout the province. Its numbers are decreasing day by day due to human pressure and hunting (Kumerloeve, 1975; Kurtonur et al., 1996; Mitchell-Jones et al. 1999; Anonymous, 2015a; Anonymous, 2015b) (Figure 21).

Figure 21. A) *Cervus elaphus* (European roe deer). B) *Sus scrofa* (Wild Boar).

3.7. Order Cetacea (Whales and Dolphins)

One species of dolphin belonging to one family and one genus within the order Whales and Dolphins has been identified. The habitat of *Tursiops truncatus* is the Saros Bay and the Aegean Sea. In 1990, a dolphin skull was found on the Enez coast by local people and presented to us for species identification (personal information). There are 13 cetacean species in Turkey. Eight of these are regularly observed. Four of these species (Tursiops truncatus, *Phocoena phocoena, Delphinus delphis* and *Grampus griseus*) are cetacean species found in the Aegean Sea. There is a possibility that the other three species may visit Saros Bay and be recorded from there in the coming years (Öztürk, 1998; Öztürk and Tonay, 2019) (Figure 22).

Figure 22. *Tursiops truncatus* (Cmmon bottlenose dolphin) (İstanbul Bosphorus – Öztürk and Tonay, 2019).

As a result of all these studies and research, the number of mammal species living within the borders of Edirne province is 62. This is an indicator of a mosaic richness in terms of mammal species at the provincial level. There are no endemic mammal species in the province. 80.7% of the species are classified as widespread (LC). 5 mammal species (8.1%) are NT (endangered), 6 mammal species (9.7%) are VU (endangered), and 1 species (1.5%) is DD (data deficient). 5 mammal species (8%) are included in CITES. According to BERN, 30 species (38%) are definitely species that need protection, and 13 species (21%) are mammal species that need protection.

According to national criteria, 40 species (85.5%) are protected mammal species, and 9 species (14.5%) are in the game animal category.

In recent years, the border fence barriers built on the Turkish-Bulgarian border in the Thrace region are hindering the passage of medium and large-sized mammals. This negatively affects the distribution of animals. Wind power plants (WPPs) pose a major threat to birds as well as bats. Illegal hunting activities, agricultural pollution, habitat degradation, and animal-traffic road accidents, especially for nocturnal animals, are negative impacts on mammals.

New mammal studies in the region could lead to an increase in mammal species numbers and pave the way for new measures to protect species from human and natural impacts.

4. REFERENCES

Ağşa, L. (1975). Su Maymunu. Av Dergisi 8: 3-4.

Albayrak, İ. (1988). Batı Türkiye Yarasaları ve Yarasa Pireleri. Türkiye Bilimsel ve Teknik Araştırma Kurumu. TBAG-663. 80 sayfa.

Albayrak, İ. (1999). Fauna: Susamuru, ATLAS-Yeşil Atlas, sayı 2, sayfa 82–83, Ekim 1999.

Altringham, J.D. (1996). Bats: Biology and Behaviour. Oxford University Press, Oxford; New York. 262 pp.

Angerman, R. (1966). Ein weitere Fundortvon *Myomimus roachi* Ognev, 1924. Z. Saugetierkde., 31: 411; Hamburg-Berlin.

Anonim. (2015a). Edirne İlinin Karasal ve İç Su Ekosistemleri Biyolojik Çeşitlilik Envanter ve İzleme Projesi. Orman ve Su İşleri III. Bölge Müdürlüğü / Edirne Şube Müdürlüğü. 783 sayfa. (Yüklenici firma: Urban Çevre ve Danışmanlık ve Müh. Tic. Ltd. Şti.) 12 Aralık 2013 – 22 Mayıs 2015.

Anonim. (2015b). Kırklareli ilinin Karasal ve İç Su Ekosistemleri Biyolojik Çeşitlilik Envanter ve İzleme Projesi. Orman ve Su İşleri I. Bölge Müdürlüğü / Kırklareli Şube Müdürlüğü, Kırklareli. (Yüklenici firma: Urban Çevre ve Danışmanlık ve Müh. Tic. Ltd. Şti.) 2014.

Anonim. (2018). Edirne ili Gala Gölü Milli Parkı'nda *Myocastor coypus* (Molina. 1782) (Su maymunu)'nun Populasyon Tespiti ve Çevreye Verdiği Zararlarının Tespitine Yönelik Araştırma Raporu. Edirne – 2018. T.C. Orman ve Su İşleri Bakanlığı Doğa Koruma ve Milli Parklar Müdürlüğü I. Bölge Müdürlüğü, Edirne İl Şube Müdürlüğü. 34 s

Anonim. (2020-2022). Türkiye'deki Karasal Ortamlarda ve İç Sularda İstilacı Yabancı Türlerin Tehditlerinin Değerlendirilmesi – Karasal İstilacı Yabancı Türler" projesi (TERİAS) 2020-2022.

Anonim. (2022). Edirne İli Meriç Nehri Havzası'nda Su maymunu (*Myocastor coypus* (Molina, 1782)'nun Kontrolü Faaliyeti'nin Acil Eylem Planı Uygulaması ve İzleme Raporu. 47 sayfa, 2022.

Anonim. 2016. Gala Gölü Milli Parkı'nın Flora, Fauna ve Vejetasyon Tespiti. T.C. Orman ve Su İşleri Bakanlığı Doğa Koruma ve Milli Parklar Müdürlüğü I. Bölge Müdürlüğü, Edirne Şube Müdürlüğü. 265 sayfa. (Poygar Planlama) 14 Temmuz 2016 – 09 Aralık 2016.

Anonim. 2023. Edirne İli Meriç Nehri Havzasında Su Maymununun (*Myocastor coypus* (Molina, 1782)) Kontrolü Faaliyetinin Uygulanması ve Orta/Uzun Vadeli Yönetim Planı ile Restorasyon / Rehabilitasyon Planı Projesi (Koordinatör, Memeli Hayvanlar Uzmanı). T.C. Orman ve Su İşler Bakanlığı

Doğa Koruma ve Milli Parklar Genel Müdürlüğü 1. Bölge Müdürlüğü Edirne İl Şube Müdürlüğü Edirne. 10.07.2023 – 10.12.2023. Yüklenici Firma: Öztürkler Orman Mühendislik Bürosu (103 sayfa).

Benda, P. and Horacek, I. (1998). Bats (Mammalia: Chiroptera) of the Eastern Mediterranean. Part 1. Review of distribution and taxonomy of bats in Turkey. ActaSoc. Zool. Bohem. 62: 255-313.

Buruldağ, E. & Kurtonur, C. (2001). Hibernation and Postnatal Development of the MouseTailed Dormouse, *Myomimus roachi* Reared Outdoor's in a Cage. Trakya University Journal of Scientific Research Series B, Volume 2, No 2, 179-186,

HCABI. (2018). *Myocastor coypus (coypu)*. [Original text by Dr. Sandro Bertolino]. In: Invasive Species Compendium. Wallingford, UK: CABI (Centre for Agriculture and Biosciences International). www.cabi.org/isc.

Can, Ö. E. (2004). Status, Conservation and management of large carnivores in Turkey. T-PVS/Inf (2004) 8. Strasbourg, France: Council of Europe, pp. 1-28.

Carter, J. and Leonard, B. P. (2002). A review of the literature on the worldwide distribution, spread of, and efforts to eradicate the coypu (*Myocastor coypus)*. Wildlife Society Bulletin 30(1):162-175. First account on the occurrence of selected invasive alien vertebrates in Greece. BioInvasions Records,Volume 5, Issue 4: 189–196.

Chloë, A. and Legakis, A. (2016). First account on the occurrence of selected invasive alien vertebrates in Greece. Bio Invasions Records, 5 (4): 189–196.

Civitelli, MV., Filuppucci, MG., Kurtonur, C., Özkan, B.,Capanna, E. (1995). Chromosome analysis of three species of Myoxidae. In: Flipppucci M. G. (ed). Proc. II. Conf. On Dormice. Hystrix (n.s.) 6 (1–2) : 117 - 126.

Corbet, C. B. (1978). The Mammals of The Palaearctic Region: A Taxonomic Review. Cornell Uninersity Press. London and Ithaca, 1–314.

Corbet, G. B. and Morris, P. A. (1967). A collection of recent and subfossil mammals from southern Turkey (Asia Minor), including dormouse *Myomimus personatus*. J. Nat. Hist., 1: 561-569.

Csorba, G. (1993). A review of the occurences of mouse–like dormouse (*Myomimus personatus*) in Turkmenia and an additional record. 57: 282-284 Mammalia.

Çağlar, M. (1965). Türkiye'nin Chiroptera Favnası. İstanbul Üniversitesi Fen Fakültesi Mecmuası, Seri B, 30(3-4): 125-134.

Çolak, E., Yiğit, N., Sözen, M., Verimli, R., Özkurt, Ö.Ş. (2000). On coloration and karyology of *Vormela peregusna*, in Turkey, Zoology in the Middle East, 21: 13-18.

Çolak, R., Çolak, E., Yiğit, N. (2005). Morphometric, Karyotypic and Electrophoretic Analysis of the Genus *Apodemus* Kaup, 1826 (Mammalia: Rodentia) in Thrace. Turkish Journal of Zoology, 29 (2): 147-153.

Doğan, M. (2010). Trakya'da Yayılış Gösteren *Microtus* (Mammalia; Rodentia) Türlerinin Morfolojik Özellikleri. Ankara Üniversitesi, Fen Bilimleri Enstitüsü (Yüksek Lisans Tezi). Ankara.

Doğramacı, S. (1974). Türkiye *Apodemus* (Mammalia; Rodentia)'larının Taksonomik Durumları. Tarım Hayvancılık Bakanlığı Zirai Mücadele Müdürlüğü Araştırma: 1-56.

Doğramacı, S. Ve Tez, Ç. (1991). Türkiye *Glis glis* (Mammalia: Rodentia) Türünün Coğrafik Varyasyonları ve Karyolojik Özellikleri. Doğa Tr. J. of Zoology, 15: 275–288.

Dönmez, Y. (1968). Trakya Bitki Coğrafyası, İstanbul Üniversitesi Coğrafya Enstitüsü Yayınları No: 51, 276 sayfa. İstanbul ISBN: 975-404-117-6

Filippucci, MG., Krystufek, B., Simson, S., Kurtonur, C., Özkan, B. (1995). Allozymic and Biometric Variation in *Dryomys nitedula* (Pallas, 1778). In: Filippuci M.G. (ed.). Proc. II Conf. on Dormice. Hystrix. (n.s.) 6 (1-2): 127 - 140.

Gosling, L. M. and Baker, S. J. (1991). Coypu *Myocastor coypus*. In: Corbet, G. B., & Harris, S. (Eds.), *The Handbook of British Mammals* (3rd ed., pp. 267–275). Blackwell, Oxford,

Gruychev, G. (2012). New Record of Nutria (*Myocastor coypus* (Molina, 1782)) Downstream of The Maritsa River in Bulgaria. Forestry Ideas vol. 18 (1): 110- 112.

Gruychev, G. (2017). Distribution And Density Of Coypu (*Myocastor Coypus* (Molina, 1782)) In Downstream Of Maritsa River Southeast Bulgaria. Forestry Ideas, 23 (1): 77-81.

https://www.iucnredlist.org/species/14087/4389146, 2019.

https://www.tramem.org/memeliler, 2026

İliker, A. (2009). Iğdır İli *Myocastor coypus* (Molina, 1782) (Sumaymunu)'un Biyolojisi ve Ekolojisi (Mammalia: Rodentia). Kırıkkale Üniversitesi, Fen Bilimleri Enstitüsü, Biyoloji Anabilim Dalı, Yüksek Lisans Tezi, 1-108.

İlker, A., Arslan, A., Pamukoğlu, N., Albayrak, İ. (2009). C-Banded karyotype of *Myocastor coypus* (Molina, 1782) from Turkey (Mammali: Rodentia). Folia Biologica, 57: 33–36.

Kıvanç, E. (1988). Türkiye Spalax'larının Coğrafik Varyasyonları (Mammalia; Rodentia). Ankara Üniversitesi, Fen Fakültesi, Biyoloji Bölümü, 88 pp. (Doktora tezi).

Krystufek, B., and Vohralik, V. (2005). Mammals of Turkey and Cyprus. Rodentia I: Sciuridae, Dipodidae, Gliridae, Arvicolinae. Zgodovinskodrustvozajuzno Primorsko Znanstveno-raziskovalnosredisce Republike Slovenije Koper. 1-292.

Krystufek, B., Buzan, V. E., and Vohralik, V., Zarerie. and Özkan, B. (2009). Mitochondrial cytochrome*b* sequence yields new insight into thes peciation of social voles in South west Asia. Biological Journal of Linnean Society. 98, 121-128,

Kryštufek, B., Murariu, D., Kurtonur, C. (1997). Present distribution of the Golden Jackal *Canis aureus* in the Balkans and adjacent regions. Mammal Review, 27(2): 109-114.

Krystufek, B., Özkan, B. and Kurtonur, C. (2004). Abnormal Skull of Roach's Mouse-tailed Dormouse (*Myomimus roachi*). Lynx (Praha), n. s., 35: 253-255.

Kryštufek, B., Tvrtkovic, N., Paunovic, M., Özkan, B. (2009). Size variation in the Northern whitebreasted hedgehog *Erinaceus roumanicus*: latitudinal cline and the island rule. Mammalia, 73: 299–306.

Kryštufek, B., Vohralik, V. (2001). Mammals of Turkey and Cyprus. Introduction, Checlist, Insectivora. Knjiznica Anneles Majora. 140 pp. Koper, Slovenia.

Kryštufek, B., Vohralik, V. (2009). Mammals of Turkey and Cyprus. Rodentia II: Cricetinae, Muridae, Spalacidae, Calomyscidae, Capromyidae, Hysticidae, Castoridae. Knjiznica Anneles Majora, 372 pp. Koper, Slovenia.

Kumerloeve, H. (ed) (1975). Die Säugetiere (Mammalia) der Türkei. Veröff. Zool. Staatssamml. München 18: 69-158.

Kurtonur, C. (1972). Trakya Rodentia'ları Üzerinde Taksonomik Bir Araştırma. İstanbul Üniversitesi. 69 sayfa. (Doktora Tezi).

Kurtonur, C. (1975). New Records of Thracian Mammals. Saugetierk. Mitt., München, 23 (1): 14 - 16.

Kurtonur, C. (1982). Trakya Glirid Türleri (Rodentia; Gliridae). -Dağılımı, Habitat, Taksonomik Karekterler- İstanbul Üniversitesi. 70 Sayfa (Doçentlik Tezi).

Kurtonur, C. (1992). First Specimens of *Glis glis* (Linneus, 1776) From Turkish Thrace (Mammalia; Rodentia; Gliridae). Senckenbergiana Biol. 71 (4-6): 1 - 6.

Kurtonur, C. and Özkan, B. (1991). New Records of *Myomimus roachi* (Bate,1937) From Turkish Tharace (Mammalia: Rodentia: Gliridae). Senckenbergiana Biol. 71: 239 - 244.

Kurtonur, C., Kryštufek, B., Özkan, B. (1994). The European polecat (*Mustela putorius*) In Turkish Thrace. Small Carnivore Conservation. (IUCN), 11: 8 – 10.

Kurtonur, C., Özkan, B. (1990). Orman Ağaç Faresi *Dryomy snitedula* (Rodentia : Gliridae)'nın Trakya'daki Dağılımı ve Üreme Mevsimi. X. Ulusal Biyoloji Kongresi, 18 - 20 Temmuz 1990, Erzurum. Zooloji. (4): 353 - 361.

Kurtonur, C., Özkan, B. (1992). Trakya *Myomimus roachi* (Bate, 1937) Örneklerinin Diş Morfolojisi (Mammalia : Gliridae). XI. Ulusal Biyoloji Kongresi. Zooloji Seksiyonu Bildiri Kitabı, s. 113 - 123, 24 - 27 Haziran 1992, Fırat Üniversitesi, Elazığ.

Kurtonur, C., Özkan, B., Albayrak, İ., Kıvanç, E., Kefelioğlu, H. (1996). Memeliler (Mammalia); Türkiye Omurgalılar Tür Listesi. Editör: Kence, A., Bilgin, C. C. : DPT/TBA G - Çevre Seksiyonu 3. 1-23. Ankara.

Lowe, S., Browne, M., Boudjelas, S. and De Poorter, M. (2000). 100 of the World's Worst Invasive Alien Species A selection from the Global Invasive Species Database. Published by The Invasive Species Specialist Group (ISSG) a specialist group of the Species Survival Commission (SSC) of the World Conservation Union (IUCN), 12 pp,

Milchev, B. and Gorgiev, V. (2012). Roach's mouse-tailed dormouse *Myomimus roachi* distribution and conservation in Bulgaria. Hystrix 23 (2) 66-70.

Mitchell-Jones, A. J., Amori, G., Bogdanowicz, W., Krystufek, B., Reijnders, P. J. H., Spitzenberger, F., Stubbe, M., Thissen, J. B. M.,Vohralik, V. And Zima J. (1999). Atlas of European Mammals. Published by T & A D Poyserforthe Societas Europaea Mammalogica. The Academic Press, London. 496 pp. (Turkey coordinators: Kurtonur, C. & Özkan, B.)

Mursaloğlu, B. (1973). New records for Turkish rodents (Mammalia). Communications de la Faculté des Sciences Series C, 17, 213–219.

Nedyalkov, N., Pogeorgiev, G. and Staneva, A. (2018). Updated distribution of the elusive Roach's mousetailed dormouse, Myomimus roachi Bate, 1937 (Mammalia: Rodentia: Gliridae) in Bulgaria. Historia Naturalis Bulgarica, 29:3-8.

Niermann, I, Biedermann, M.., Bogdanowicz, W., Brinkmann, R., Bris, Y. Le; Ciechanowski, M., Dietz, C., Dietz, I., Estók, P., Helversen, O., Houédec, A. Le; Paksuz, S., Petrov, B., Özkan, B., Piksa, K., Rachwald, A., Roué, Sébastien Y.; Sachanowicz, K., Schorcht, W., Tereba, A., Mayer, F. (2007). Biogeography of the recently described *Myotis alcathoe* von Helversen and Heller, 2001.Acta Chiropterologica, Volume 9, Number 2, December 2007, pp. 361-378 (18).

Özkan, B. (1987). Edirne Kemiricileri. Trakya Üniversitesi, Fen Bilimleri Enstitüsü, Biyoloji Anabilim Dalı. 42 sayfa. (Yüksek Lisans Tezi). 17.04.1987 (Danışman: Prof. Dr. Cengiz Kurtonur).

Özkan, B. (1995). Gökçeada ve Bozcaada Adalarının Kemiricileri. Trakya Üniversitesi, Fen Bilimleri Enstitüsü, Biyoloji Anabilim Dalı. 150 sayfa. (Doktora Tezi) (Danışman: Prof. Dr. Cengiz Kurtonur)..

Özkan, B. (1999a). Feral coypus, *Myocastor coypus* (Molina, 1782), in the European part of Turkey. **Israel Journal of Zoology,** 45, 289–291.

Özkan, B. (1999b). Gökçeada ve Bozcaada Kemirici Faunası (Mammalia; Rodentia). Tr.J. of Zoology, Ek sayı 1, 133-147.

Özkan, B. (2006a). An Observation on the Reproductive Biology of *Glis glis* (Linnaeus, 1766) (Rodentia; Gliridae) and Body Weight Gaining of Pups in the Istranca Mountains of Turkish Thrace. International Journal of Zoological Research 2 (2) 129-135.

Özkan, B. (2006b). Trakya Bölgesinde Yaban Kedisi (*Felis silvestris* Schreber, 1775)'in Dağılımı. 18. Ulusal Biyoloji Kongresi, 26-30 Haziran 2006, Zooloji Özetler; s. 280. Kuşadası/AYDIN.

Özkan, B. (2018). Current Distribution of *Myocastor coypus* in Gala Lake, Environmental Problems Caused and Suggested Solution, International Symposium. Ecology 2018. 19-23.06.2018. Abbstract Book 297. Kastamonu University, Turkey, Kastamonu-Türkiye

Özkan, B. (2019). Mammals of Gala Lake National Park. Journal of the Institute of Science and Technology, 9(2): 699-707.

Özkan, B. (2019a). Current Distribution of the Mouse-tailed Dormouse (*Myomimus roachi*, Bate, 1937) in Turkey. 1st International Symposium on Biodiversity Research.ISBR 02-04.05.2019, pp. 398-405, Çanakkale Onsekizmart University. Çanakkale –Türkiye.

Özkan, B. (2026). Current Current Distribution of the Coypu (*Myocastor coypus* (Molina, 1782)) in Turkish Thrace. Trend and Innovative

Research in Natural Science and Mathematics. All Sciences Academy. 5-18.

Özkan, B. and Paksuz, S. (2015). Yer Yediuyuru (*Myomimus roachi*) Tür Koruma Eylem Planı. T.C. Orman ve Su İşleri Bakanlığı Doğa Koruma ve Milli Parklar Müdürlüğü II. Bölge Müdürlüğü. 198 sayfa (Urban Çevre ve Danışmanlık ve Müh. Tic. Ltd. Şti.) 25 Mayıs 2015 – 06 Aralık 2015 Edirne.

Özkan, B. ve Kurtonur, C. (1994). Trakya Bölgesi'nde *Myocastor coypus* (Molina, 1782) (Su maymunu) (Rodentia: Mammalia)'a Ait İlk Kayıt. XII. Ulusal Biyoloji Kongresi. Zooloji Seksiyonu Bildiri Kitabı, s. 273 - 276, 6 - 8 Temmuz 1994,Trakya Üniversitesi, Edirne.

Özkan, B., and Krystufek, B. (1999). Wood Mice*, Apodemus* of Two Turkish Island: Gökçeada and Bozcaada, Folia Zool.-48 (1), pp.17-24.

Özkan, B., Yiğit, N., Çolak, E. (2003). A study on *Micromys minutus* Pallas, 1771 (Mammalia: Rodentia) in TurkishT hrace. Tr. J. of Zoology. 27, 55–60.

Özturk, A.A., Tonay, A.M. (eds.) 2019. Cetacean Studies in Turkey by TUDAV. TUDAV, Istanbul, Turkey. TUDAV Publication No: 52.

Öztürk, B. (1998). Türkiye'nin Balinaları, Türk Deniz Araştırmaları Vakfı, ATLAS-Yeşil Atlas, sayı 1, sayfa 60-65, Kasım.

Paksuz, S. (2009). Koyunbaba Mağarası (Kırklareli – Türkiye) Yarasa Faunasının Mevsimsel Populasyon Değişimleri ve Tünek Seçimi. Trakya Üniversitesi, Fen Bilimleri Enstitüsü, Biyoloji Anabilim Dalı. - (Doktora Tezi) 96 (+10) sayfa. 26.10.2009. (Tez Danışmanı: Dr. Öğrt. Üyesi Beytullah Özkan).

Paksuz, S. and Özkan, B. (2011). New Distribution Records and Some Notes for Greater Noctule, *Nyctalus lasiopterus* (Mammalia: Chiroptera) fromTurkey. Acta zool. Bul., 63 (2), 217-220.

Pechev, Z. Kh., Dinev, T. S. and Angelova, V. I. (1960). *Myomimus personatus* Ogn. (Mammalia, Myoxidae) – a new rodent in the fauna of Bulgaria. Zool. Zh., 39: 784-785.

Simson, S.; Ferruccı, L.; Kurtonur, C.; Özkan, B.; Fılıppuccı, M.G. (1995). Phalli and Bacula of European Dormice: Description and Comparıson. In: Filippuci M.G. (ed.). Proc. II Conf. on Dormice. Hystrix. (n.s.) 6 (1-2):231 -244.

Sözen, M. and Çolak, F. (2025). An updated checklist of the mammals of Türkiye. Turk J Zool 49: 252-280 TÜBİTAK doi: 10.55730/1300-0179.3232

Spitzenberger, F. (1968). Zur Verbreitung und Systematik türkischer Soricinae (Insectivora, Mamm.). Ann. Naturhistor. Mus. Wien, 72: 273-289.

Walker, N. K. et al. (1975). *Mammals of the World* (3rd ed.). Johns Hopkins University Press, Baltimore,

Wilson, D. E., & Reeder, D. A. M. (Eds.) (1993). *Mammal Species of the World: A Taxonomic and Geographic Reference* (2rd ed.). Smithsonian Institution Press, Washington and London. 1206 pp.

Yiğit, N., Çolak, E., Çolak, R. Özkan, B.and Özkurt, Ş. (2003). On the Turkish Populations of *Dryomys nitedula* (Pallas, 1779) and *Dryomys laniger* Felten and Storch, 1968 (Mammalia: Rodentia). Acta Zoologica Academiae Scientiarum Hungaricae 49 (Supl. 1), pp. 147-158.

Yiğit, N., Çolak, E., Sözen, M., Karataş, A. (2006). Rodents of Türkiye (Türkiye Kemiricileri). (Ed. Ali Demirsoy). Meteksan Co. Ankara. 1-154.

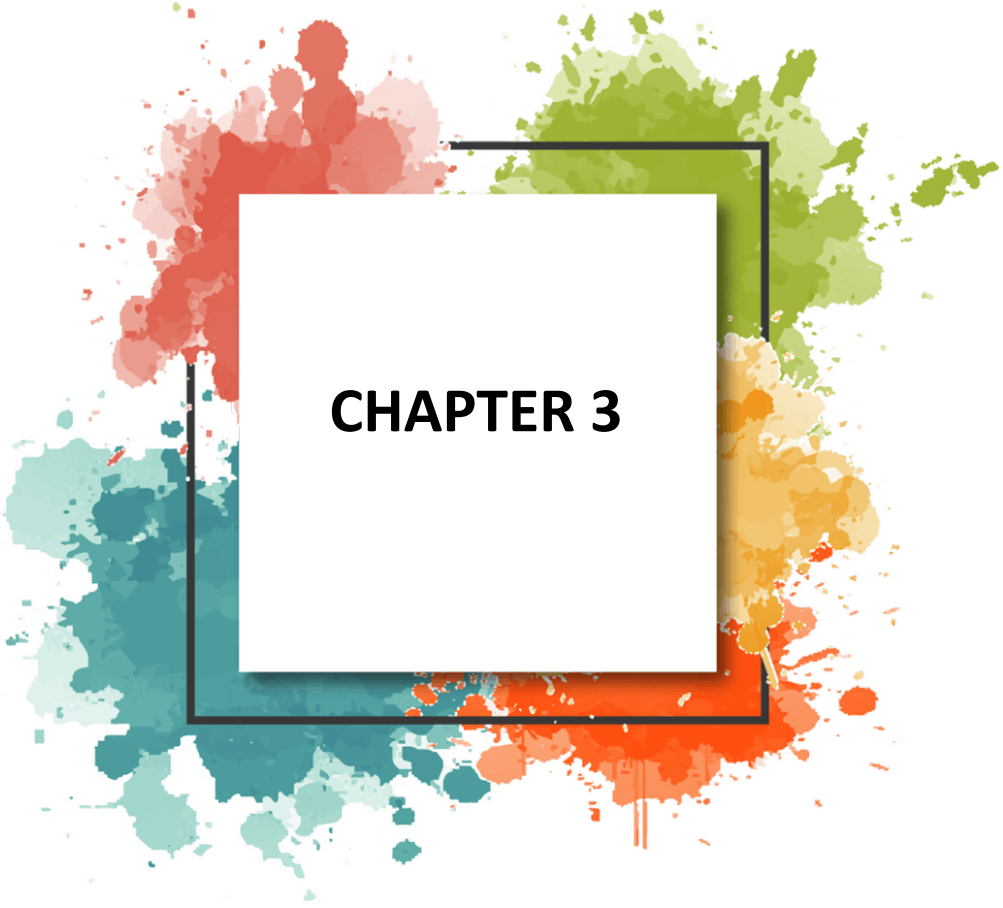
CHAPTER 3

The Lambert-Garima Distribution: A Flexible Extension for Positive Data Modeling

Aslıhan Demir[1] & Sinan Çalık[2] & Ayşe Metin Karakaş[3]

INTRODUCTION

Probability distributions play a central role in statistics, probability theory, and many applied scientific fields (Johnson, Kotz, & Balakrishnan, 1994). They are used to describe random phenomena and to model the behavior of real-world data. In disciplines such as reliability engineering, survival analysis (Collett, 2023), finance (Ruppert, 2014), and biological sciences (Quinn & Keough, 2002), selecting an appropriate probability distribution is crucial for accurate statistical inference and prediction. However, classical probability distributions such as the exponential, normal, and gamma distributions are often not sufficiently flexible to model complex datasets that exhibit skewness, heavy tails, or non-standard hazard rate functions.

To address these limitations, statisticians have developed several techniques for constructing new families of probability distributions. One widely used approach is the **generator method**, where an existing baseline distribution is transformed through a mathematical function to produce a more flexible model. Notable generator families include the beta-generated family (Eugene, Lee, & Famoye, 2002) and the Kumaraswamy-generated family (Cordeiro & de Castro, 2011).

Among the various generator approaches proposed in the literature, the **Lambert-type transformation** has received increasing attention due to its mathematical tractability and flexibility. The Lambert *W* function, introduced by Corless, Gonnet, Hare, Jeffrey, and Knuth (1996), provides a convenient way to modify the cumulative distribution function of a baseline distribution and generate new probability models. More recently, Astorga and Iriarte (2025) introduced the Lambert-Topp-Leone distribution, and Gemay et al. (2023)

[1] Department of Statistics, Firat University, Elazığ, Turkey,
Orcid: 0000-0003-4532-1564
[2] Department of Statistics, Firat University, Elazığ, Turkey,
Orcid: 0000-0002-4258-1662
[3] Department of Statistics, Bitlis Eren University, Bitlis, Turkey,
Orcid: 000-0003-3552-0105

developed the Power Lambert uniform distribution, demonstrating the applicability of Lambert-type transformations.

In recent years, researchers have focused on constructing new distributions derived from existing lifetime models to better describe reliability and survival data. One such model is the **Garima distribution**, introduced by Shukla, Shanker, and Tiwari (2023) as an alternative to the Lindley (Lindley, 1958) and exponential distributions for modeling positively skewed data. The Garima distribution has been shown to provide better fits than some classical lifetime models in certain applications, particularly when analyzing failure times and reliability data.

Despite its usefulness, the Garima distribution may still lack sufficient flexibility when dealing with highly complex datasets. For this reason, extending the Garima distribution through a generator technique can significantly enhance its modeling capability. By introducing an additional parameter, the resulting distribution can adapt to a wider range of data behaviors and hazard rate structures.

Motivated by these considerations, this chapter applies the Lambert-type transformation to the Garima distribution to develop a new model called the **Lambert-Garima (LG) distribution**. The proposed distribution extends the baseline Garima model (Shukla, Shanker, & Tiwari, 2023) by incorporating an additional parameter $\alpha \in (0,e)$ that improves flexibility in modeling skewed and lifetime data. The Lambert transformation, as utilized by Astorga and Iriarte (2025) and Gemay et al. (2023), provides a mathematically tractable framework that preserves the positive support of the baseline distribution while introducing an additional shape parameter that controls skewness, kurtosis, and tail behavior.

The main objectives of this chapter are as follows:

1. To construct the Lambert-Garima distribution using the Garima distribution (Shukla, Shanker, & Tiwari, 2023) as the baseline model
2. To derive its fundamental statistical properties, including the probability density function, cumulative distribution function, quantile function, hazard rate function, and moments
3. To discuss parameter estimation methods, including maximum likelihood
4. To illustrate potential applications in statistical modeling and reliability analysis

The Lambert-Garima distribution represents a novel two-parameter extension of the classical Garima distribution. The Garima distribution, originally proposed

by Shukla, Shanker, and Tiwari (2023) as an alternative to the Lindley (Lindley, 1958) and exponential models for lifetime data, is limited by its single-parameter structure, which restricts its ability to capture varying levels of skewness and kurtosis observed in real-world applications. By applying the Lambert transformation, we obtain the Lambert-Garima distribution, which retains the positive support of the original model but offers enhanced flexibility through an extra parameter $\alpha \in (0,e)$.

The remainder of this chapter is organized as follows. Section 2 presents the Lambert-Garima distribution and derives its fundamental functions. Section 3 establishes the identifiability of the model parameters. Section 4 derives the moments and related statistical measures. Section 5 discusses parameter estimation methods. Section 6 illustrates the practical applicability of the proposed distribution using real datasets. Section 7 provides concluding remarks.

1. The Garima Distribution

The Garima distribution, introduced by Shukla et al. (2023), is a one-parameter lifetime distribution that serves as an alternative to the Lindley and exponential distributions. A random variable X is said to follow the Garima distribution with parameter $\theta>0$, denoted by $X \sim G(\theta)$, if its probability density function (PDF), cumulative distribution function (CDF), and quantile function (QF) are given respectively by:

$$f_G(x;\theta) = \frac{\theta^3}{\theta^2+2\theta+2}(1+x+x^2)e^{-\theta x}, \quad x>0,\ \theta>0 \tag{1}$$

$$F_G(x;\theta) = 1-\left(1+\frac{\theta x(\theta x+\theta+2)}{\theta^2+2\theta+2}\right)e^{-\theta x},\ x>0,\ \theta>0 \tag{2}$$

$$Q_G(u;\theta) = -\frac{1}{\theta}-\frac{1}{\theta}W_{-1}\left((u-1)(\theta^2+2\theta+2)e^{-(1+\theta)}\right)-\frac{1}{\theta}, \quad u \in (0,1) \tag{3}$$

where $W_{-1}(\cdot)$ denotes the negative branch of the Lambert W function (Corless et al., 1996). The Garima distribution exhibits decreasing and unimodal shapes depending on the parameter θ, making it suitable for various lifetime data applications.

2. The Lambert-F Generator

The Lambert-F generator, proposed by Iriarte et al. (2020), provides a systematic method for introducing an additional shape parameter into any baseline distribution with CDF $F(x;\xi)$ and PDF $f(x;\xi)$. For a random variable Y following a Lambert-F distribution, the CDF is defined as:

$$G(x;\eta,\alpha) = 1 - (1 - F(x;\eta))\alpha^{F(x;\eta)}, \quad \alpha \in (0, e) \tag{4}$$

where α is the shape parameter introduced by the generator. The corresponding PDF is obtained by differentiating (4):

$$g(x;\eta,\alpha) = f(x;\eta)\alpha^{F(x;\eta)}[1 - log(\alpha)(1 - F(x;\eta))] \tag{5}$$

The Lambert-F generator transforms any continuous baseline distribution into a more flexible family while preserving its support and fundamental characteristics. The parameter $\alpha\alpha$ controls the tail behavior and skewness: When $\alpha<1$, the distribution exhibits heavier tails and increased skewness, When $\alpha=1$, the Lambert-F distribution reduces to the baseline distribution, When $\alpha>1$, the distribution exhibits lighter tails and decreased skewness.

If we take the standard Garima distribution as the base distribution:

$$f_G(x;\theta) = \frac{\theta^2}{\theta + 2}(1 + \theta + \theta x)e^{-\theta x}, \quad x > 0,\ \theta > 0$$

$$F_G(x;\theta) = 1 - \left(1 + \frac{\theta x}{\theta + 2}\right)e^{-\theta x}$$

Here, the survival function:

$$\bar{F}_G(x;\theta) = 1 - F_G(x;\theta) = \left(1 + \frac{\theta x}{\theta + 2}\right)e^{-\theta x}$$

is expressed as.

3. The Lambert-Garima Distribution

By applying the Lambert-F generator to the Garima baseline distribution, we obtain a new two-parameter distribution called the **Lambert-Garima (LG) distribution**. A random variable X is said to follow a Lambert-Garima distribution with parameters $\theta>0$ and $\alpha\in(0,e)$, denoted by $X\sim LG(\theta,\alpha)$, if its cumulative distribution function (CDF) is given by:

$$\overline{F}_{LG}(x;\theta,\alpha) = 1 - \overline{F}_G(x;\theta)\alpha^{F_G(x;\theta)}$$

so, explicitly:

$$F_{LG}(x;\theta,\alpha) = 1 - \left[(1 + \frac{\theta x}{\theta + 2})\right] e^{-\theta x} \alpha^{1-(1+\theta+\frac{\theta x}{\theta+2})e^{-\theta x}}, \quad x > 0,\ \theta > 0,\ \alpha \in (0, e)$$

(6)

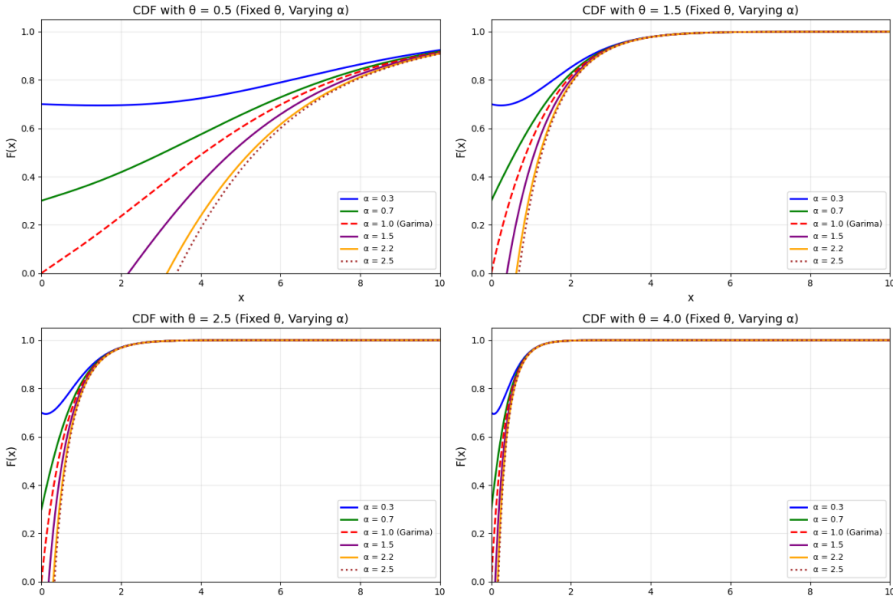

Figure 1. Lambert-Garima CDF with Fixed θ and Varying ∝

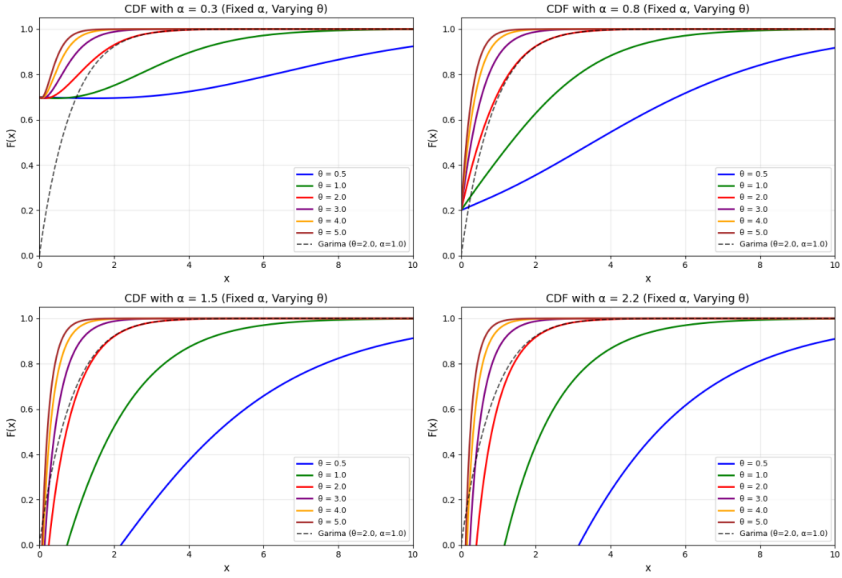

Figure 2. Lambert-Garima CDF with Fixed ∝ and Varying θ

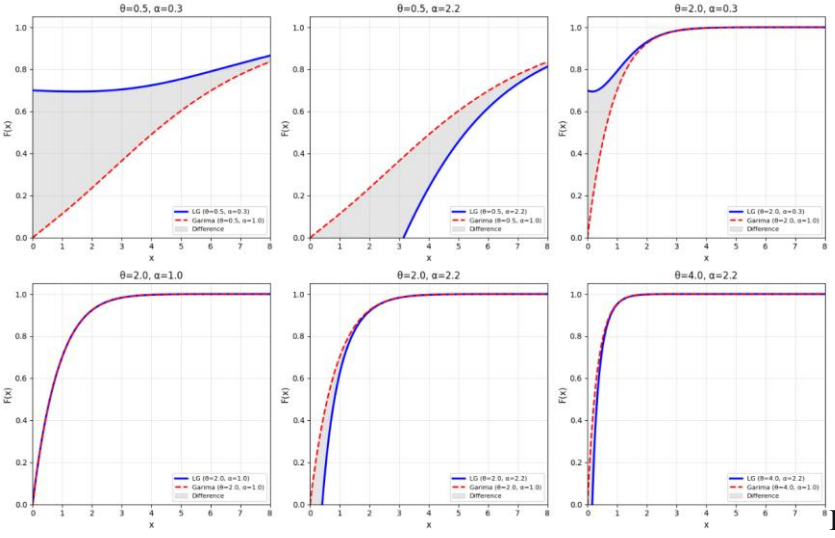

Figure 3. Lambert-Garima vs Garima CDF Comparison

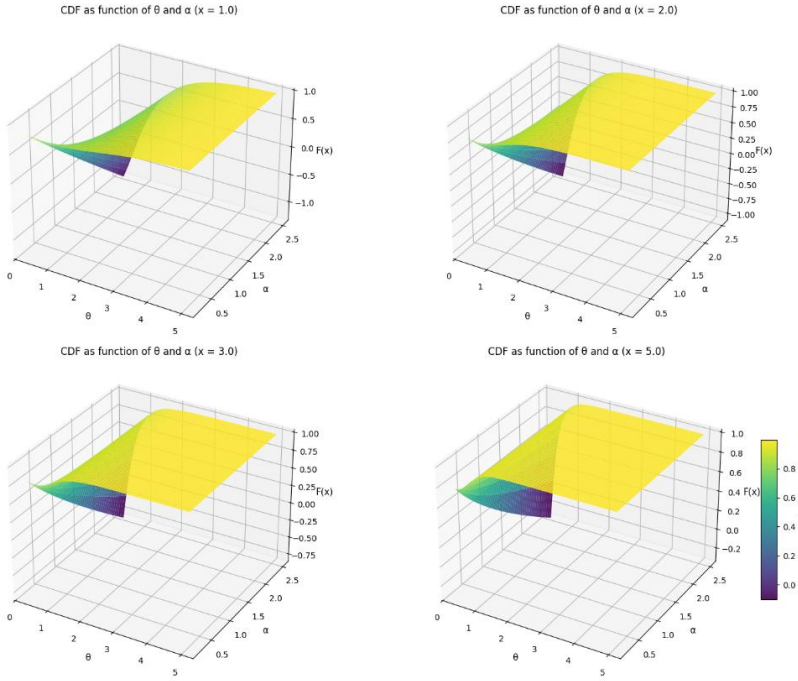

Figure 4. 3D Surface Plots of Lambert-Garima CDF

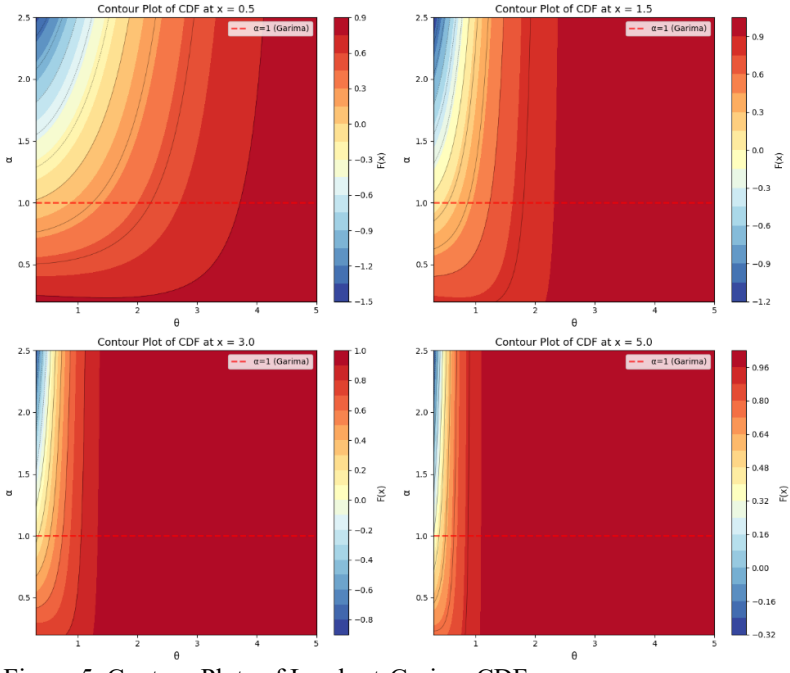

Figure 5. Contour Plots of Lambert-Garima CDF

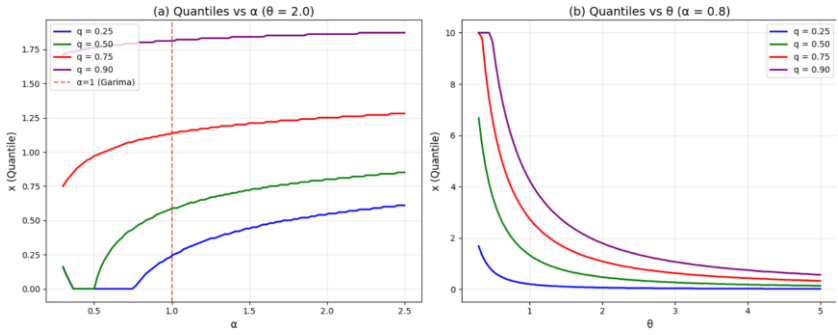

Figure 6. Quantile Analysis of Lambert-Garima Distribution

where $FG(x;\theta)$ is the CDF of the Garima distribution given in (2).

The probability density function (PDF) of the Lambert-Garima distribution is obtained by differentiating (6) with respect to x:

$$f_{LG}(x;\theta,\alpha) = f_G(x;\theta)\alpha^{F_G(x;\theta)}\left[1 - log(\alpha)\overline{F}_G(x;\theta)\right] \quad (7)$$

If we write it in explicit form:

$$f_{LG}(x;\theta,\alpha) = \frac{\theta}{\theta+2}(1+\theta + \theta x)e^{-\theta x}\alpha^{1-\left(1+\frac{\theta_x}{\theta+2}\right)e^{-\theta x}}\left[1 - log(\alpha)\left(1+\frac{\theta_x}{\theta+2}\right)e^{-\theta x}\right]$$

Substituting the explicit expressions for $fG(x;\theta)$ and $FG(x;\theta)$ from (1) and (2) into (7) yields the expanded form:

$$f_{LG}(x;\theta,\alpha) = \frac{\theta^3}{\theta^2+2\theta+2}(1+x+x^2)e^{-\theta x}, \quad x>0, \theta>0$$

$$= \alpha^{\frac{(1+\theta x)(\theta x+\theta+2)}{\theta^2+2\theta+2}e^{-\theta x}}\left[1 - log(\alpha)\frac{(1+\theta x)(\theta x+\theta+2)}{\theta^2+2\theta+2}e^{-\theta x}\right], \quad x>0,\ \theta>0,\ \alpha\in(0,e) \quad (8)$$

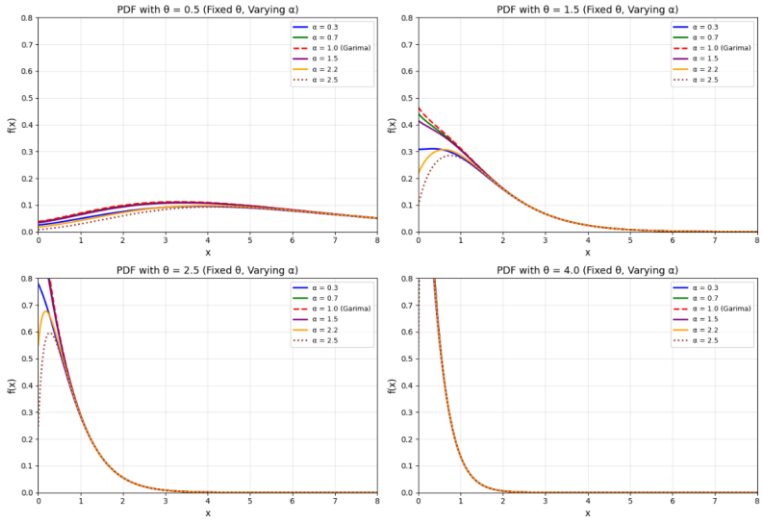

Figure 7. Lambert-Garima PDF with Fixed θ and Varying ∝

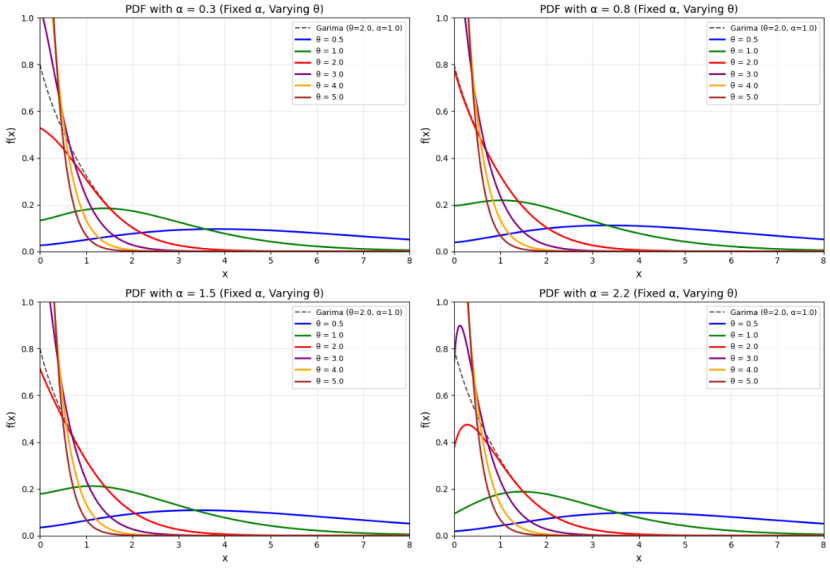

Figure 8. Lambert-Garima PDF with Fixed ∝ and Varying θ

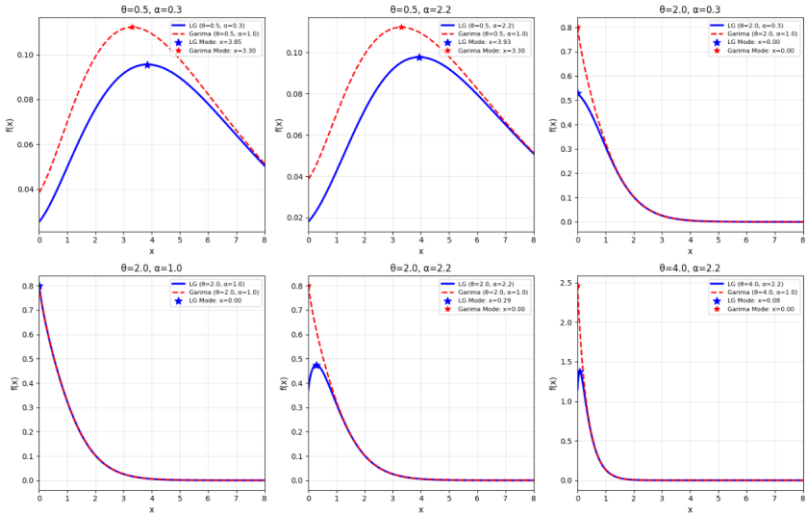

Figure 9. Lambert-Garima vs Garima PDF Comparison

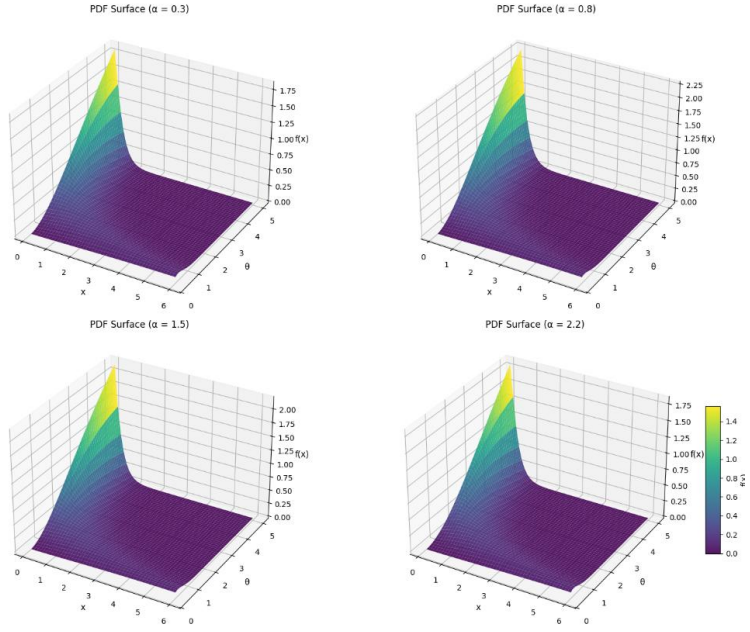

Figure 10. 3D Surface Plots of Lambert-Garima PDF

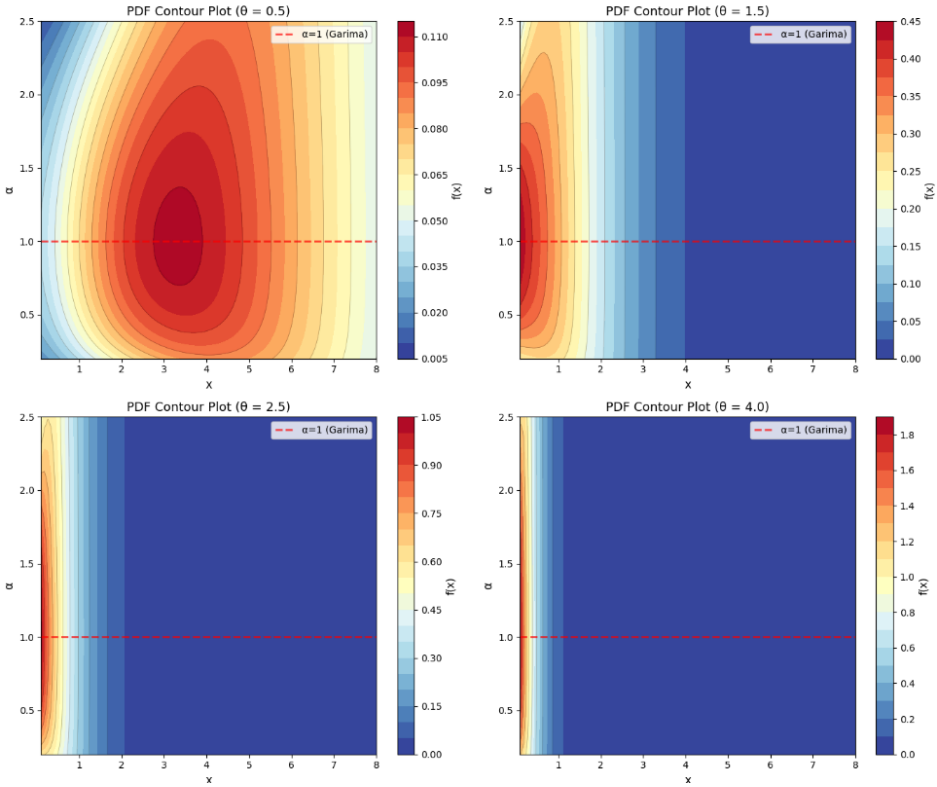

Figure 11. Contour Plots of Lambert-Garima PDF

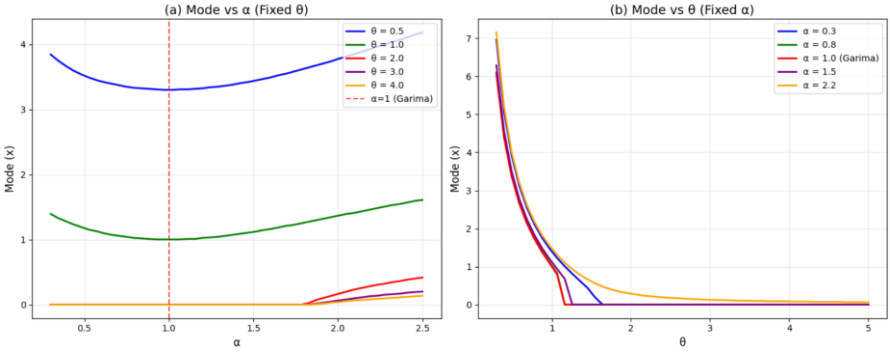

Figure 12. Mode Analysis of Lambert-Garima Distribution

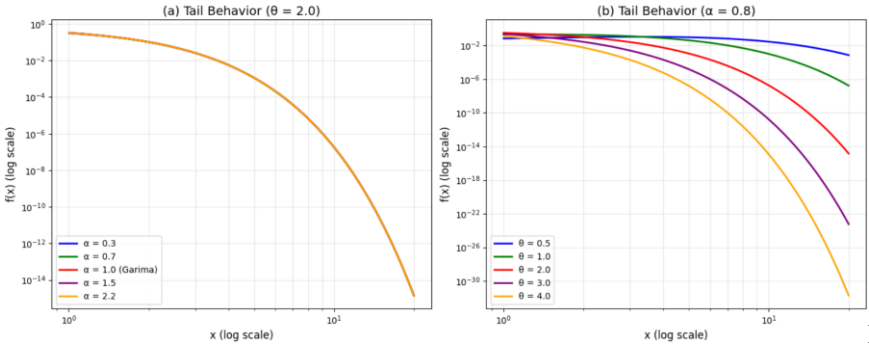

Figure 13. Tail Behavior Analysis of Lambert-Garima PDF

3.3 Quantile Function

The quantile function of the Lambert-Garima distribution does not have a simple closed-form expression but can be obtained through the composition of the Garima quantile function and the Lambert-F quantile transformation. Following the approach of Iriarte et al. (2020), if U~Uniform(0,1), then:

$$Q_{LG}(u;\theta,\alpha) = F_G^{-1}\left(\frac{1}{log(\alpha)}W_0\left(\frac{log(\alpha)(u-1)}{\alpha}\right)+1\right), \quad \alpha \neq 1 \tag{9}$$

For Garima distribution F_G^{-1} can be written in closed form. If $z \in (0,1)$:

$$F_G^{-1}(z;\theta) = -\frac{W_{-1}\left(-(\theta+2)(1-z)e^{-(\theta+2)}\right)-(\theta+2)}{\theta}$$

Therefore:

$$Q_{LG}(u;\theta,\alpha) = -\frac{W_{-1}\left(-(\theta+2)(1-z_u)e^{-(\theta+2)}\right)-(\theta+2)}{\theta}$$

$$z_u = \frac{1}{log(\alpha)}W_0\left(\frac{log(\alpha)(u-1)}{\alpha}\right)+1$$

Besides, when α=1, we directly revert to the Garima distribution:

$$F_{LG}(x;\theta,1) = F_G(x;\theta), \quad f_{LG}(x;\theta,1) = f_G(x;\theta)$$

where $QG(\cdot;\theta)$ is the Garima quantile function given in (3), $W_{-1}(\cdot)$ is the negative branch of the Lambert W function, and $\alpha \in (0,e)$ with $\alpha \neq 1$. When α=1, the quantile function reduces to that of the Garima distribution: $QLG(U;\theta,1)=QG(U;\theta)$.

This representation is particularly useful for random number generation via the inversion method.

3.4 Survival Function of the Lambert-Garima Distribution

The survival function (also known as the reliability function or survivor function) gives the probability that a unit survives beyond time *t*. Mathematically, it is defined as:

$$S(t) = \mathrm{P(X>t)} = 1 - \mathrm{F}(t)$$

The CDF of the Lambert-Garima distribution was given in Equation (6):

$$G_{LG}(x;\theta,\alpha) = 1 - \alpha^{1-F_G(x;\theta)}[1 - F_G(x;\theta)]$$

From this, we obtain the survival function:

$$S_{LG}(t;\theta,\alpha) = 1 - G_{LG}(t;\theta,\alpha) = \alpha^{1-F_G(t;\theta)}[1 - F_G(t;\theta)], \quad t > 0,\ \theta > 0,\ \alpha \in (0, e)$$

where $FG(t;\theta)$ is the CDF of the baseline Garima distribution:

$$F_G(t;\theta) = 1 - \left(1 + \frac{\theta t(\theta t + \theta + 2)}{\theta^2 + 2\theta + 2}\right) e^{-\theta t}$$

Substituting $FG(t;\theta)$ into the survival function yields:

$$S_{LG}(t;\theta,\alpha) = \left(1 + \frac{\theta t(\theta t + \theta + 2)}{\theta^2 + 2\theta + 2}\right) e^{-\theta t} \cdot \alpha^{\left(1+\frac{\theta t(\theta t+\theta+2)}{\theta^2+2\theta+2}\right)e^{-\theta t}}$$

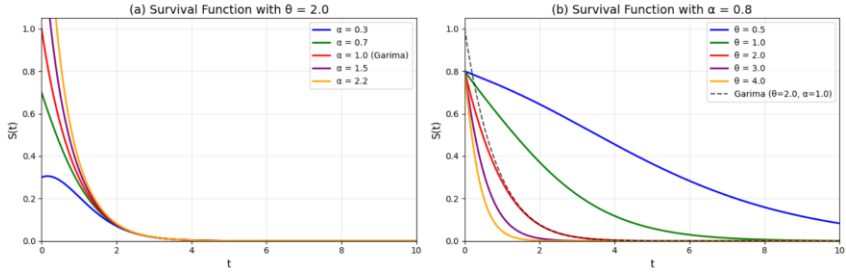

Figure 14. Survival Function of the Lambert-Garima Distribution

3.5 Hazard Rate Function

The hazard rate function (HRF), also known as the failure rate function, is a fundamental concept in reliability and survival analysis. For a continuous random variable *X* with PDF $g(x)$ and CDF $G(x)$, the HRF is defined as:

$$h(x) = \frac{g(x)}{1 - G(x)}, \quad x > 0$$

Proposition 1. Let $X \sim LG(\theta,\alpha)$. Then the hazard rate function of X is given by:

$$h_{LG}(x;\theta,\alpha) = h_G(x;\theta)\left\lfloor 1-\log(\alpha)\left(1-F_G(x;\theta)\right)\right\rfloor, \quad x>0 \qquad (10)$$

where $hG(x;\theta)=fG(x;\theta)/[1-FG(x;\theta)]$ is the hazard rate function of the baseline Garima distribution.

Proof. From the definition of the HRF and using (6) and (7):

$$h_{LG}(x;\theta,\alpha) = \frac{f_{LG}(x;\theta,\alpha)}{1-F_{LG}(x;\theta,\alpha)} = \frac{f_G(x;\theta)}{\overline{F}_{LG}(x;\theta,\alpha)}[1-log(\alpha)\overline{F}_G(x;\theta)]$$

$$h_{LG}(x;\theta,\alpha) = \frac{\theta(1+\theta+\theta x)}{1+2+\theta x}\left[1-log(\alpha)\left(1-(1+\theta+\frac{\theta x}{\theta+2})e^{-\theta x}\right)\right]$$

which completes the proof.

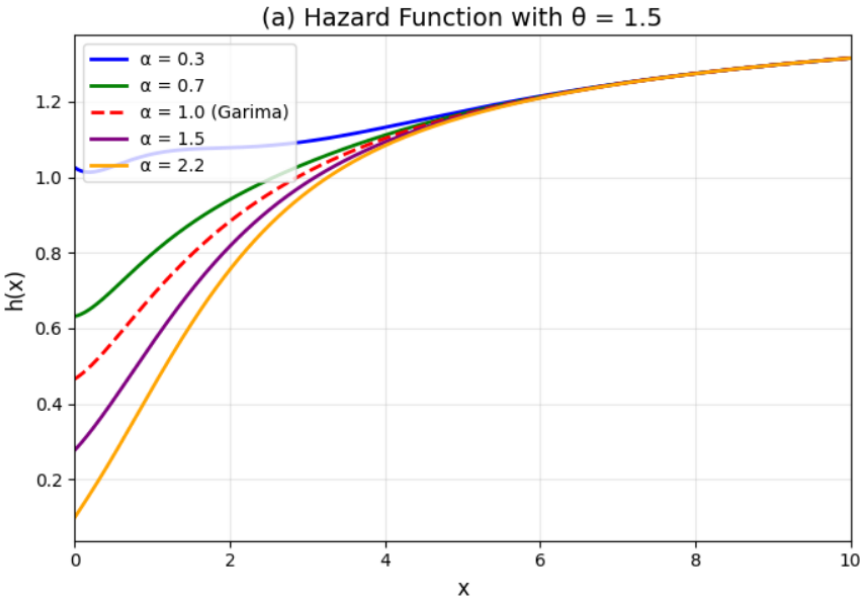

Figure 15. The hazard rate function of Lambert-Garima distribution

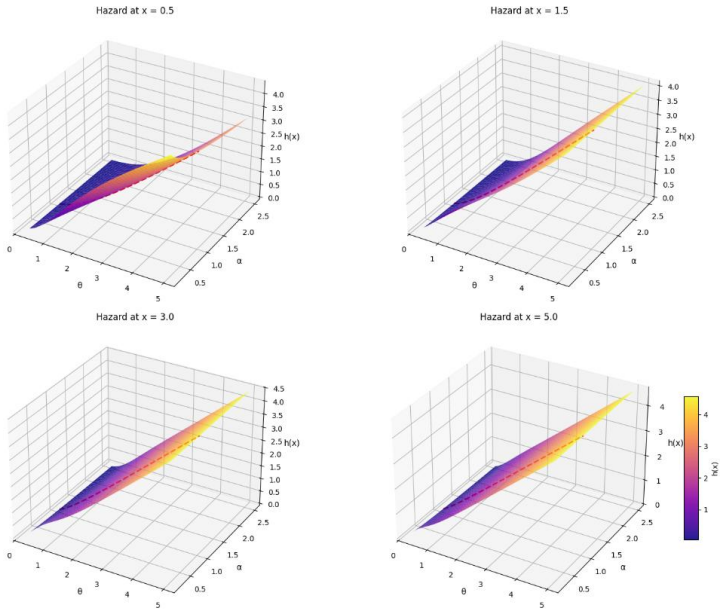

Figure 16. 3D Surface Plots of Lambert-Garima Hazard Function

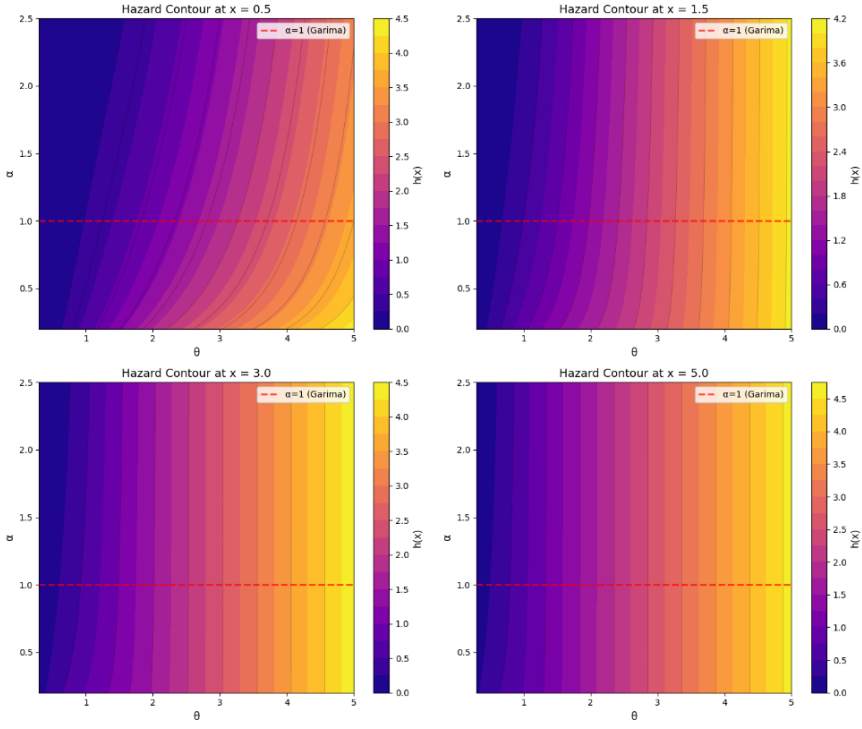

Figure 17. Contour Plots of Lambert-Garima Hazard Function

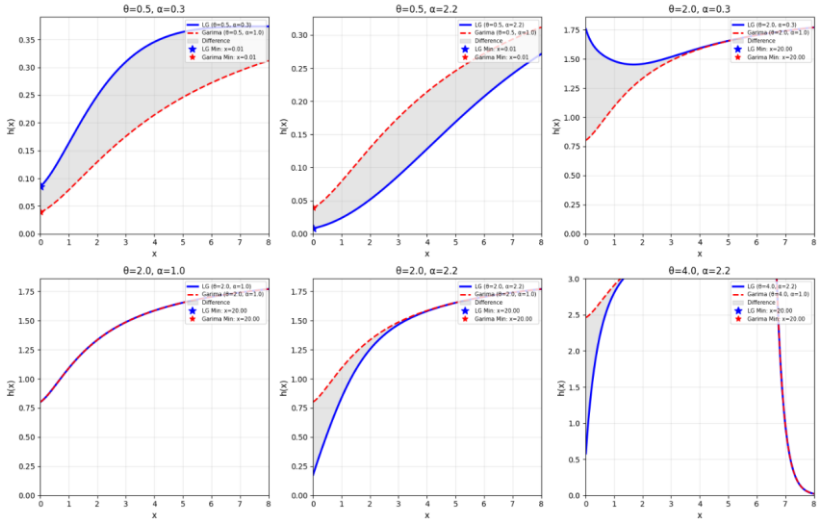

Figure 18. Lambert Garima vs Garima Hazard Function Comparison

Equation (10) reveals an important property: the Lambert-Garima hazard rate is a multiplicative modification of the baseline Garima hazard rate. The modifying factor depends on α and the baseline CDF. At the lower bound of the support, as $x \to 0+$, we have:

$$\lim_{x \to 0^+} \frac{h_{LG}(x;\theta,\alpha)}{h_G(x;\theta)} = 1 - log(\alpha)$$

Thus, the LG distribution can exhibit either higher ($\alpha<1$) or lower ($\alpha>1$) initial hazard compared to the baseline Garima distribution. As $x \to \infty$, since $FG(x;\theta) \to 1$, we obtain:

$$\lim_{x \to \infty} \frac{h_G(x;\theta)}{h_{LG}(x;\theta,\alpha)} = 1$$

indicating that both distributions share the same asymptotic tail behavior.

3.6 Odds Function of the Lambert-Garima Distribution

The odds function (also known as the odds of failure) is defined as the ratio of the cumulative distribution function (CDF) to the survival function. It represents the odds that an event occurs by time t*t* versus surviving beyond time *t*.

For a random variable X with CDF $F(t)$ and survival function $S(t)=1-F(t)$, the odds function is defined as:

$$O(t) = \frac{1 - F(t)}{F(t)} = \frac{S(t)}{F(t)}$$

For the Lambert-Garima distribution, the CDF is given by Equation (6):

$$G_{LG}(t;\theta,\alpha) = 1 - \alpha^{1-F_G(t;\theta)}[1 - F_G(t;\theta)]$$

and the survival function is:

$$S_{LG}(t;\theta,\alpha) = \alpha^{1-F_G(t;\theta)}[1 - F_G(t;\theta)]$$

Therefore, the odds function is:

$$O_{LG}(t;\theta,\alpha) = \frac{G_{LG}(t;\theta,\alpha)}{S_{LG}(t;\theta,\alpha)} = \frac{1 - \alpha^{1-F_G(t;\theta)}[1 - F_G(t;\theta)]}{\alpha^{1-F_G(t;\theta)}[1 - F_G(t;\theta)]}, \quad t > 0, \theta > 0, \alpha \in (0, e)$$

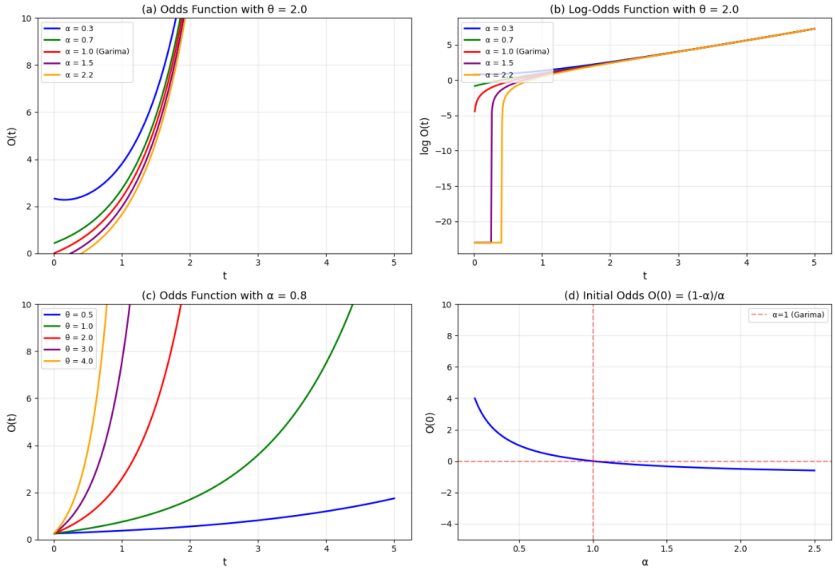

Figure 19. Odds Function of the Lambert-Garima Distribution

3.7 Order Statistics of the Lambert-Garima Distribution

Let $X1,X2,\ldots,Xn$ be a random sample from the Lambert-Garima distribution with parameters $\theta>0$ and $\alpha\in(0,e)$. Let $X(1)\leq X(2)\leq\cdots\leq X(n)$ denote the **order statistics** of the sample, where $X(k)$ is the k-th smallest observation. The probability density function (PDF) of the k-th order statistic $X(k)$ is given by:

$$f_{X_{(k)}}(x;\theta,\alpha)=\frac{n!}{(k-1)!\,(n-k)!}[G_{LG}(x;\theta,\alpha)]^{k-1}[1-G_{LG}(x;\theta,\alpha)]^{n-k}g_{LG}(x;\theta,\alpha)$$

where:

$GLG(x;\theta,\alpha)$ is the CDF of the Lambert-Garima distribution (Equation 6) and $gLG(x;\theta,\alpha)$ is the PDF of the Lambert-Garima distribution (Equation 7)

Substituting the expressions for GLG and gLG:

$$f_{X_{(k)}}(x;\theta,\alpha)=\frac{n!}{(k-1)!\,(n-k)!}\left[1-\alpha^{1-F_G(x;\theta)}(1-F_G(x;\theta))\right]^{k-1}\times\left[\alpha^{1-F_G(x;\theta)}(1-F_G(x;\theta))\right]^{n-k}\times f_G(x;\theta)\alpha^{1-F_G(x;\theta)}[1-log(\alpha)(1-F_G(x;\theta))]$$

The cumulative distribution function (CDF) of

$$F_{X_{(k)}}(x;\theta,\alpha)=\sum_{j=k}^{n}\binom{n}{j}[G_{LG}(x;\theta,\alpha)]^{j}[1-G_{LG}(x;\theta,\alpha)]^{n-j}$$

The CDF of the minimum is:

$$f_{X_{(1)}}(x;\theta,\alpha)=n[1-G_{LG}(x;\theta,\alpha)]^{n-1}g_{LG}(x;\theta,\alpha)$$

The CDF of the maximum is:

$$f_{X_{(n)}}(x;\theta,\alpha)=n[G_{LG}(x;\theta,\alpha)]^{n-1}g_{LG}(x;\theta,\alpha)$$

The range $R=X(n)-X(1)$ has PDF:

$$f_R(r;\theta,\alpha)=\int_0^{\infty}f_{X_{(1)},X_{(n)}}(x,x+r;\theta,\alpha)dx,\quad r>0$$

3.8 Maximum Likelihood Estimation (MLE) for the Lambert-Garima Distribution

Let $X1,X2,\ldots,Xn$ be a random sample from the Lambert-Garima distribution with parameters $\theta>0$ and $\alpha\in(0,e)$. The probability density function (PDF) is:

$$g_{LG}(x;\theta,\alpha) = f_G(x;\theta)\alpha^{1-F_G(x;\theta)}\left[1-\log(\alpha)(1-F_G(x;\theta))\right]$$

where:

$$f_G(x;\theta) = \frac{\theta^2+2\theta+2}{\theta^3}(1+x+x^2)e^{-\theta x}$$

$$F_G(x;\theta) = 1-\left(1+\frac{\theta x(\theta x+\theta+2)}{\theta^2+2\theta+2}\right)e^{-\theta x}$$

The likelihood function is:

$$L(\theta,\alpha;x) = \prod_{i=1}^{n} g_{LG}\,(x_i;\theta,\alpha)$$

$$\frac{\partial \ell}{\partial \theta} = \frac{3n}{\theta} - \frac{n(2\theta+2)}{\theta^2+2\theta+2} - \sum_{i=1}^{n} x_i$$
$$+ log\,\alpha \sum_{i=1}^{n} \frac{\partial}{\partial \theta}\left[\left(1+\frac{\theta x_i(\theta x_i+\theta+2)}{\theta^2+2\theta+2}\right)e^{-\theta x_i}\right]$$
$$-\sum_{i=1}^{n} \frac{log(\alpha)\frac{\partial}{\partial \theta}\left[\left(1+\frac{\theta x_i(\theta x_i+\theta+2)}{\theta^2+2\theta+2}\right)e^{-\theta x_i}\right]}{1-log(\alpha)\left(1+\frac{\theta x_i(\theta x_i+\theta+2)}{\theta^2+2\theta+2}\right)e^{-\theta x_i}}$$

4. Identifiability

A fundamental requirement for any parametric statistical model is identifiability: different parameter values must produce different distributions.

Proposition 2. The Lambert-Garima distribution is identifiable; that is,

$$g_{LG}(\cdot;\theta_1,\alpha_1) = g_{LG}(\cdot;\theta_2,\alpha_2) \text{ almost everywhere on } (0,\infty) \Rightarrow (\theta_1,\alpha_1) = (\theta_2,\alpha_2)$$

Proof. Assume that $gLG(x;\theta1,\alpha1)=gLG(x;\theta2,\alpha2)$ for all $x>0$. As $x\to\infty$, we have $FG(x;\theta)\to1$, and from (7):

$$g_{LG}(x;\theta,\alpha)\sim\alpha f_G(x;\theta)$$

The baseline Garima PDF has exponential decay governed by $f_G(x;\theta)\sim e^{-\theta x}$, as $x\to\infty$. If $\theta1\neq\theta2$, the exponential tails would differ, contradicting the equality of the densities for all x. Therefore, $\theta1=\theta2=\theta$.

With θ fixed, dividing both sides of the equality by $fG(x;\theta)$ yields:

$$\alpha_1^{\frac{1}{1-F_G(x;\theta)}}[1-log(\alpha_1)(1-F_G(x;\theta))] = \alpha_2^{\frac{1}{1-F_G(x;\theta)}}[1-log(\alpha_2)(1-F_G(x;\theta))]$$

Taking the limit as $x\to\infty$ (so $FG(x;\theta)\to1$):

$$\lim_{x\to\infty}\alpha_i^{\frac{1}{1-F_G(x;\theta)}}[1-log(\alpha_i)(1-F_G(x;\theta))] = \alpha_i, \quad i=1,2$$

Thus $\alpha1=\alpha2$, completing the proof.

5. Moments and Related Measures

The moments of the Lambert-Garima distribution do not have simple closed-form expressions but can be represented through integrals involving the Lambert W function.

Proposition 3. Let $X\sim LG(\theta,\alpha)$. Then the r-th moment of X is given by:

$$E(X^r) = \int_0^\infty x^r f_G(x;\theta)\alpha^{\frac{1}{1-F_G(x;\theta)}}[1-log(\alpha)(1-F_G(x;\theta))]dx, \quad r=1,2,\ldots \tag{11}$$

Using the transformation $u=FG(x;\theta)$, we obtain an alternative expression:

$$E(X^r) = \int_0^1 [Q_G(u;\theta)]^r\,\alpha^{1-u}[1-log(\alpha)(1-u)]du \tag{12}$$

where $QG(u;\theta)$ is the Garima quantile function given in (3). For practical purposes, these moments must be evaluated using numerical integration techniques.

The mean, variance, coefficient of variation, skewness, and kurtosis can be computed from (11) or (12) using standard formulas. These measures demonstrate that:

For α<1, the LG distribution exhibits greater dispersion, skewness, and kurtosis than the baseline Garima , For α>1, the LG distribution exhibits lower dispersion, skewness, and kurtosis, The parameter α provides effective control over the tail behavior and shape of the distribution

6. Special Cases and Limiting Behavior

The Lambert-Garima distribution encompasses several important special cases:

Case 1: α=1 (Garima distribution)

When α=1, equation (7) reduces to:

$$g_{LG}(x;\theta,1) = f_G(x;\theta)\cdot\frac{1}{1-F_G(x;\theta)}[1-0\cdot(1-F_G(x;\theta))] = f_G(x;\theta)$$

Thus, the LG distribution coincides with the classical Garima distribution when α=1.

Case 2: $\alpha \to 0^+$ (Degenerate case)

As $\alpha \to 0^+$, for any fixed x>0 with $FG(x;\theta)$<1, we have $\alpha^{1-FG(x;\theta)} \to 0$. Consequently, $gLG(x;\theta,\alpha)\to 0$ for all x>0, indicating that the probability mass concentrates near zero.

Case 3: $\alpha \to e^-$ (Upper limit)

As $\alpha \to e^-$, $\log(\alpha) \to 1$, and the PDF converges to:

$$\lim_{\alpha\to e^{-1}} g_{LG}(x;\theta,\alpha) = f_G(x;\theta)e^{1-F_G(x;\theta)}[2-F_G(x;\theta)]$$

This limiting case yields a one-parameter distribution with specific skewness and kurtosis properties.

Boundary behavior of the PDF:

$$\text{As } x\to 0^+: \quad \lim_{x\to 0^+} g_{LG}(x;\theta,\alpha) = [1-log(\alpha)]\cdot\frac{\theta^3}{\theta^2+2\theta+2}$$

$$\text{As } x\to \infty: \quad \lim_{x\to\infty} g_{LG}(x;\theta,\alpha) = 0$$

This shows that at the lower bound, the LG density can be either higher (α<1) or lower (α>1) than the baseline Garima density, while both distributions share the same asymptotic decay at the upper bound.

Table X. Bladder Cancer Remission Duration Data (n = 128)

0.08	2.09	3.48	4.87	6.94	8.66	13.11	23.63
0.20	2.23	3.52	4.98	6.97	9.02	9.02	0.40
2.26	3.57	5.06	7.09	9.22	13.80	25.74	0.50
2.46	3.64	5.09	7.26	9.47	14.24	25.82	0.51
2.54	3.70	5.17	7.28	9.74	14.76	26.31	0.81
2.62	3.82	5.32	7.32	10.06	14.77	32.15	2.64
3.88	5.32	7.39	10.34	10.34	14.83	34.26	0.90
4.18	5.34	7.59	10.36	10.64	15.96	36.66	1.05
4.23	5.41	7.62	10.75	10.75	16.62	43.01	1.19
4.26	5.41	7.63	17.62	17.12	46.12	1.26	2.83
5.49	7.66	11.25	17.14	79.05	1.35	2.87	5.62
7.87	11.64	17.36	1.40	3.02	4.34	5.71	7.93
1.46	18.10	11.79	4.40	5.85	8.26	11.98	19.13
1.76	3.25	4.50	6.25	8.37	12.02	2.02	13.31
4.51	6.54	8.53	12.03	20.28	2.02	3.36	12.07

Table 1. Descriptive Statistics of the Data

Statistic	Value
n	128.0000
Mean	9.4438
Median	6.6500
Std.Dev	10.5001
Variance	110.2526
Minimum	0.0800
Q1	3.3600
Q2 (Median)	6.6500
Q3	11.9900
Maximum	79.0500
Range	78.9700
IQR	8.6300

CV (%)	111.1859
Skewness	3.2355
Kurtosis	18.1550

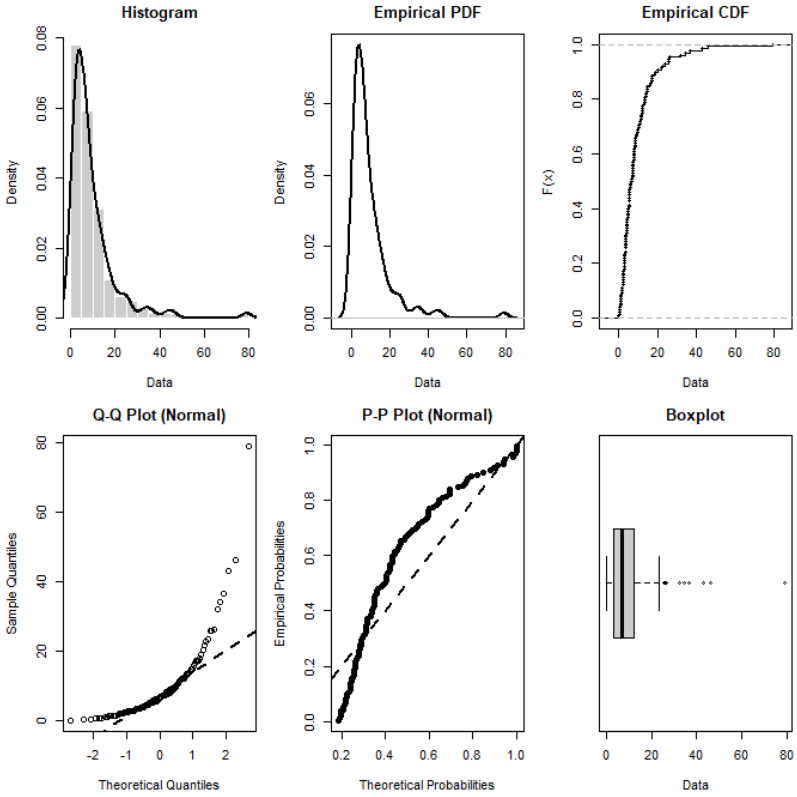

	Lambert Garima	GARİMA
theta	0.052431(SE=0.056962)	0.15434(SE=0.011935)
alpha	0.041084(SE=0.188934)	
LogL	-412.364003	-416.374102
AIC	828.728006	834.748203
BIC	834.432067	837.600233
HQIC	831.045595	835.906998
CAIC	836.432067	838.600233
KS TEST	0.074676	0.081996
P VALUE	0.201387	0.355678
Anderson-Darling Test	1.005957	1.031779
P VALUE	0.230390	0.340874

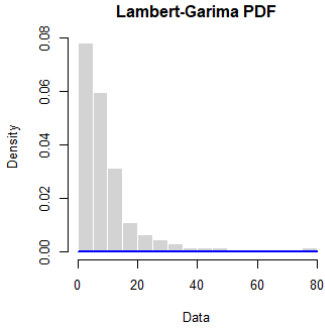
Lambert-Garima PDF
Density
Data

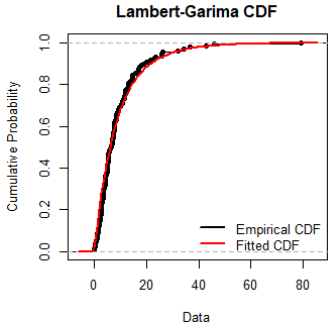
Lambert-Garima CDF
Cumulative Probability
Empirical CDF
Fitted CDF
Data

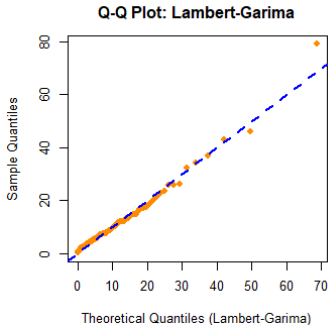
Q-Q Plot: Lambert-Garima
Sample Quantiles
Theoretical Quantiles (Lambert-Garima)

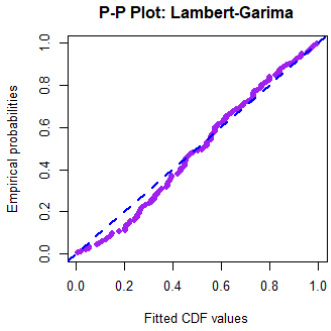
P-P Plot: Lambert-Garima
Empirical probabilities
Fitted CDF values

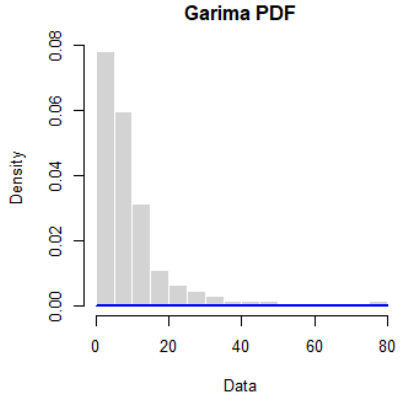
Garima PDF
Density
Data

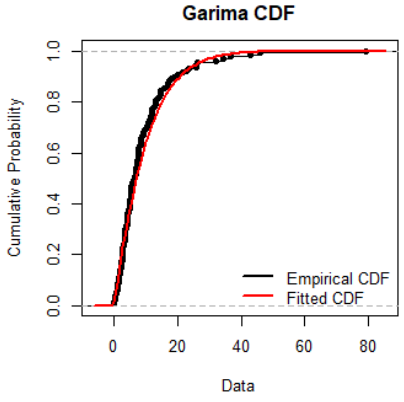
Garima CDF
Cumulative Probability
Empirical CDF
Fitted CDF
Data

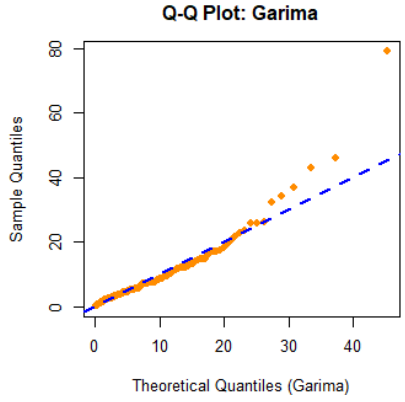
Q-Q Plot: Garima
Sample Quantiles
Theoretical Quantiles (Garima)

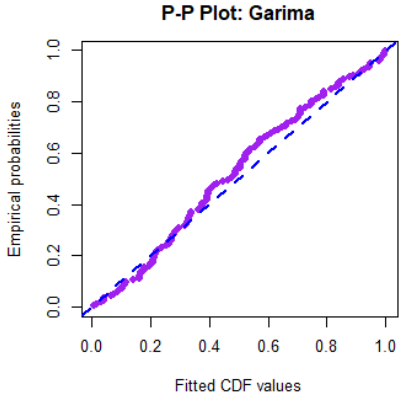
P-P Plot: Garima
Empirical probabilities
Fitted CDF values

7. Conclusions

The descriptive statistics clearly indicate that the dataset is significantly right-skewed, exhibits high variability, and shows a structure with a long right tail. The mean being 9.4438 while the median is 6.65, along with skewness of 3.2355 and kurtosis of 18.1550, clearly shows that a few large observations pull the distribution upward. The minimum being 0.08, maximum 79.05, range 78.97, and the coefficient of variation being 111.19% are also consistent with this. Therefore, the data is neither symmetric nor light-tailed; on the contrary, it appears as challenging survival data for classical unimodal and less flexible models.

Examining the descriptive statistics, with Q1 = 3.36, median = 6.65, Q3 = 11.99, the middle 50% of the observations are concentrated approximately between 3.36 and 11.99. Despite this, the maximum being 79.05 suggests that the upper tail of the dataset is very long. This is an expected situation for survival data such as bladder cancer remission times that extend to the right. In other words, the descriptive statistics in the document are internally consistent and reflect the structure of the data well.

Regarding model comparison, the Lambert–Garima model appears to provide a better fit than the Garima model. The strongest indicator of this is the log-likelihood value: -412.364003 for Lambert–Garima, -416.374102 for Garima. A larger log-likelihood indicates a better fit; here Lambert–Garima is ahead. The same result is maintained in the information criteria: all AIC, BIC, HQIC, and CAIC values are smaller for Lambert–Garima. Particularly, the AIC being 828.728006 compared to 834.748203 for Garima suggests that the improvement is not merely coincidental but meaningful in terms of modeling. In other words, despite the penalty for the additional parameter, Lambert–Garima remains superior. This indicates that the transformation adds additional flexibility to the data.

The KS test results also show that neither model is completely poor. The KS statistic for Lambert–Garima is 0.074676, for Garima 0.081996; both p-values are above 0.05. This means that neither model shows a serious discrepancy with the empirical distribution. However, the fact that the KS statistic is smaller for Lambert–Garima is again a sign in its favor. In the Anderson–Darling test, similarly neither model is rejected; however here too Lambert–Garima's statistic is slightly lower. Particularly since Anderson–Darling is more sensitive to the tail, this small superiority is important considering the right-tailed data structure.

In terms of parameter estimates, in the Lambert–Garima model $\theta = 0.052431$ and $\alpha = 0.041084$ are given. However, the point to note here is that the standard errors are quite large; especially for α, the standard error is larger than the estimate itself. This could mean two things: either the data explains the Lambert transformation with a parameter close to the boundary region, or even though this additional parameter provides improvement on the data, the estimation stability is not very high. In other words, Lambert–Garima provides a better fit; but one needs to be somewhat cautious in terms of parameter interpretation. In the Garima model, $\theta = 0.15434$ and the standard error is much smaller; that is, the parameter estimate of the simpler model is more stable. Therefore, Lambert–Garima appears more advantageous in terms of "fit quality," while Garima appears more advantageous in terms of "parametric simplicity and stability."

The overall scientific message in the document can be summarized as follows: Because this dataset is heavily right-tailed and has high variability, although it can be explained by the basic Garima model alone, the Lambert-type transformation provides additional flexibility to the data, resulting in a better fit. Due to its superiority in all information criteria and better results in fit tests, the main preference for this dataset could be the Lambert–Garima model. On the other hand, because of parameter uncertainty, when writing the results it should be stated that "Lambert–Garima provided the best fit," but a note that "parameter estimates contain high uncertainty" should also be added.

REFERENCES

1. Shanker, R. (2016). Garima distribution and its application to model behavioral science data. *Biometrics & Biostatistics International Journal, 4*(7), 1–9.
2. Topp, C. W., & Leone, F. C. (1955). A family of J-shaped frequency functions. *Journal of the American Statistical Association, 50*, 209–219.
3. Abebe, B., Tesfay, M., Eyob, T., & Shanker, R. (2019). A two-parameter power Rama distribution with properties and applications. *Biometrics & Biostatistics International Journal, 8*(1), 6–11.
4. Al-Shomrani, A., Arif, O., Hanif, S., Shahbaz, M. Q., & Shawky, A. (2016). Topp–Leone family of distributions: Some properties and application. *Pakistan Journal of Statistics and Operation Research, 12*(3), 443–451.
5. Corless, R. M., Gonnet, G. H., Hare, D. E. G., Jeffrey, D. J., & Knuth, D. E. (1996). On the Lambert W function. *Advances in Computational Mathematics, 5*(1), 329–359.
6. Iriarte, Y. A., de Castro, M., & Gómez, H. W. (2020). The Lambert-F distributions class: An alternative family for positive data analysis. *Mathematics, 8*(8), 1398.
7. Shukla, K. K., Shanker, R., & Tiwari, M. K. (2023). Garima distribution and its applications. *Journal of Statistics and Management Systems, 26*(3), 671–688.
8. Lee, E. T., & Wang, J. (2003). *Statistical methods for survival data analysis* (3rd ed.). Hoboken, NJ: John Wiley & Sons.
9. Astorga, J. M., & Iriarte, Y. A. (2025). The Lambert-Topp-Leone distribution: An alternative for modeling proportion and lifetime data. *Frontiers in Applied Mathematics and Statistics*, *11*, 1527833.
10. Collett, D. (2023). *Modelling survival data in medical research* (4th ed.). Chapman and Hall/CRC.
11. Cordeiro, G. M., & de Castro, M. (2011). A new family of generalized distributions. *Journal of Statistical Computation and Simulation*, *81*(7), 883-898.
12. Eugene, N., Lee, C., & Famoye, F. (2002). Beta-normal distribution and its applications. *Communications in Statistics - Theory and Methods*, *31*(4), 497-512.
13. Gemay, A. M., Karakaya, K., Bakr, M., Balogun, O. S., Atchade, M. N., & Hussam, E. (2023). Power Lambert uniform distribution: Statistical

properties, actuarial measures, regression analysis, and applications. *AIP Advances*, *13*(9), 095319.

14. Ghitany, M. E., Atieh, B., & Nadarajah, S. (2008). Lindley distribution and its application. *Mathematics and Computers in Simulation*, *78*(4), 493-506.
15. Johnson, N. L., Kotz, S., & Balakrishnan, N. (1994). *Continuous univariate distributions* (2nd ed., Vol. 1). John Wiley & Sons.
16. Lindley, D. V. (1958). Fiducial distributions and Bayes' theorem. *Journal of the Royal Statistical Society: Series B (Methodological)*, *20*(1), 102-107.
17. Quinn, G. P., & Keough, M. J. (2002). *Experimental design and data analysis for biologists*. Cambridge University Press.
18. Ruppert, D. (2014). *Statistics and data analysis for financial engineering* (2nd ed.). Springer.
19. Shukla, K. K., Shanker, R., & Tiwari, M. K. (2023). Garima distribution and its applications. *Journal of Statistics and Management Systems*, *26*(3), 671-688.
20. Weibull, W. (1951). A statistical distribution function of wide applicability. *Journal of Applied Mechanics*, *18*(3), 293-297.